Generation of High Value Fuel Gas from a Pilot Scale Downdraft Biomass Gasification Unit by Process Integration

By

RENNY ANDREW MOONJELY

COLLEGE OF ENGINEERING

Submitted

IN PARTIAL FULFILLMENT OF THE REQUIREMENT OF THE DEGREE OF DOCTOR OF PHILOSOPHY

TO

UNIVERSITY OF PETROLEUM AND ENERGY STUDIES
Dehradun
February, 2018
Under the Guidance of

Dr. Pankaj Kumar Sharma, Senior Associate Professor, UPES
Dr. D.T. Gokak, Dy. General Manager (R&D), BPCL

DECLARATION

I hereby declare that this submission is my own work and that, to the best of my knowledge and belief, it contains no material previously published or written by another person nor material which has been accepted for the award of any other degree or diploma of the university or other institute of higher learning, except where due acknowledgement has been made in the text.

Renny Andrew Moonjely

(Signature/ Name/ Date)

SAP ID : 500017676

ACKNOWLEDGEMENTS

Albert Einstein once said- “*there are only two ways to live your life; one as though nothing is a miracle; the other is as though everything is a miracle*”. Life has been full of miracles for me. Born in a middle class family, blessed with lovable parents, aspired to become an oil & gas engineer, destined to do research in oil and gas area, it was a dream journey for me. Suddenly, the opportunity came for doing Ph.D. while serving my company. I’m thankful to Bharat Petroleum Corporation Ltd. for giving me the opportunity to pursue Ph.D.

Thanks to merciful God for all the countless gifts you have offered me, and thanks to my family for their love and support.

It is a great pleasure to acknowledge my deepest thanks and gratitude to Prof. Pankaj Kumar Sharma, Associate Professor at UPES Dehradun and Dr. D.T Gokak, Dy. General Manager at BPCL Corporate R&D Centre for suggesting the topic for this research work and relentless advice. It is a great honour to work under their supervision and mentoring. I would also remember Mr. Janardan Sharma for his generous advice during the study. I am fully indebted to my previous R&D heads, Mr. K.V. Sheshadri, Dr. P.S. Viswanathan and current R&D head, Mr. Sanjay Bhargava for allowing me to carry out the Ph.D. work.

Emerson once reflected- “A friend is a person with whom I may be sincere. Before him, I may think aloud. I’m arrived at last in the presence of a man so real and equal, that I may even drop even those undermost garments of dissimulation, courtesy and second thought, which men never put off, and may deal with him with the simplicity and wholeness with which one chemical atom meets another”. I’m very fortunate to have two such friends - Mr. Nitin Somkuwar and Mr. Mel George. They were very supportive during the research work. I’m equally indebted to my other colleagues Mrs. Chithra Viswanath and Dr. Biswanath Saha for their consistent encouragement. I’m also thankful to Dr. Shalini Gupta and Mr. Amit Kunte for their timely back-end support.

I am extremely grateful for the assistance and help provided by project assistants Mr. Santhosh Viswanathan, Mr. Avneesh Kumar, Mr. Mahesh Chand and Mr. Hakeem and Mr. Surjeet Singh.

I would also be thankful to Mr. Pappu Kumar Singh for the fabrication help provided during the initial phase of the project.

Wittgenstein had remarked- “whereof one cannot speak, thereof one must be silent”. I have to remain silent on what the love of my life,- my wife, Remya means for me, and what all she has done for me. No words to praise her efforts. Thank You dear!.

Last but not the least; it is my son Lian, whose birthday every year comes as reminder for me to complete my Ph.D. work as he was born on the days I registered for Ph.D.

Once again thank each and every person in my life for their consistent support and prayers.

CONTENTS

Page

1. Chapter 1 Introduction and organization of thesis

2. Chapter 2 Review of Literature

3. Chapter 3 Research methodology

4. Chapter 4 Results and Discussion

List of Figures

List of Tables

THESIS COMPLETION CERTIFICATE

This is to certify that the thesis on "**Generation of High Value Fuel Gas from a Pilot Scale Downdraft Biomass Gasification Unit by Process Integration**" by **RENNY ANDREW MOONJELY** in partial completion of the requirements for the award of the Degree of Doctor of Philosophy (Engineering) is an original work carried out by him under our joint supervision and guidance.

It is certified that the work has not been submitted anywhere else for the award of any other diploma or degree of this or any other University.

External Guide	Internal Guide
Dr. D. T. Gokak	Dr. Pankaj Kumar Sharma

DY. GEN. MANAGER
BPCL CORPORATE R&D CENTRE
PLOT NO. 2A, UDYOG KENDRA
GREATER NOIDA - 201306
PH. 0120-2354125
MOB: 9999673130
EMAIL: gokakdt@bharatpetroleum.in

Executive Summary

The production and use of biofuels have grown rapidly over the years. Despite its less attractive economic stature as compared to fossil fuels, the increased use of biomass derived fuels is mainly driven by policies and emission norms. With respect to alternative fuels, especially biofuels, a clear focus needs to be placed on those fuels that actually minimize the fossil fuel usage and emissions. Here, the importance of biomass gasification is pretty high so as to efficiently convert biomass to generate fuels without additional release of greenhouse gases and avoid further environmental damages. In this pursuit, hydrogen qualifies as the ideal alternative fuel, which contributes zero emission when put to use.

Purpose of this research work was to devise an efficient process scheme to produce hydrogen rich syngas stream devoid of impurities. For this study, a downdraft gasification reactor was chosen as the benchmark owing to its advantages in terms of feedstock flexibility and product gas purity. In spite of its existence as a very near-the-best system, downdraft reactor faces several drawbacks. These are i) limited operability with low density biomass feedstock due to flow problems, ii) excessive pressure drops, iii) slagging of ash, iv) moderate efficiency due to lack of internal heat exchange and (v) tar formation.

One factor which determines the gasification efficiency is the type of reactor. It has been understood from the literature that the conversion levels in the conventional downdraft gasification reactors are less than 80% due to the limitations of improper heat and mass transfer and absence of proper temperature control of the reaction regime. In case of fluidized bed gasification schemes, there are many short-comings such as narrow size range of feed, moisture content of the feed, short residence time etc.

Here, an attempt has been made to design a new reactor configuration which suits wide variety of feedstock varying in terms of size and bulk density. The new design is built on a tubular reactor platform with a screw conveyor inside the reactor. The advantages of the new screw conveyor reactor design include its linear design, which facilitates positive displacement of biomass from one end to the other end through the reaction regime. This also

ensured efficient heat and mass transfer within the system by continuous mixing of the biomass due to rotation of the screw in the downdraft direction. An externally heated screw conveyor reactor was designed, fabricated and assembled.

Among all gasification schemes, superheated steam gasification was found to be advantageous as compared to oxygen or air aided gasification, mainly due to higher calorific value of syngas, production of less carbon dioxide due to indirect combustion and relatively clean gasification products. Superheated steam was generated with an electrically heated vaporizer. Known quantity of steam and biomass were inducted into the heated reactor system through a screw conveyor feeder. The resultant syngas yield (1.252 Nm^3/kg biomass) and carbon conversions (92%) were higher than the reported values from steam gasification on different reactor platforms. Once the proof-of-concept was established in the benchscale gasification reactor, the target shifted to integration of the process with suitable fixed bed catalytic reactor schemes, so that the heavy and residual vapour and carbon monoxide conversion to hydrogen enriched gas could be maximized. By this, a hydrogen rich product gas stream containing upto 53% hydrogen was obtained.

The primary steam gasification stage was optimized for temperature, steam-to-biomass ratio and residence time using rice husk as biomass feed. The gasified vapour from the primary gasification stage was reformed in the second stage reactor to yield hydrogen rich syngas. The second stage reactor was actually meant to do mainly two reactions in presence of steam, namely, steam reforming of residual hydrocarbons and Water Gas Shift reaction of carbon monoxide to hydrogen and carbon dioxide. Hence the fixed bed reactor was loaded with two types of commercial catalysts in such a way that the top layer aids steam reforming reaction and the bottom layer caters to CO shift reaction. The temperatures of both the reaction zones also have been varied to get desired reaction temperature in the 'subsections'. A thermodynamic model was also developed using ASPEN Plus to theoretically analyse the equilibrium conversion of biomass to hydrogen.

The operating conditions of the reactor are optimized using simulated gas mixture to get maximum conversion of residual hydrocarbons and CO. In the next step, the real product gas from the primary gasification stage was fed directly in the second stage reactor. The conversion obtained was in parity with the simulated gas mixture case.

After successful steam gasification experiments with rice husk, a different high density biomass- deoiled cake of Jatropha Curcas seeds was tried. The initial experimental studies revealed that deoiled cake biomass is a good feedstock for thermal pyrolysis. Benchscale pyrolysis experiments in both nitrogen atmosphere and steam were carried out at moderate temperatures of 500- 600°C. The products were condensed and analysed for its constituents. The condensate was distilled to eliminate heavy hydrocarbon fractions. From the component analysis, the amount of nitrogenous and oxygenated species was quantified. The distilled hydrocarbons were then separately fed to the fixed bed reactor loaded with reforming and Water-Gas-Shift catalysts along with steam to study the steam reforming characteristics of the pyrolysis liquid condensate. The conversion of hydrocarbon liquid was nearly 90% initially with product gas containing 82% hydrogen. But the hydrogen concentration in the product gas as well as conversion went down gradually. The rate of decay of catalytic activity was varying form one sample to the other. From the results, it was concluded that this could be attributed more to the nitrogen content in the pyrolysis liquid condensate. Hence, for this type of a process to work on continuous mode, a reactor swing mode of operation is required, in which reactors would undergo reaction and regeneration alternatively.

In order to demonstrate steam gasification on continuous mode, few engineering measures were taken into effect, which include continuous feeding, reduction of char carry-over, main drive seal cooling and hot gas clean-up. A continuous process (1 kg/h) was conceptualized and the pilot plant was designed, fabricated and assembled. The pilot plant was made fully automatic so that all relevant process data can be controlled and monitored on real time basis. On pilot run with rice husk biomass, biomass conversion upto 95% (on ash-free basis) and product gas yield upto 89% in first stage and 118% from the second stage with a steady hydrogen content upto 61% could be obtained. The product gas yield has gone above 100% due to hydrogen extraction from superheated steam fed to both gasification reactor and the secondary fixed bed converter. This shall also be attributed to the extended char gasification taking place in presence of excess steam.

Finally, an energy and economic analysis of the process was carried out to understand the scalability aspects of the process and future scope of research. The thermal conversion efficiency of biomass based hydrogen process was determined in terms of actual Hydrogen Production Efficiency (HPE) and Overall Energy Efficiency (OEE) of the process. An HPE of 105% and OEE of 52% were obtained without taking any heat integration measures into consideration. This study depicts potential of scaling up this process to large scale.

CHAPTER-1

Introduction and Organization of Thesis

1. Introduction and organization of thesis

1.1 Introduction

Biofuels are considered as the promising means to achieve energy independence and reduce Green House Gas (GHG) emissions. In spite of an ever-increasing trend of biofuels technologies, the use of biofuels is quite low as compared to petroleum fuels. The major impediments for the adaptation of biofuels are the widely varying feedstock, adaptation of the right technology and the economics. Gasification provides a competitive way to convert diverse, highly distributed and low-value lignocellulosic biomass to syngas for combined heat and power generation. This has been successfully demonstrated and commercialized by many in the past by use of gas engines or gas turbines coupled with gasifiers. Hydrogen from biomass is the most promising option provided we adopt efficient gasification technologies via. controlled combustion/ oxidation.

Most of the industrial gasifiers are either fixed bed or fluidized bed type. In the fixed bed gasifiers, there are up-draft and down-draft configurations being used. In the up-draft mode, biomass moves counter-currently to the gas flow, and passes through the drying zone, the pyrolysis zone, the reduction zone and the oxidation zone. Although this offers use of feedstock having wide variation in size, major drawback is high amount of tar and pyrolysis products, because the pyrolysis gas is not combusted. In case of down-draft mode, the feed biomass and the gas move in the same direction and pass through the drying zone, the pyrolysis zone, the oxidation zone and the reduction zone. This configuration is advantageous in terms of low tar and pyrolysis products. The disadvantages include presence of high amount of ash and dust particles leaving with the product gas and comparatively lower efficiency, because the product gas leaves at very high temperatures. In addition to the above, being a self-propagated process both the updraft and downdraft gasifiers give away lot of variabilities in product gas flow and quality [1].

Fluidized-bed reactors operate with a fluidized mix of bed material and biomass. The oxidant stream flows from the bottom and fluidize the bed material and the biomass is uniformly mixed all over the reactor and the temperature is maintained uniform throughout the length of the reactor. The advantages of fluidized bed gasifiers include fast biomass devolatilization due to uniform heat exchange and intense mixing. This configuration is limited by the following aspects- fine and very narrow feed size range, short residence time, low allowable moisture content of feed, high tar and condensable hydrocarbon content, high energy consumption and suitability at very large capacity [2-3].

Here, it requires to combine the advantages of both down-draft and fluidized bed gasifiers and develop a new gasification reactor and its auxiliaries for better biomass conversion, less operational problems and high energy efficiency. It was also required to look at the scalability aspects of the new design. Key parameters of design considered here are uniform temperature along the length of the reactor, longer residence time, control over flow of oxidizing media and other principal attributes such as axial conveyance of the biomass and oxidant stream and fast devolatilization of volatile and decomposable matter. The new gasifier aims to handle comparatively bigger and non-uniform size of biomass feed, because the axial conveyance is mechanically done instead of compressed gas used in case of fluidized bed reactors.

More research is needed to improve syngas quality for its commercial use in a highly energy-efficient manner, and for the production of liquid fuels and H_2. Most of the advanced studies have focused on achieving high calorific value fuel gas which is comparatively better than those from conventional air-gasification processes. The present gasification systems are generally designed and operated to produce fuel gas for heat and power. The produced fuel gas contain primarily CO, H_2, CO_2, H_2O (g), and hydrocarbons. Average product gas composition obtained from the conventional type downdraft gasifier is CO: 15-19%, H_2: 10-14%, CO_2: 10%, CH_4 upto 3%, N_2: 50-55%. The formation of tar (complex mixture of aromatic condensable hydrocarbons) is one of the major problems in the gasification process.

There is lack of authentic information in terms of process integration which could provide a promising way to improve the syngas yield and quality. The syngas quality (cleanliness) and composition are critical factors for its value added application. In order to utilize biomass derived syngas for applications like synthesis of liquid fuels and H_2, process integration measures like tar decomposition at high temperatures, enhanced biomass and char conversion, CO shift under steam atmosphere were required to be studied on a gasification platform. Biomass and agro-residues from one source to other widely differ in terms of their elemental composition, ash content and bulk density. This calls for process integration (*appropriate selection of processing steps and their interconnection to form a manufacturing* *system to transform raw materials into desired products*) of biomass feed preparation and gasification followed by gas clean-up steps. Significant progress has been made by researchers over past 10 years or so towards developing a better understanding of biomass derived gas handling and conditioning processes for use in advanced power production and processes making liquid fuels from syngas. However, there is need for further R&D for enhancement of calorific value of the fuel gas and removal or elimination of particulates, alkali compounds, tar etc.

Apart from the new gasification reactor design, this research was aimed to investigate some of the above process integration schemes on pilot scale biomass gasification to produce high value fuel gas enriched mainly with CO and $H_{2.}$ The process was conceptualized based on a clear theoretical background that a plug flow reactor leads to better conversion levels. Fundamental and applied research was required to improve product selectivity, to produce essentially H_2 with/ without CO, CO_2, and H_2O. The role of catalytic and non-catalytic downstream processes on raw product gas yield and thermodynamic limitations were to be investigated. Objective was total carbon conversion to produce raw gas containing more of H_2, CO and less of CO_2. Further to this, the overall process can be sustainable only when effluents from the process are minimized by appropriate methodology or recycles. Minimization of effluents from the process by hot gas filtration and application of secondary char conversion schemes were also investigated.

Typically, in the present work, a unique gasification scheme has been conceptualized and experiments were carried out to understand the effect of various operating parameters along with use of secondary reactor for meeting final product quality.

1.2 Selection of the thermochemical process scheme

Downdraft gasification systems are better represented in terms of their flow configuration that both the oxidant stream and the solid feed, flow in the same direction from top to bottom and hence it is called as "*downdraft*". The temperature increases along the direction of flow and during the process the biomass inside the downdraft gasifier undergoes various steps such as drying, pyrolysis, partial combustion and reduction. Through the new design, the advantages of downdraft reactor (flexibility in handling varied biomass materials, ability to handle biomass containing more than 10% moisture, high solid and vapour residence time) and fluidized bed reactor (uniform temperature profile, efficient heat and mass transfer) have been combined.

Several drawbacks of the downdraft system can be identified as limitation to 1) operation with low density biomass feedstock due to flow problems and 2) excessive pressure drops, 3) slagging of ash 4) non-uniform temperature profile and 5) lower efficiency due to lack of internal heat exchange and tar formation.

The sensitivity of these gasifiers with respect to feedstock size and quality are widely reported [4]. Moreover, feeding of biomass is done from top from a hopper and it requires opening of the top lid. This causes lot of air leakage and heat losses. Also, the gases inside the gasifier come out and it is a safety issue. Hence, the present design aims for a volumetric screw feeding system which is continuous in nature.

Excessive pressure drop actually results from the blockage of biomass and char movement in the gasifier, especially when they are not mechanically mixed or moved. This becomes a bitter problem in case of downdraft gasifiers when operated with biomass having moisture level more than 10% and higher size feed. It is required to progressively move the biomass steadily along the length of the reactor.

The slag formation is the result of incomplete pyrolysis, where the heavy hydrocarbons bond with the ash present in the char and agglomerates. Slagging can be removed by giving sufficiently large time for pyrolysis reactions to get complete at high temperatures. Thus, it requires steady temperature profile in the thermal zones of the reactor and tight control over residence time.

Heat transfer inside the downdraft reactor is not very efficient due to the unmixed nature of the biomass and char particles. Condensation of tars also causes severe problems in downstream processes such as fouling of pipes, filters etc. Also, formation of tar reduces the gasification efficiency by lowering the yield of product gas. The tars contain large amount of energy. The tars are generally formed from the pyrolysis stage as the pyrolysis temperature is not sufficiently high enough to completely decompose biomass into gases [5]. Tar composition depends on many parameters including the operating conditions, the design of gasifiers and the type of biomass. Tar removal methods are clubbed as i) chemical methods (thermal cracking and catalytic cracking), ii) physical methods, iii) improved reactor design.

Thermal cracking normally happens at a very high temperature greater than 800^{o}C, which is highly energy intensive. Catalytic tar conversion is practically feasible at moderate temperatures; but still has disadvantages like catalyst deactivation due to coke formation and other degradation in textural properties [6-7].

Physical tar capture techniques such as filters, cyclone, spray tower are effective in cleaning the product gas; but they are unable to improve gasification characteristics and efficiency. Thus, design of a new configuration gasifier is considered as a very impressive option, because it aims to produce syngas by retaining maximum calorific value. There were few research attempts made by earlier researchers [8], to develop a continuous downdraft reactor with internal recycle of pyrolysis gas to the combustion zone. In the present study, basic role of the new gasifier design is to enhance the residence time of biomass in the high temperature zone. A uniform surface heat flux along the length of the reactor was also aimed. Also, the cracking of tar is highly aided by steam at high temperature [9].

1.3 Design specifics of new thermochemical reactor

The design configuration for biomass gasifiers were deliberated in the past by many researchers [10-11]. Considering the design improvements required in the downdraft gasification system, a new *tubular downdraft reactor* was conceptualized addressing all the aforementioned issues. The three major factors governing all the aforementioned discussions were 1) forced draft movement of biomass particles within a gasification system to maintain ***steady and uniform flow parameters*** (flow rate, solid residence time and vapour velocity), 2) external heating of the reactor to ensure ***uniform temperature profile*** along the length of reactor and control of thermal zone lengths and 3) use of ***superheated steam*** for gasification of biomass.

To address the issue of forced draft movement, fluidized bed reactors can also be used. But literature points out to the following disadvantages of fluidized bed reactors for use in biomass gasification.

- Requirement of large scale of operation to become economically viable.
- Biomass particles have to be ground to very small and uniform size.
- Moisture content in the biomass un-favours fluidization of the particles.
- Residence time is very low.
- Product gas gets diluted with the fluidizing media

It is apparent that the fluidized bed configuration is not suitable for varied types and sizes of biomass and it can originate additional operational issues over and above the aforementioned three governing factors. Thus, it is reasoned that only mechanical displacement of biomass positively along the length of the reactor could be the viable solution.

The second factor of uniform temperature profile and control of thermal zones could be addressed by means of external heating by means of furnaces, which are pretty good in terms of temperature control and uniformity of temperature profiles. For lab scale studies, the furnace shall be electrically heated type.

Combining both the factors, it culminates that a tubular reactor with a downdraft flow pattern (biomass and gasification media flow down in the same direction by application of a partial vacuum from the product end) consisting of a rotating element inside the reactor to progressively move biomass, coupled with uniformly heated external furnaces could eventually improve the heat and mass transfer within the reactor system.

The mixing element or the screw conveyor in the reactor system is actually designed to achieve the theoretical ***reactor residence time*** ($t_{reactor}$) for the biomass solid that depends on the number of screw pitches (N_p) and screw rotation speed (N) as shown in equation 1.1.

$$t_{reactor} = N_p / N \qquad \text{................ (Eq. 1.1)}$$

Here, it is possible to achieve very high $t_{reactor}$ values (more than 7 minutes) in order to ensure complete gasification and optimize according to the particle size and nature of biomass. The design calculations are given in Appendix- I.

The optimum ***vapour velocity*** in the gasification reactor is also crucial in order to have sufficient tar cracking and reforming reactions inside the gasification reactor so that yield of hydrogen and CO can be maximized. Vapour velocity is in-turn dependant on the porosity of the reactor bed and the pressure drop across the reactor length [12].

The pressure drop across the porous bed of length L can be predicted by the Ergun equation;

$$\Delta P_{bed} / L = \frac{150\,(1-\varepsilon)^2\,\mu . U_g}{\varepsilon^3\,(dp.\phi)^2} + \frac{1.75(1-\varepsilon)\,\rho\,U_g^2}{\varepsilon^3\,(dp.\phi)} \qquad \text{.................. (Eq. 1.2)}$$

Where, ε is the porosity of the biomass bed inside the reactor, μ is the viscosity of the product gas, Ug is the superficial velocity of the product gas inside the reactor, ρ is the density of the product gas, dp is the biomass particle size and ϕ is the sphericity.

The pressure drop due to the mixing element inside the reactor is represented by $\Delta P_{C;}$

$$\Delta P_C = k.\ \rho\, U_g^2/2 \qquad \text{.................. (Eq. 1.3)}$$

Here, *k* is the head-loss coefficient corresponding to the mixing element inside the reactor. This loss is considered constant for the designed system.

The total pressure drop across the system,

$$\Delta P_T = \Delta P_{bed} + \Delta P_C \qquad \text{.................. (Eq. 1.4)}$$

The design of the reactor system takes care of the total pressure drop across the reactor and thus the superficial velocity is lower as compared to that in fluidized bed reactors.

Moreover, the vacuum pump is used to control the product gas flow rate from the reactor system, which ensures constant superficial velocity of product gas through the reactor system. The pressure drop calculations for the new reactor design are given in Appendix-I.

The other important factor for design of the new reactor configuration is the ***heat transfer rate***. In the new reactor design, the screw conveyor inside the reactor facilitates conductive, convective and radiative heat transfer. The conductive heat transfer takes place among the particles, and from the reactor walls and conveyor mixing elements by intimate contact of hot surfaces and particles; whereas the convective heat transfer from furnace through the walls to the particles is assumed to be highly predominant compared to conductive heat transfer. Considering that the particle environment is at a constant temperature, the heat flux density at the particle surface is given by;

$$Q = h_w .A.(T_w - T_b) \qquad \text{.................. (Eq. 1.5)}$$

Where,

T_w *and* T_b are respectively the temperature of the reactor wall and bulk surroundings inside the reactor.

A is the heat transfer area

h_w is the heat transfer coefficient between the wall of the reactor and both the phases (solid and gaseous material inside reactor)

The difference between a conventional downdraft reactor and the new reactor design is mainly in $h_{w,}$ which is in-turn dependant on the *velocity of the media, temperature and turbulence.*

In the new 'thermal screw conveyor' reactor design, velocity of the media can be increased by increasing rpm of the screw conveyor and vacuum level inside the reactor. Also, the boundary layer breakage due to rotation of the screw inside the reactor causes more turbulence inside the reactor.

Convection with uniform surface heat flux is ensured by the tubular reactor based 'thermal screw conveyor' design chosen for the present work. Moreover for this design, the internal thermal resistance of the metallic reactor body and mixing element (conveyor) is considered to be far less than the thermal resistance of the fluid/ metal interface. This is because, the characteristic length Lc; which in-turn is defined as the ratio of volume of the body to surface area of the body= $V_{body}/A_{surface}$ is very less. Hence the Biot number (*$Bi = h. Lc/k$; where h is film heat transfer coefficient, k is thermal conductivity of the metal body of reactor*) is less, which is very important for a constant high surface heat flux in the reactor through conductive heat transfer. The convective heat transfer inside the reactor is taken care by the rotational speed of the screw conveyor and the superheated steam.

Use of ***superheated steam*** is advantageous in many ways. There are clear evidences cited in literature about enhancement of biomass conversion and quality of syngas produced by use of superheated steam as oxidant [13-14].

1.4 Objectives of the research

- Investigation of gasification schemes with use of superheated steam
- Investigation of process integration measures
  1) Enhanced carbon conversion by novel reactor design
  2) Enhanced carbon conversion by pyrolysis coupled with reforming
  3) Tar decomposition at various temperatures and in presence of catalysts/ promoters

4) Enhanced secondary carbon conversion by fixed bed subsection temperature controlled reforming and water gas shift reactions to produce hydrogen rich product gas.

- Optimize process scheme to produce high value fuel gas enriched mainly with CO, H_2 and devoid of tar, particulates and other impurities.

1.5 Scope of research work

The scope of the study is divided into four parts.

- To design a novel gasification scheme, wherein superheated steam can be used to gasify biomass and positively displace the char from the primary gasification zone
- Optimize process variables of the superheated steam gasification scheme by integration of various improvement schemes such as extended char gasification to increase carbon conversion efficiency and also to improve the overall product gas yield and hydrogen yield.
- To study the catalytic conversion of residual hydrocarbons, CO and heavy hydrocarbon liquids to H_2 rich gas.
- The feasibility study of the process in finding process economics towards producing a high calorific value fuel containing majority of H_2 without other combustion impurities.

1.6 Plan of the thesis

The present work has been reported in a thesis comprising of five chapters - Introduction, Review of literature, Research methodology, Results and discussion, Conclusions and recommendations and References.

Chapter 1 represents the complete introduction to the present study including need for this research, selection of process scheme, research objectives and scope of work in the current research.

Chapter 2 deals with the literature review - the research works which have previously been carried out in the areas of biomass gasification, gap areas in the earlier research works, various reactor configurations and process integration techniques adopted by earlier researchers.

Chapter 3 deals with the research outline - the experimental methodology, target parameters and procedures, feed and product analysis procedures, design of experimental platform, theoretical considerations and thermodynamic model, and basis for parametric studies on steam gasification and pyrolysis in the new reactor platform.

Chapter 4 describes the results of steam gasification and pyrolysis experiments to produce syngas. The steam gasification and pyrolysis conditions were varied to get high biomass conversion and product yield and quality. Secondary conversion of the gasified vapour and pyrolytic liquid (bio-oil) reforming to hydrogen rich gas were carried out in a second stage fixed bed reactor. Based on the process integration, scale-up parameters were identified and a continuous mode process was conceptualized and demonstrated. The steady state results were interpreted and other process efficiency factors were determined. Also, scalability and economic aspects, conclusions from present work and recommendations for future research feature at the end of this chapter.

◊◊

CHAPTER-2

Review of Literature

2.1 Chapter overview

With increasing demand for alternative source of energy, biomass energy conversion and utilization attracts much attention. Thermo-chemical conversion is the most commonly used biomass conversion method to upgrade biomass energy quality. Gasification is a complex thermochemical process in which a solid carbonaceous fuel is transformed into a gas having usable heating value (called producer gas or synthesis gas depending on its composition) at high temperatures (800–1800°C) and in the presence of a gasifying agent (air, oxygen, steam, carbon dioxide, hydrogen, and mixtures of them).

The effect of the way of introducing oxygen into the gasifier (as air or steam) is different. Gasification reaction is very fast when oxygen or air is used as the medium. The quality of gas obtained is of low grade, which could only be useful for heat and power applications. Steam is less reactive than oxygen, and steam reforming reactions are endothermic and slower than those of combustion. Thus, it is necessary to supply heat to the process externally. A possible way to solve this latter drawback is gasifying using air–steam mixtures, so the process efficiency is considerably increased without significantly raising the capital costs. In the first part of the chapter, various thermochemical conversion processes developed in the past for conversion of biomass to fuels have been discussed in detail along with various reactor configurations. In the second part, specific researches on steam gasification and pyrolysis of rice husk and deoiled cake of Jatropha were discussed. The gap areas identified were reactor design suitable for all types of biomass, high carbon conversion efficiency at moderately high temperature of operation, tar conversion to gaseous components, enrichment of hydrogen in product gas stream by downstream process integration, steam reforming of pyrolysis oil to produce hydrogen and effect of catalyst deactivation and continuous process on biomass-to-hydrogen concept.

2.2 Literature Survey

Gasification is a process that converts organic or fossil-based carbonaceous materials into carbon monoxide, hydrogen, carbon dioxide, methane and nitrogen. This is achieved by reaction of the carbonaceous material with a controlled amount of oxidant stream at high temperatures.

2.2.1 Fundamental chemistry

The reaction gets completed with a series of steps: drying, devolatilization, char gasification and gas phase reactions. The exothermic reactions provide heat to support the endothermic reactions through partial combustion. The major challenge of gasification technology is to improve quality of the product gas which determines the extent of the post-treatment. Tar formation (complex hydrocarbons CxHy), multiphase flow, gas-solid interaction, chemical reactions and turbulence are responsible for the composition of the raw output gas.

The main reactions taking place during the conversion process are described in Table 2.1.

The producer gas must be properly conditioned (cooling, particles and tar cleaning, composition adjustment) prior to its use as a fuel in internal combustion engines, gas turbines, or fuel cells for the production of heat, power or mechanical energy, or as a feedstock for the synthesis of fuels and chemicals. Both the gas composition and the process performance (gas yield, cold gas efficiency, fuel conversion, etc.) depend on a series of factors, namely the physical and chemical fuel properties, the type of gasifier, the type of gasifying agent and the operating conditions (pressure, fuel/gasifying agent ratio, temperature, heating rate, residence time, use of catalysts, etc.) [15,16].

Table 2.1 Major gasification reactions

Devolatilization	Reaction
Biomass + Q → Carbonaceous residue (char) + tars and oils + gases (CO, CO_2, H_2, CH_4+ CnHm)	R.1
Pyrolysis: Secondary cracking and reforming	
Tars+Q → Char + gases (CH_4, H_2, CnHm)	R.2
Tars +H_2O ↔ CO, H_2	R.3
Combustion	
$C + O_2 \rightarrow CO_2$	R.4
$C + \frac{1}{2} O_2 \rightarrow CO$	R.5
$CO + \frac{1}{2} O_2 \rightarrow CO_2$	R.6
$H_2 + \frac{1}{2} O_2 \rightarrow H_2O$	R.7
Reduction /Gasification	

Boudouard reaction

$C + CO_2 \leftrightarrow 2CO$ R.8

Hydrogasification

$C + 2H_2 \leftrightarrow CH_4$ R.9

Char Steam Reforming

$C + H_2O \leftrightarrow CO + H_2$ R.10

$C + 2H_2O \leftrightarrow CO_2 + H_2$ R.11

$C + H_2O \rightarrow \frac{1}{2} CH_4 + \frac{1}{2} CO_2$ R.12

Water Gas Shift

$CO + H_2O \leftrightarrow CO_2 + H_2$ R.13

Methane reforming

$CH_4 + H_2O \rightarrow CO + 3H_2$ R.14

$C_nH_m + 2n H_2O \rightarrow (2n + m/2) H_2 + nCO_2$ R.15

The advantages of air gasification are the availability and economy of air, and the possibility of a self-sustained process; however, the gas obtained has a low heating value (~5 MJ/Nm^3) owing to its dilution in nitrogen. The use of oxygen in the process increases the calorific value of the gas, although the need for an air separation unit makes the process expensive, this option thus being feasible only for large scale facilities. Steam gasification offers some advantages- it is an affordable process, and the resulting gas has a higher heating value and is rich in H_2 [17-21].

2.2.2 Thermochemical conversion processes

Thermo-conversion processes are combustion, pyrolysis, and gasification. Combustion produces gases at a temperature range of 800 to 1000°C, with very little solid residue; whereas the pyrolysis process produces gases, liquids, and solids. It is feasible to combust a biomass that has a moisture content of less than 50%, whereas conventional biomass pyrolysis produces fractions of gases, liquids, and solids. There is a great amount of research work going on in the area of up-gradation of liquid products to fuel grades or hydrogen, but they have not yet been fully developed [22]. Gasification is an attractive thermo-chemical process and has a higher efficiency than combustion. Gasification adds value to low or negative-value feed stocks in terms of usefulness by converting them to marketable fuels and products. Gasification converts biomass to gas and diminishes the content of char and tar.

2.2.3 Biomass gasification processes

By gasification process, biomass can be broken down to H_2, CH_4, CO, CO_2 and others in the presence of a gasification agent(s). The agent may be oxygen, air, steam or a combination of them. Steam gasification produces a gas rich in hydrogen [19]. It gives a medium heating value gas of ~15–20MJm^{-3}, which is higher than that from air gasification and costs less compared with oxygen gasification [23]. The type of gasification process varies with end application. The application can be use of product gas in gas engines, gas turbines, fuel cells, hydrogen production, Fischer-Tropsch synthesis etc.

In case of use in gas engines and gas turbines for power production, a low calorific value fuel is sufficient and hence air can be used as the gasifying medium. In case of Fischer-Tropsch synthesis, the ratio of CO to H_2 is critical and hence a combination of oxygen and steam blown gasification system is preferred. For hydrogen production and fuel cell application, hydrogen rich gas is required to be produced. Here, a steam gasification system is advantageous.

Gasifier configurations:

There are many types of gasifiers available ranging from simple to more complicated geometries. As there is an interaction of air or oxygen and biomass in the gasifier, these are classified according to the way air or oxygen is introduced into it. Thus, there are 4 types of gasifiers widely practiced depending on the end application.

- Fixed bed gasifier (Up - draft, Down - draft)
- Fluidized bed gasifier (bubbling bed, circulating fluidized bed)
- Entrained bed gasifier
- Auger reactors

Fig. 2.1 shows the configuration for different types of gasifiers, based on their feeding design and geometries.

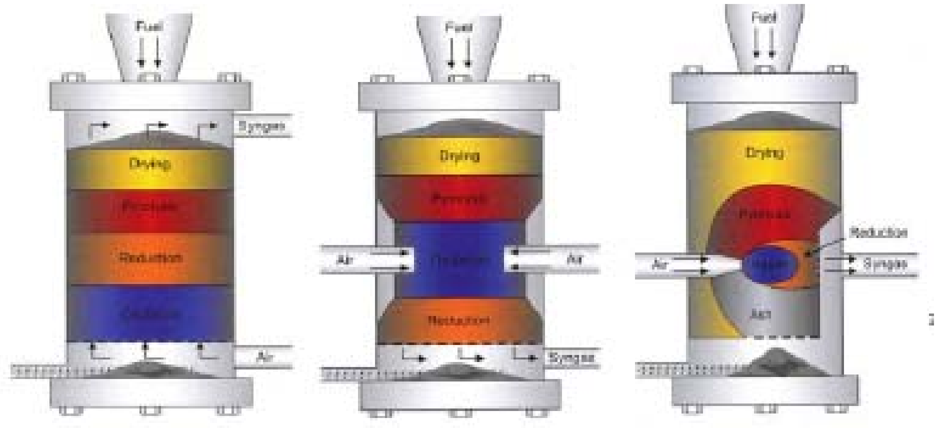

Fig 2.1 From left to right: Updraft, Downdraft and Cross-draft gasifiers [24]

Updraft gasifier:

This is the simplest type of gasifier. Biomass moves counter-currently to the gas flow, and passes through the drying zone, the pyrolysis zone, the reduction zone and the oxidation zone. The major advantages of this type of gasifier are its simplicity, high charcoal burn-out and internal heat exchange leading to relatively low gas exit temperatures and high gasification efficiencies. Furthermore, this type of gasifier can even process relatively small sized fuel particles and accepts some size variation in the fuel feedstock. Major drawbacks are the high amounts of tar and pyrolysis products, because the pyrolysis gas is not combusted, hence extensive gas cleaning is required.

Downdraft gasifier:

In downdraft reactor, the feed biomass and the gas move in the same direction. Downdraft gasifiers produce the lowest level of tar and are therefore the best option for engine applications. Scaling-up of this type of gasifier is however limited.

Drawbacks of the downdraft gasifier are the high amounts of ash and dust particles in the gas. This leads also to a relative high temperature of the leaving gases resulting in lower gasification efficiency.

Crossdraft gasifiers:

In the crossdraft gasifier, the contact time is very less and due to very short reduction zone, hence the quality of gas is not very good.

Fluidized bed gasifiers:

Fluidized-bed reactors function with a fluidized mix of bed material and biomass. The gasification medium flows through the nozzle bottom and fluidize the bed material. This can be inert, as for example quartz sand or also catalytically active with regard to the conversion of organic contaminants in the crude gas through possible after reactions in the gas phases. For this purpose, substances like dolomite or olivine can be used. The air passes upwards through the bed, and when the point where the pressure drop equals the gravity force of the particles, the particles become suspended and termed fluidized at the minimum fluidization velocity. This is an important parameter in designing fluid bed reactors. Further increase of the air velocity causes the particles to move more and more vigorously resembling a boiling liquid.

Due to the intense mixing, the different zones (drying, pyrolysis, oxidation, reduction) cannot be distinguished like at fixed bed gasifiers; the temperature is uniform throughout the bed. Contrary to fixed bed gasifiers the air-biomass ratio can be changed, and as a result the bed temperature can be controlled, usually between 700 to 900ºC.

The advantages of fluidised bed reactors in comparison with fixed bed reactors are compact construction, high heat exchange due to the intensive mixing in the bed.

But the drawbacks are high tar and dust content of the produced gas, high producer gas temperatures containing alkali metals in the vapor state, incomplete carbon burn out, complex operation because of the need to control the supply of air and solid fuel supply, relatively high power consumption for the compression of the gas stream.

The main fluidized bed reactor designs are the Bubbling Fluidized Bed reactors (BFB) and Circulating Fluidized Bed (CFB) reactors.

Bubbling fluidised bed (BFB):

The BFB gasifier (Fig 2.2) is well known and commonly used because of its robust properties. The BFB utilizes the minimum fluidisation velocity of the bed material to achieve fluidization state and has a distinct interface between the freeboard above the bed surface and fluidised bed reaction zone. Tar production is 1% to 2% because the unit operates like a continuous stirred thermal reactor, so there is some biomass and tar slip.

Circulating fluidised bed (CFB):

The CFB gasifier (Fig. 2.2) has no distinct interface between the fluidized sand bed and the freeboard. It uses a velocity higher than the minimum fluidization velocity and requires a cyclone separator to transport the elutriated bed material back to the gasifier. CFB operates with higher superficial velocities, typically in the range of 2-5 m/s, whereas the velocity in the BFB is only 0.5-2 m/s, maintaining the ratio of fuel to fluidization gas. This type of gasifier increases the rate of gasification, has a high conversion rate of tar and is suitable for large scale power generations. The carbon burn out in circulating fluidized bed gasifiers is considerably better than in bubbling fluidized beds.

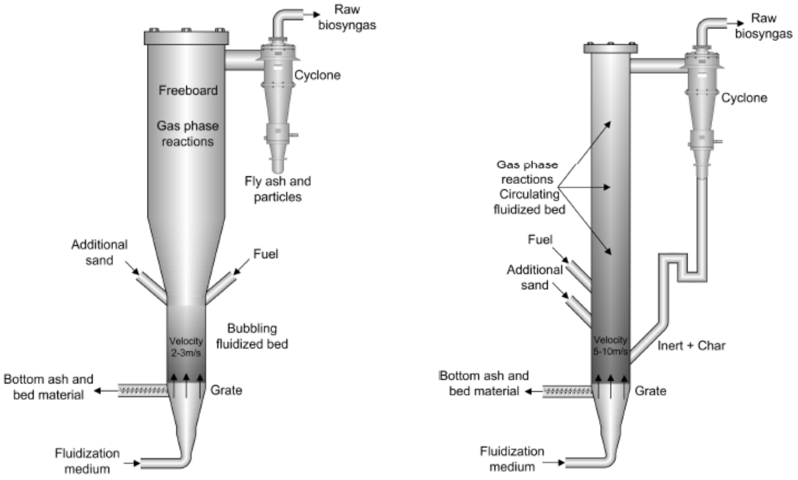

Fig 2.2 Diagram of a bubbling fluidised bed gasifier (left) and a circulating fluidised bed gasifier (right) [24]

Auger gasifier/Rotary kiln gasifier:

The class of rotary kiln reactor consists of a cylindrical chamber that slowly rotates in its on axis. The auger reactor consists of a screw conveyor rotating inside the tubular reactor with the help of a motor. The gas–solid contact takes place due to the rotation of the reactor that exposes the new solid surfaces to the gasification agent. The conditions for mass transfer and heat transfer between the solid and the gas are not very effective, and then, the residence time is higher than those with the other gasification technologies. Table 2.2 shows the main advantages and disadvantages of the various gasification reactors, as reported in the scientific literatures.

Table 2.2: Summary of gasification techniques

S.N.	Gasifier Types	Merits	Demerits
1	Updraft	- Small pressure drop - Good thermal efficiency - Little tendency towards slag formation	- Great sensitivity to tar formation - Relatively high start-up time - Heavy formation of particulates
2	Downdraft	- Flexible adaptation of gas production to load - Low sensitivity to charcoal dust & tar content - Greater temperature control - Higher LHV ~ 11 MJ/Nm^3 reported - High (H_2+CO) ~ upto 72% - Large scope for improvement of the gas yield by hot clean-up methods - Suitable for small scale standalone installations	- Not feasible for very small particle size of feed - Moderate gas yield: 1.5 Nm^3/Kg feed
3	Cross-Draft	- Short design height - Very fast response time to variation in load (el.)	- Very high sensitivity to slag formation - High pressure drop
4	Fluid Bed	- Flexibility with regard to feed rate and rate of consumption - High gas yield upto 2.5 Nm^3/kg reported - Highest carbon conversion efficiency ~ 97%	- Not suitable for small scale - Requires reduced feed size and good particle distribution - Produces more dust & tar as compared to downdraft - High operating cost

5	Entrained Bed	- Gasified with oxygen in co-current flow - Very high temperatures and very less particulates and heaviers	- High oxygen requirement - Low calorific value of gas
6	Auger Gasifiers	- Very easy to operate - Control of temperature along length is possible	- High chances of wear and tear - Moderate heat transfer

2.2.4 Effect of operating parameters on gasification efficiency

To get the best-quality exit gas, the gasifier performance has to be optimized. For an optimized performance of the gasifier, the main attractive factors are the design and the operation of the gasifier. In the operation of the gasifier, both steam and steam–air gasification processes have been studied by several authors, in theoretical as well as in experimental works [25, 26]. In general, all researchers agree to the trend that depicts increase in the gas H_2 content when adding steam to the process; and many of them point at the importance of the Water Gas Shift reaction (WGS, R.13 in Table 2.1) in the final adjustment of the synthesis gas composition [27-32]. Most of the experimental works have been carried out in fluidised-bed [33-39], fixed-bed [40-46], or batch reactors [31, 47-49]. The feasibility of the process lies in finding favourable process economics towards producing a high calorific value fuel containing majority of CO and H_2.

The most important influencing parameters include temperature, pressure, gasifying medium, catalyst and additives, equivalence ratio (ER), residence time, etc.

Effect of temperature:

To achieve a high carbon conversion of the biomass and low tar content in the resultant product gas, a high operating temperature (above 800°C) in the gasifier is preferred. To produce a relatively clean gas by increased temperature, several temperature ranges are reported in the literature. Some of these works are cited in the present work. Temperature not only affects the amount of tar formed, but also the composition of tar by influencing the chemical reactions involved in the whole gasification network.

Turn et al. [18] observed during sawdust gasification in a fixed bed gasifier that the total number of detectable tar species decreased with increasing temperature. Oxygen-containing compounds such as phenol, cresol and benzofuran exist in significant quantities only at temperature below 800°C. They also confirmed that higher temperature favour the formation of fewer aromatic tar species without substituent groups such as benzene, naphthalene, phenanthrene, etc. Destruction of these aromatic hydrocarbons occurs only at temperatures above 850°C. An increasing temperature promotes the formation of gaseous products at the expense of total tar. More than 40% reduction in tar yield was reported when the temperature was raised from 700°C to 900°C. With increase in temperature, the amount of total oxygen-containing components drastically goes down.

Effect of pressure:

Several researchers have investigated pressurized biomass gasification. Knight [50] investigated the effect of system pressure for biomass gasification. When the pressure was increased, almost complete elimination of phenols and oxygenates was observed. The trend was the same when amount of steam was increased at constant pressure and temperature. Although the amount of total tar decreased, the fraction of Poly Aromatic Hydrocarbons (PAH) have increased with increasing pressure. The pressure was raised from 1 to 15 bar of CO_2 and H_2O at temperatures of 750°C and 850°C. Increase in CO_2 pressure slightly reduced char gasification whereas this increased with increasing H_2O pressure.

Effect of residence time:

According to Turn et al. [18] residence time has little influence on the tar yield. Gil et al. [16] observed a decrease in the total tar content when the space time was increased for biomass gasification with in-bed use of dolomite. Amounts of O_2-containing compounds tend to decrease with increasing residence time.

Effect of gasifying media:

Different gasifying agents such as air, steam, steam–oxygen and carbon dioxide have been reported in the literature. Selectivity of the gasification reactions varies with different gasifying media, thus affecting the product gas composition as well as the heating value.

Gasification under air:

Heating value of the product gas with air as gasifying medium is lower because of dilution of the gas by nitrogen. Ismail et al. [51] reported a gas composition of 8% H_2, 14% CO, 15% CO_2 (vol%) from a gasifier with gasification temperature of 800°C with an Equivalence Ratio (ER) of 0.35. But the tar content decrease sharply as the ER was increased, being as low as 2 g m^{-3}. The ER strongly influences the type of gasification products. Tar yield and tar concentration decreases as the ER increases because of more availability of oxygen to react with volatiles in the pyrolysis zone. This effect of ER is more significant at higher temperature.

The ER is very crucial because its higher value results in lower concentration of H_2, CO and higher CO_2 content in the product gas, thus decreasing the heating value of the gas. Although the total tar concentration decreased by almost 30% when the ER was increased from 0.22 to 0.32 for a temperature of 700°C.

Gasification under oxygen enriched air:

As far as the purity of product gas is concerned, gasification under oxygen is preferred over the conventional air-gasification process. Although the gas is free from N_2, the operational difficulties and cost of oxygen make the process not suitable for medium scale applications.

Gasification under CO_2:

The use of CO_2 as gasifying medium is promising because of its presence in the gasification atmosphere. Tar reduction is also enhanced by dry reforming reactions of CO_2, which is a gasification product. According to Minkova et al. [52], a mixture of steam–CO_2 gives highest degree of carbonization for pyrolysis and gasification of biomass in a horizontal rotating reactor. They also mentioned that a steam–CO_2 mixture produced the highest activity char, which resulted in high ash content. Garcia et al. [53] investigated CO_2 gasification in the presence of Ni/Al co-precipitated catalyst and compared the results with those of steam gasification. CO_2 gasification in the presence of a catalyst transformed tars into useful products and also causes a decrease of the amounts of CH_4 and C_2-fraction (C_2H_2; C_2H_4; C_2H_6) as well as an increase in H_2 and CO yields. Significant decrease in the CO_2 content was observed with a CO_2/biomass ratio of 1.16 indicating that CO_2 itself converts to other products. Deposition of carbon in the catalyst particles can be avoided to a certain extent by feeding CO_2 in excess and the Ni/Al co-precipitated catalyst remained active. The catalyst quantity also plays an important role. At lower catalyst/ biomass ratios, the H_2 and CO decreased and CO_2, CH_4 and C_2H_4 increased. The main chemical reactions with H_2O and CO_2 as gasifying media are listed below:

$Tar + H_2O \rightarrow mH_2 + nCO$	$Tar + CO_2 \rightarrow pH_2 + qCO$
$CH_4 + H_2O \rightarrow 3H_2 + CO$	$CH_4 + CO_2 \rightarrow 2H_2 + 2CO$
$C_2H_4 + 2H_2O \rightarrow 4H_2 + 2CO$	$C_2H_4 + 2CO_2 \rightarrow 2H_2 + 4CO$
$C + CO_2 \rightarrow 2CO$	

2.2.5 Biomass gasification under steam

In view of lower heating value as well as poor gas composition, pure steam was used by many as oxidant and they observed a completely different product gas distribution [54-56]. The steam gasification product is more or less free from N_2 and more than 50% H_2 in the product gas.

An increase in H_2 (as high as 60%) and CO_2 (from 10 to 30%) contents, a sharp decrease in CO (from 35 to 10%) content, a slight decrease in CH_4 content and relatively no change of C_2-fractions (C_2H_2; C_2H_4; C_2H_6) were observed when the S/B ratio was increased from 0.5 to 2.5, without using any catalyst or additive. Steam gasification is endothermic and hence sometimes requires complex design for heat supply in the process. The main reactions are given below.

$$\text{Biomass} + \text{Steam} \rightarrow H_2 + CO + CO_2 + CH_4 + \text{Light and heavy HC} + \text{Tar} + \text{Char (C)} \quad (1)$$

$$C + H_2O \rightarrow CO + H_2 \quad (2)$$

$$CH_4 + H_2O \rightarrow CO + 3H_2 \quad (3)$$

$$CnHy + H_2O \rightarrow CO + CH_4 + C_2H_4 + H_2 \quad (4)$$

$$CO + H_2O \rightarrow CO_2 + H_2 \quad (5)$$

Steam gasification is believed to be an effective mode of producing renewable hydrogen without leaving any carbon footprint in the environment. Only lesser amounts of char and tar are produced during steam gasification since steam initiates more water gas reactions. Steam gasification technology is suitable for biomass having moisture content less than 35%.

Hydrogen production by steam gasification of biomass is a complex process that is influenced by a number of factors, such as *biomass feed types, biomass feed particle size*, *temperature*, *steam-to-biomass ratio*, *residence time*, *addition of catalysts* and *sorbent-to-biomass ratio*.
Bridgwater [15] in his work stated that relative yields of gas, liquid and char depend mostly on the *rate of heating* and the *final temperature*. The researcher further asserted gas composition is influenced by many factors such as feed composition, water content, reaction temperature, and the extent of oxidation of the pyrolysis products.

Some other researchers had the opinion that catalysts enhance decomposition of volatiles and tar produced from biomass and consequently increase the production of gases like hydrogen [57]. The same researcher also revealed that the smallest biomass particles yielded more gas per kg of biomass.

The effect of biomass particle size on hydrogen production is significant. Some researchers have worked on the effect of biomass particle size on the product gas yield [58-63]. Lv et al. [64] reported that larger particles possess greater heat transfer resistance which result in incomplete pyrolysis leading to more amount of residual char. On the other hand, smaller particles possess larger surface area per unit mass. This improves the heat and mass transfer between particles. Effective heat transfer increases the gasification efficiency significantly. This results in increased CO and H_2 production at the expense of CO_2 and decreased tar and char formation.

Effect of temperature on hydrogen production during steam gasification was studied by many researchers [65, 66]. Generally, increase in temperature increases the heating rate among the particles. This leads to effective destruction of the particles and proceeds for completion in gasification reactions. Moreover, thermal decomposition of tar molecules and Boudouard reaction of carbon in char lead to more gaseous products. Demirbas [67] ascertained that increase in temperature not only increases the hydrogen yield but also decreases tar yield. Biomass with larger composition of Cellulose and Lignin yields more gaseous products. Thus hydrogen production from biomass is based on its intrinsic nature and moisture content. Inayat et al. [68] in his experiments observed decrease in methane and CO_2 concentration with increase in temperature.

Steam has a significant influence on the biomass conversion and gas composition. Many researchers have reported increase in hydrogen yield with steam gasification [69, 70]. Low values of steam produce methane and carbon. At higher values of steam, carbon, higher hydrocarbons and methane are reformed to CO and H_2. Excess steam has a negative effect as it may reduce the reaction temperature and that induces more tar into the product stream.

Many researchers have studied the effect of catalysts on biomass steam gasification. The catalysts used majorly are dolomite, Ni-Alumina, Alumino-silicate, K_2CO_3, Na_2CO_3, Alkali metal oxides etc. Catalysts work in improving the various gasification reaction efficiencies and promote destruction of tar. Ni et al. [71] reported that dolomite, Ni-based catalysts and alkaline metal oxides catalysts are best for gasification reactions. Corte et al. [72] found that the Alumino-Silicate catalyst is good for carbon gasification and Ni- catalyst is more active for higher hydrocarbon reforming. Extensive research is underway by many researchers to develop a stable, cheap and highly reactive catalyst for hydrogen production from biomass [73-77]. Some of the works on high temperature CO_2 adsorbents also gained attention in the past. Some find CaO, Calcium Aluminate, MgO based adsorbents are very good for in-situ CO_2 adsorption during gasification reactions. They require cyclic regeneration also after saturation in CO_2 uptake.

2.2.6 Effect of feedstock on gasification characteristics

The biomass materials vary in terms of the following characteristics. They are 1) Moisture content, 2) Ash content, 3) Proximate analysis (volatile content), 4) Ultimate analysis (CHNO content), 5) Biomass particle size and 6) Bulk density.

Moisture content: Biomass with moisture content above 20% is normally not suitable for steam gasification due to the need to evaporate the additional moisture before combustion/gasification can occur. High moisture content reduces the temperature achieved in the oxidation zone, resulting in the incomplete cracking of the hydrocarbons released from the pyrolysis reactions. However, lower levels of moisture in presence of CO produce H_2 by the water gas shift reaction.

Ash content: High amount of ash in the feed makes the gasification tough. If the oxidation temperature is above the melting point of the biomass ash, it can lead to clinkering/ slagging and can cause blockages. Clinker is a problem for ash contents above 5%. Most of the biomass materials contain moderate ash to the tune of 5-15%. In case of steam gasification, due to low gasification temperatures, clinkering is normally avoided.

Elemental composition: The elemental composition of the fuel is important with respect to the heating value and the emission levels in almost all applications. The production of nitrogen and sulphur compounds is generally small in biomass gasification because of the low nitrogen and sulphur content in biomass. The mass percentage of carbon, hydrogen and oxygen actually contribute to the heating value of the fuel.

Heating value: The heating value is determined by the elemental composition, ash content and moisture content of the biomass. On a dry and ash free basis, most biomass species have a heating value of about 19 MJ/kg.

Volatile compounds: Besides operating conditions, reactor designs, etc. the amount of volatiles has an impact on the tar production levels in gasifiers. The gasifier must be designed to destruct tars and the heavy hydrocarbons released during the pyrolysis stage of the gasification process.

Bulk density and morphology: The bulk density refers to the weight of material per unit volume. Biomass of low bulk density is expensive to handle, transport and store. The particle size of the feedstock material depends on the reactor dimensions but is typically 10–20% of the reactor diameter. Larger particles can form bridges which prevent the feed moving down, while smaller particles tend to clog the available air voidage, leading to a high pressure drop and the subsequent shutdown of the gasifier. Feedstock pre-treatment/preparation is required for almost all types of biomass materials because of a large variety in physical, chemical and morphological characteristics. The degree of pre-treatment of the biomass feedstock depends on the gasification technology used.

Considering the advantages and disadvantages of the primary and secondary methods, in the present study, a combination of the methodologies was adopted in such a way that the biomass gasification and extended char gasification by excess steam are targeted in the first stage ‘rotary tubular gasification’ and conversion of CO and hydrocarbons into H_2 in the second stage ‘fixed bed catalytic conversion’.

In the present study, the combination of catalysts is chosen such a way that the top bed is filled with catalyst of higher stability and reforming activity and the bottom bed is filled with catalyst of higher selectivity and higher coke deposition resistance.

2.2.7 Secondary conversion and downstream processes for hydrogen rich gas

Steam reforming is the most popular but energy intensive hydrogen production process wherein naphtha or natural gas is used as the feed. Gasification of biomass followed by catalytic conversion is considered as another alternative process to steam reforming, particularly when biomass is abundantly available. The present trend of research is majorly focused on fast pyrolysis to produce bio-oil followed by steam reforming [78-80] and catalytic steam gasification [81, 82]. Although both the processes yield high quality gas, there are many problems such as incomplete conversion of biomass, formation of tar (heavy hydrocarbons and chemicals) and particulate matter etc. Also, this has caused problems in the effluent treatment, especially in case of processes where water is used as a scrubbing medium. Tar is a complex mixture of condensable hydrocarbons and it causes problems in application of the product gas.

Literature reveals that tar and particulates are removed by two methods: 1) primary tar and particulate reduction in the gasifier (in-situ), 2) secondary tar and char reduction outside the gasifier (ex-situ). In the primary method, the gasifier reactor design is crucial for overall efficiency and product gas quality. This method has advantages like low investment and less maintenance. In the secondary method, hot gas filtration and catalytic conversion are employed. Secondary method has advantages like, better particulate control and better catalyst life; but it is more expensive compared to primary method.

Primary process: The first stage gasification involves various reactions including pyrolysis or decomposition, gasification or combustion and reduction. As these reactions are diffusion and mass transfer limited, gasification efficiency is dependent on particle size, temperature, steam-to-biomass ratio, residence time, internal solid mixing and heat exchange. Compared to a conventional fixed bed downdraft gasifier producing large amounts of contaminants like char, ash and tar, primarily due to less contact of oxidants or steam with the biomass particles and inept heat and mass transfer, the present system ensures radial mixing of each particle in the reactor due to rotation of the tubular furnace. Also the screw conveyor inside the rector allows better heat and mass transfer within the system.

In conventional gasification processes, gasification efficiency gets affected easily by change in the particle size of the feed and residence time [83]. In a conventional downdraft gasifier, it is relatively easy to tune and control the above reactions in segregated oxidative and reductive sections within the same reactor. In spite of this, poor mass and heat transfer hampers the overall efficiency of the process. In the present work, a rotary tubular furnace consisted of a helical coil conveyor was used, wherein residence time of biomass within the rotary tubular furnace was controlled by the speed of rotation of the tube. Also the use of superheated steam enhances the biomass conversion to lighter components.

Autothermal gasification processes have already been investigated by many in the past [84, 85]. The main drawback is that the process is largely diluted with nitrogen. On the other hand, steam gasification is endothermic and external heating is required to be given, in order to carry out the gasification at specific temperatures. In recent studies, fluidized bed gasifiers are used to gasify the biomass in presence of steam [86]. The produced volatiles and nascent char involved in the gasification reactions concurrently fall into the moving bed. The tar and heavy hydrocarbons will pass through a hot catalyst bed at the lower part of the gasifier, which favors reduction of heavy pyrolytic vapour and hydrogen production. In this process, coke will deposit on the surface of the catalyst, and the deactivated catalyst (bed material) will need to be regenerated. The coke deposition shall reduce the life of the catalyst. Hence in the present study, extended char gasification with the help of steam reforming of carbon-char and control of biomass residence time has been realized. The final residual char and ash is then collected in the char collection bottle. The disengaged product vapour was then sent to the secondary fixed bed catalytic converter for maximization of hydrogen.

Secondary process: Catalytic cracking has provided a big thrust to biomass gasification for converting the heavy pyrolytic vapour into useful gases and hydrocarbons. Recent reviews on up-gradation of biomass gasification vapours classify the catalysts into four categories; Ni based catalysts, alkali metal catalysts, dolomite catalysts and mixed metal oxide catalysts [87-89]. Ni-based catalysts are extensively applied in the petrochemical industry for naphtha and methane reforming. Meanwhile, a wide variety of Ni-based catalysts are commercially available. Especially, some studies showed that nickel based catalysts help in reduction of biochar, heavy pyrolytic vapour to produce more hydrogen [90]. Compared to the un-promoted catalysts, K_2CO_3 impregnated catalyst significantly suppressed the coke deposited on the catalyst surface, but only had marginal effect on the product selectivity. Mohammed et al. [91] reviewed various catalysts used and suggested Ni supported by dolomite catalyst by its high activity and stability for a long contact time. Moreover, carbon deposition at the Ni/dolomite catalysts surface was negligible.

2.2.8 Pyrolysis of biomass followed by catalytic conversion to hydrogen

Fast pyrolysis is a process in which biomass is converted in the absence of oxygen into a liquid, often called pyrolysis oil or bio-oil. Pyrolysis oil has the potential to become an important intermediate energy carrier for the production of bio-based chemicals, transportation fuels, heat, and electricity. Recently, there has been a shift in research attention from maximizing bio-oil yield to approaches and process designs aiming to improve bio-oil quality. For co-processing stabilized bio-oil in standard crude oil refinery units, molecular weight (distribution), oxygen content, hydrogen/carbon (H/C) ratio, total acid number, corrosivity, and thermal stability are key characteristics. These quality indicators are directly related to the chemical composition of these oils. Bio-oil is a complex multi-component mixture of molecules derived from depolymerization and fractionation of biomass building blocks, namely, *cellulose, hemicellulose, and lignin*. It can be classified into the following generalized categories: hydroxyaldehydes, hydroxyketones, sugars and dehydrosugars, carboxylic acids, and phenolic compounds. However, unlike oil, its high content of oxygenated compounds makes it difficult to be processed in traditional petroleum refineries. These significant amounts of oxygen are related to undesirable properties, such as high viscosity, corrosiveness, and instability. Pyrolysis is generally chosen as a recommended process to achieve this goal. This process has gained much attention in recent times as it can produce highest liquid yield upto 75wt%. This is accomplished at moderate temperatures (~500^{o}C) and short hot vapour residence times (~ 1s) [92]. The liquids from this process are called as pyrolysis oil or bio-oil. Bio-oil has got application as heating fuels in furnaces and boilers or as feedstock for commodity chemicals. The high percentage of Oxygenated compounds in the bio-oil makes it less attractive to become a high calorific value fuel and is prone to corrosion problems and instability. The oxygen content in bio-oil is reported as 35-60% by many researchers [93-95]. But the greatest advantage is its suitability for conversion into an environmentally clean fuel like H_2. Hence the efforts are in the direction of elimination of oxygen from the bio-oil. The entire pyrolysis process consists of three stages. 1. Feed preparation, 2. Closed system pyrolysis, and 3. Condensation. High moisture content feed may lead to pyrolysis oil containing more water. Bridgewater [96] suggested that the maximum moisture content in the feed biomass should be 10%. These properties can be quite problematic with respect to equipment, operations, catalysts, and the overall quality of the final product.

One of the options to steer the bio-oil composition is by controlling the pyrolysis conditions, i.e. reactor temperature and residence time of solids and vapors. Another option is fractionation of the vapors produced.

At present, the steam reforming of natural gas or fossil fuels is the widespread technology for hydrogen production. However, in the long term, hydrogen produced from renewable sources or biomass derivatives is a more promising method.

For steam based pyrolysis of biomass to produce additional hydrogen, fast-heating rate is necessary. Under fast-heating conditions, both drying and pyrolysis occurred in a relative shorter time and thus enhance the interactions between the steam and the intermediate products (volatile and nascent char) to produce more hydrogen. Sweeping gas flow rate greatly affects the H_2 yield. With the decrease of the flow rate the H_2 yield increases, especially for the fast-heating pyrolysis. High reactor temperature favors hydrogen production. Several studies indicate that the presence of steam atmosphere during biomass pyrolysis influences the products distribution, increasing the yield of the liquids [97-101].

It is well known that the Ni-based catalyst on Al_2O_3 support is widely used for steam reforming of natural gas. It is cheap and high in activity for both steam and dry reforming processes. It is found that Ni-based catalysts deactivate easily and quickly due to the coking and sintering problems. Several researchers have reported that the Ceria is an excellent catalyst for several chemical processes, such as steam reforming [102], CO combustion [103,104], water gas shift reaction [105] and reduction of NO [106,107], due to its ability to increase oxygen capacity and excellent redox properties. Overall, the ceria plays a dominant role in improving the reaction efficiency in several processes by taking up oxygen under oxidizing conditions and releasing it under reducing ones.

Further, iron oxide is also beneficial for H_2 production by taking the reaction

$Fe_xO_{y\_1} + H_2O \rightarrow Fe_xO_y + H_2$ and

$(2n + m)Fe_xO_y + C_nH_{2m} \rightarrow (2n + m)Fe_xO_{y\_1} + nCO_2 + mH_2O$

It is also reported that Fe supported on Al_2O_3 could promote the cracking of the coke on the iron oxide particles to increase H_2 yield. Besides, it also could boost the catalyst activity in the steam reforming ($CH_4 + 2H_2O \rightarrow CO_2 + 4H_2$) to maximize the CH_4 conversion to hydrogen and selectivity towards the formation of CO_2 both in the steam reforming and in the water gas shift reaction ($CO + H_2O \rightarrow CO_2 + H_2$).

Calcined dolomite is a low-cost catalyst that was effective for bio-oil deoxygenation through cracking/decomposition, reforming reactions, and interconversion reactions of oxygenates, thus reducing the O/C ratio in the upgraded oil. The relative prevalence of each reaction depended on the operating temperature and time on stream, as these parameters affected the dolomite deactivation. Although dolomite was effective for CO_2 capture, it has low activity for reforming/cracking below 500 °C, and the inter-conversion of oxygenates were the prevailing reactions. Temperatures above 600 °C were required for promoting the bio-oil and ethanol reforming/cracking reactions [108].

While maximizing hydrogen production is the primary goal for steam reforming studies, catalyst stability has been reported to be a major issue, limiting times on stream to around 5 h in some cases even at low space velocities. Carbon deposition has been identified as the primary cause for catalyst deactivation, which leads to compromised hydrogen yields. This effect is even more problematic when reforming whole bio-oils. The formation of carbon deposits is complex because it may arise from a combination of cracking, dehydration, and polymerization reactions. Ni as well as noble metal-based catalysts have been tested in fixed-bed and fluid-bed reactors at elevated temperatures (700-900^{o}C) and steam/carbon (S/C) molar ratios (between 6 and 11) to try to mitigate this issue [109-113].

Regarding the reactor system for closed loop pyrolysis, there are lot comparative research works available in literature. Most of the studies were conducted on either a fluidized bed reactor or a fixed bed reactor or an auger reactor. Fluidized bed reactor was chosen by many of them as it is easy to scale up. Liquid yield in auger reactor was found to be more than that in a fixed bed reactor. There was also remarkable difference in the composition and quality of the bio-oil obtained in both cases [114].

In fluidized bed, the fluidizing gas is sent from the bottom. The residence time is controlled by adjusting the velocity of the fluidizing gas, which holds up the weight of the feed in the reactor. For this purpose, the size of the feed particle must be smaller (less than 2-3mm). To process large quantity of the feed, large size of the reactor is required with high fluidizing gas requirement. There is another type of Fluidized bed called as Circulating Fluidized bed reactor. The major difference is that the heat carrier along with the char and catalyst is sent to a regenerator and burnt to remove coke deposition and efficient circulation of heat carrier. Catalyst is usually loaded in the reactor for upgrading the pyrolysis vapours. The up-gradation is hindered by the solid deposition on the catalyst surface resulting in catalyst deactivation. Also, the mineral deposit de-activates the catalyst permanently. In rotating cone reactor configuration, the feed along with the heat carrier such as sand is injected into the rotating cone which is heated. The pyrolysis is carried by contact of the feed material with the heated walls of the rotated cone. The heat carrier along with char is burnt off in the combustor where the heat carrier is heated partially. The heat carrier is then mixed with the fresh feed and the process is carried out. Rotating cone is a complex design with a rotating cone pyrolyser, combustor and riser reactors [115]. Another class of reactor, ablative reactors operate in a way that is entirely different from the other reactors. The reactor walls are heated to high temperatures and the heat melts the biomass when pressed. The feed melts forming vapors which are then condensed. This process has the advantage of handling feeds with high particle size which can effectively reduce the cost of size reduction. Also there is no gas requirement. However large scale handling of feed and char removal is a major problem [116].

Auger reactors or screw reactors are the simplest design among the reactors discussed. The feed is conveyed by a screw within a tubular reactor which is heated externally. Because of the continuous movement of feed, a smaller reactor can operate large volumes of feed, thus reducing the capital cost [117]. Previous literature reveals potential of pyrolysis of biomass residues in a screw reactor and obtained a bio-oil yield of 51% at 580^{o}C [118].

While maximizing hydrogen production from bio-oil by steam reforming has been the primary goal in the previous studies, catalyst stability has been reported to be a major issue, limiting times on stream to around 5 hr in some cases even at low space velocities [119]. Carbon deposition has been identified as the primary cause for catalyst deactivation, which leads to compromised hydrogen yields. This effect is even more problematic when reforming whole bio-oil. The formation of carbon deposits is complex because it may arise from a combination of cracking, dehydration, and polymerization reactions. Ni as well as noble metal- based catalysts have been tested in fixed-bed and fluid-bed reactors at elevated temperatures (700-900^{o}C) and steam/ carbon (S/C) molar ratios (between 6 and 11) to try to mitigate this issue [120-123]. Unfortunately, the chemical complexity of whole bio-oils does not readily allow for a systematic approach for determining how best to maximize hydrogen productivity while alleviating carbon deposition issues. Catalytic reforming of bio-oil by Ni based catalyst in a fixed bed reactor has been the most researched process. Some of the two staged processes yielded hydrogen yields upto 10wt% based on woody biomass [124,125].

2.3 Literature summary

Gasification of biomass followed by catalytic conversion is considered as another alternative process to steam reforming for hydrogen production, particularly when biomass is abundantly available. In the literature review, the relative advantages and disadvantages of each of the processes were discussed in detail. The objective of the present work was getting highest carbon conversion and gas and hydrogen yields irrespective of the particle size of the biomass. Keeping the larger objective in mind, selection criteria for the appropriate type of biomass gasifier was discussed. The concept of biomass-derived hydrogen is well known and profusely presented by many authors. Although both the processes yield high quality gas, there are many problems such as incomplete conversion of biomass, formation of tar (heavy hydrocarbons and chemicals) and particulate matter etc. Also, this has caused problems in the effluent treatment, especially in case of processes where water is used as a scrubbing medium.

Tar is a complex mixture of condensable hydrocarbons, and it causes problems in application of the product gas. Literature reveals that tar and particulates are removed by two methods: (i) primary tar and particulate reduction in the gasifier (in-situ) and (ii) secondary tar and char reduction outside the gasifier (ex-situ).

In the primary method, the gasifier reactor design is crucial for overall efficiency and product gas quality. This method has advantages like low investment and less maintenance. In the secondary method, hot gas filtration and catalytic conversion are employed. Secondary method has advantages like, better particulate control and better catalyst life, but it is more expensive compared to primary method.

1) Primary biomass conversion

The first stage gasification involves various reactions including pyrolysis or decomposition, gasification or combustion and reduction. As these reactions are diffusion and mass transfer limited, gasification efficiency is dependent on particle size, temperature, steam-to-biomass ratio, residence time, internal solid mixing and heat exchange. Compared to a conventional fixed bed downdraft gasifier producing large amounts of contaminants like char, ash and tar, primarily because of less contact of oxidants or steam with the biomass particles and inept heat and mass transfer, the present system ensures radial mixing of each particle in the reactor because of rotation of the tubular furnace. Also the screw conveyor inside the rector allows better heat and mass transfer within the system. In conventional gasification processes, gasification efficiency gets affected easily by change in the particle size of the feed and residence time. In conventional gasification reactors, poor mass and heat transfer hampers the overall efficiency of the process. In the present work, a rotary tubular furnace consisted of a helical coil conveyor was used, wherein residence time of biomass within the rotary tubular furnace was controlled by the speed of rotation of the tube. Also the use of superheated steam enhances the biomass conversion to lighter components. Autothermal gasification processes have already been investigated by many in the past. The main drawback is that the process is largely diluted with nitrogen. On the other hand, steam gasification is endothermic, and external heating is required to be given, in order to carry out the gasification at specific temperatures. In recent studies, fluidized bed gasifiers are used to gasify the biomass in the presence of steam. The tar and heavy hydrocarbons will pass through a hot catalyst bed at the lower part of the gasifier, which favors reduction of heavy pyrolytic vapor and hydrogen production. In this process, coke will deposit on the surface of the catalyst, and the deactivated catalyst (bed material) will need to be regenerated. The coke deposition shall reduce the life of the catalyst. Hence in the present study, extended char gasification with the help of steam reforming of carbon-char and control of biomass residence time has been realized. The final residual char and ash is then collected in the char collection bottle. The disengaged product vapour was then sent to the secondary fixed bed catalytic converter for maximization of hydrogen.

Secondary catalytic conversion:

Catalytic cracking has provided a big thrust to biomass gasification for converting the heavy pyrolytic vapor into useful gases and hydrocarbons. Recent reviews on upgradation of biomass gasification vapors classify the catalysts into four categories; Ni based catalysts, alkali metal catalysts, dolomite catalysts and mixed metal oxide catalysts. Ni-based catalysts are extensively applied in the petrochemical industry for naphtha and methane reforming. Meanwhile, a wide variety of Ni-based catalysts are commercially available. Especially, some studies showed that nickel based catalysts help in reduction of biochar, heavy pyrolytic vapour to produce more hydrogen. Compared to the un-promoted catalysts, K_2CO_3 impregnated catalyst significantly suppressed the coke deposited on the catalyst surface, but only had a marginal effect on the product selectivity. Out of various catalysts under study, Ni-supported by dolomite catalyst is reviewed to be very high in activity and stability for a long contact time. Moreover, carbon deposition at the Ni/dolomite catalysts surface was negligible. In the present study, the combination of catalysts is chosen such a way that the top bed is filled with catalyst of higher stability and reforming activity and the bottom bed is filled with catalyst of higher selectivity and higher coke deposition resistance.

Also, low temperature pyrolysis of biomass followed by steam reforming of the pyrolysis oil by steam reforming catalysts was also studied. From literature review, it was also revealed that the life of the catalyst increases when a combination of catalysts having higher activity and coke resistance is used. Also, the intrinsic properties of the biomass pyrolysis oil also contribute to the overall efficiency of the process.

Pyrolysis is generally chosen as a recommended process to achieve this goal. This process has gained much attention in recent times as it can produce highest liquid yield upto 75wt%.

This is accomplished at moderate temperatures (~500^{o}C) and short hot vapour residence times (~ 1s) [92]. The liquids from this process are called as pyrolysis oil or bio-oil. Bio-oil has got application as heating fuels in furnaces and boilers or as feedstock for commodity chemicals. The high percentage of Oxygenated compounds in the bio-oil makes it less attractive to become a high calorific value fuel and is prone to corrosion problems and instability. The oxygen content in bio-oil is reported as 35-60% by many researchers [93-95]. But the greatest advantage is its suitability for conversion into an environmentally clean fuel like H_2. Hence the efforts are in the direction of elimination of oxygen from the bio-oil. The entire pyrolysis process consists of three stages: 1. Feed preparation, 2. Closed system pyrolysis and 3. Condensation. High moisture content feed may lead to pyrolysis oil containing more water. Bridgewater [96] suggested that the maximum moisture content in the feed biomass should be 10%.

In overall, considering the advantages and disadvantages of the primary and secondary methods, a combination of the methodologies by integrating a primary gasification stage with a secondary catalytic conversion stage was adopted in the present study. It was envisaged to design a novel 'rotary tubular screw conveyor reactor system' in the primary stage, which enhances the overall heat flux and mass transfer in the reactor, so that the biomass gasification and extended char gasification by excess steam could be targeted in the first stage. In the second stage, conversion of CO and hydrocarbons into H_2 using a second stage 'fixed bed catalytic converter' has been envisioned.

It was also aimed that the process conditions in both the stage could be varied so that pyrolysis of biomass can be carried out in the primary stage (screw conveyor reactor) followed by catalytic conversion (steam reforming and Water Gas Shift reaction) of the pyrolysis oil in the second stage fixed bed reactor, without de-coupling the two stages.

##

CHAPTER-3

Research Methodology

3.1 Chapter Overview

The primary purpose of gasification is to convert chemical energy in the biomass feedstock into chemical energy in syngas. In gasification reactors, biomass undergoes several sequential processes as temperature increases: drying, devolatilization/ pyrolysis, primary combustion/gasification followed by secondary char gasification. There are no clear boundaries dividing these steps and often they overlap. As per reaction thermodynamics, the gasification efficiency is highly dependent on the *heating rate* of biomass in each of these thermal zones. Along with *heating rate, oxidant (oxygen/ steam)-to-biomass ratio* and *biomass particle size* are also important to achieve high gasification efficiency. When heating rate is slow, all the temperature dependant reactions like pyrolysis and gasification take place sequentially and that result in lot of condensable hydrocarbons. On the other hand if heating rate is high, all the thermochemical reactions happen simultaneously including the steam reforming of organic vapour and thus conversion completes in a very short period.

Considering the aforementioned objectives, a novel modified downdraft reactor has been conceptualized and designed. The new configuration matches with a downdraft reactor; but it has an internal screw conveyor to move the biomass along the length and reactor heated externally. The major advantage of this type of a reactor is that residence time and heating rates can be controlled precisely. Also, the system is not limited by feedstock particle size. Unlike coal, biomass contains low ash and hence, the thermochemical conversion rate for biomass is far high and all the reactions take place very fast. Hence it was not required to go for a very complex reactor design. Screw conveyor reactor is one of the less complex reactor systems of its kind for carrying out gasification reactions. The overall reaction rate is affected by intrinsic reaction rate, distribution of lumps, porosity of biomass particles and mass and heat transfer in the biomass particles. The distribution of lumps is taken care by the rotational motion of the reactor. Heat and mass transfer is also very high due to high metallic contact area (low characteristic length) in the screw conveyor reactor and rotation of the screw conveyor.

Although hydrogen production from biomass by thermo-chemical conversion was considered as a promising route, there were only very few who actually practiced the same and demonstrated the process on an end-to-end basis. The present work was focused on the following aspects;

a) to design a plug flow based thermochemical reactor, with very precise feed and residence time control and high heat and mass transfer.
b) to optimize hydrogen production by a two stage process
c) to determine the economics of hydrogen production by thermochemical conversion of agri-waste biomass materials.

In order to accomplish the same, the approach has been depicted as below, which involves design of a new or modified thermo-chemical process scheme and parametric studies.

Steam gasification of biomass to produce hydrogen generates CO_2 during the process of conversion, but it is a carbon neutral system for the whole life cycle if the origin of feedstock biomass is regenerated via photosynthesis in a sustainable way. The advantages envisaged with the current system are;
1) Simple structure, 2) feed flexible, 3) uniform high temperature thermal zones, 4) low tar content, 5) high carbon conversion, 6) high quality syngas, 7) easy control of gaseous components, 8) secondary catalytic conversion to maximize gas yield.

In this chapter, the rationale behind selection of this particular reactor for biomass gasification is elucidated. Also, the mechanistic features such as various critical parts of the reactor and auxiliary equipment that ultimately plays important role in improving reliability of the reactor system and enhancing the carbon conversion and gas yield are discussed in detail. Subsequently, the experimental methodology adopted for systematic evaluation of the reactor set-up followed by parametric study has been explained. Both gasification and pyrolysis studies were carried out using two different type of biomass materials.

Steam blown gasification system is adopted for the present study since steam enhances production of CO and H_2 from biomass and yields high calorific value product gas. Thermodynamic studies using ASPEN Plus was carried out in order to find the theoretical potential of the process in terms of biomass conversion and product gas yield. Parametric studies were aimed at obtaining optimum process conditions; temperature, steam-to-biomass ratio and residence time yielding high biomass conversion and product gas.
Secondary conversion of the product gas and condensable hydrocarbons was carried out in fixed bed catalytic reactor loaded with two types of reforming catalysts varying in Nickel content and support. The catalyst activity and optimum operating conditions were determined

by simulated gas mixture and toluene, before introducing the real feed of product vapour from first stage gasification process.

The same reactor system has been extended to use as a pyrolysis reactor. Pyrolysis reaction conditions were chosen for parametric study. The pyrolytic condensate liquid obtained has been characterized for major constituent compounds. Hydrogen production by steam reforming of pyrolytic liquid has been explored as second stage conversion. Effect of steam reforming conditions for production of hydrogen from pyrolytic liquid has been investigated in detail.

Finally, a continuous mode process has been conceptualized based on the experimental results. The scale-up parameters for scale-up and demonstration have also been determined.

3.2 Introduction

A majority of the biomass gasification systems have been designed and operated based on either fixed bed or fluidized bed concepts. Major indicators leading to efficient and economic application of these technologies are capital and operating costs, fuel flexibility, improved performance in terms of conversion and gas yield, and reduced emissions. Although both the configurations were successful at very large scale in industrial processes, utilization of the same reactor systems in biomass gasification and pyrolysis invites lot of disadvantages.

Disadvantages in fixed bed reactor system are;

- Inefficient heat transfer and mass transfer due to static internals, causing hot spots and irregularity in the product gas flow and quality
- Uncontrolled combustion
- Accumulation of char, ash or clinkers in the system over a period of time leading to low efficiency of operation
- Maintenance is not easy

Disadvantages in fluidized bed reactor system are;

- Reduced conversion due to intimate mixing of both fully and partially gasified biomass
- Very short residence time (< 2 s) , which leads to incomplete carbon conversion
- Losses occurring due to particle entrainment
- Lack of flexibility in handling different types of feed, especially those varying in terms of moisture content, size, shape and density

- Requirement of fluidizing media, which actually reduces the purity of the product gas. Sometimes the gasification media itself was used as fluidizing media; this reduces the flexibility in terms of optimization of both flows.

Thus, the objective of the present work was to design a robust, simple, feed flexible and efficient biomass gasification and pyrolysis system which combines advantages of fluidized bed and fixed bed gasification systems.

Biomass feedstock generally contain high amount of volatile matter. Hence, a sufficiently long residence time in the high temperature reactor is preferred so as to dissociate them into lighter hydrocarbons and syngas before getting entered to downstream processing vessels, otherwise results in high tar content which makes the clean-up very difficult. Also the perfectly mixed atmosphere inside the fluidized bed system induces similar time scales to completely gasified components and partially gasified components. This may not favourably lead to conditions for getting complete conversion.

In case of fluidized bed reactor, the superficial velocity of the gas is very high which leads to entrainment of the biomass particles to downstream vessels. Actually, during biomass gasification considerable size reduction of biomass particles takes place and that leads to entrainment of light particles. As the fluidizing media flow rate is controlled by the biomass feed rate, biomass particle size and density, reduction of fluidizing media velocity to take care of the fines would not be possible. In order to defy the above effects a reactor configuration with a plug flow/ stratified flow behaviour with a sufficiently long residence time in the reactor is envisaged.

On the basis of gasifying medium used, the gasification efficiency varies. Air gasification produces low heating value fuel, due to presence of large quantity of nitrogen in air. Oxygen blown gasification system is attractive in terms of high calorific value of the product gas but requires air separation unit for pure oxygen supply. Steam blown gasification system is efficient in terms of quality of product gas in terms of high calorific value of the product gas but requires external heat source to drive endothermic reactions. Moreover, it is reported that superheated steam aids in reduction of fixed carbon and hydrogen associated with the biomass and thus leads to maximum carbon conversion and product gas yield as compared to any other gasifying media. As the objective of the project was to design an efficient biomass gasification system, steam blown gasification was considered. Thus, the mode of heating chosen was indirect type. The bench scale system made for evaluation is electrically heated. For an industrial system, the heating will have to be done by external inert hot air media, which can be produced by combustion of the char produced from gasification itself in a separate furnace system.

Biomass feed reactivity is dependent on the type of feed used. The reactivity in gasification increases with surface area of the feed. The particle size and porosity of feed have significant effect on the kinetics of gasification. Hence the particle size chosen for the study is in the range 450 micron – 1.45 mm. In case of fluidized bed gasification, the biomass particles having a definite narrow size and density range can only be used. Also, it becomes difficult to fluidize particles with higher moisture content. The ash content in the feed biomass doesn't decide the product gas composition but it does have a profound impact on the practical operation of the gasifier. It is removed along with the biochar in solid form. Ash takes along carbon in the biomass and thus affects the overall conversion.

A new biomass gasification reactor has been designed taking consideration of the above factors. The new design is more leaned towards a downdraft reactor system. The enhancements as compared to downdraft gasification reactor have been depicted in fig. 3.1 to 3.3.

The new biomass gasification system is mainly focused on char conversion and tar elimination to the extent possible, because the main loss from the plant is *carbon in the ash* and *loss of volatiles as tar*. Operation of the reactor at high temperatures in presence of steam has aided extraction of carbon from the ash and tar conversion could be favored by increasing the vapour residence time [126]. All these depend on both the design of the gasifier as well as the operating conditions. Hence, it was required to design a gasification reactor, wherein the biomass feed rate, vapour and solid residence time, reaction temperatures could be controlled efficiently.

Due to the vertical orientation of fixed-bed gasification systems, the thermal zones of the gasifier are fixed and movement of thermal front is static in nature, which sometimes creates clinkers of biomass materials having higher ash content and are responsible for break-down maintenance of the process. *In order to overcome the above limitations, a time adjusted movement of the thermal zones namely, drying, pyrolysis, combustion and reduction using a screw conveyor fitted inside an inclined tubular reactor was envisaged.* The reactor tube was made to rotate externally so that the biomass is moved constantly in to the high temperature thermal zones. The system was designed, developed and successfully tested to prove that the concept is viable. Conventional downdraft gasifiers report inconsistent overall energy efficiency mainly due to wide variation in conversion levels and measurement difficulties inherent in these gasification systems. In case of fluidized beds, it is difficult to measure the exact energy transferred to the fluidizing media. The new configuration of the gasifier was intended to bring in the following benefits.

- An increased and uniform particle residence time in thermal zone as compared to a vertical fixed-bed system or a fluidized bed system.
- Extended char and tar gasification by using steam (for reduction of residual carbon and hydrogen content in the residual char)
- Intimate mixing of biomass particles and oxidant (steam).
- Adequate measurement hardware: flow rates, temperature, pressure, composition
- Uniform thermal zone temperatures along the length of the reactor
- Higher heating value of syngas due to absence of air and any fluidizing media.
- More surface contact between biomass particles and internal metal surface, which results in enhanced heat transfer, thus increasing conversion.
- Due to prolonged exposure to high temperature, this new configuration should produce less tar and particulate matter compared to a downdraft gasifier.
- Ability to process a wide range of feed-stocks having varied moisture content, ash content and size range.
- Less dependence on scale-up parameters.

Fig. 3.1 shows the internal temperature increase along the length of the reactor for the conventional downdraft gasifier and for the new configuration gasifier. This clearly shows the lag in conventional downdraft gasifiers in reaching the gasification temperature. Similarly the mixing pattern in the conventional downdraft is found to be local and does not show a uniform pattern all along and across the gasifier. Both mixing pattern and temperature excursions obtained based on literature data available [127] for a downdraft gasifier is pictorially represented Fig. 3.2. The spiral flow pattern is normally seen for downdraft rector with a rotating grate at the bottom. In the contrary, the mixing pattern and temperature profiles for the new configuration gasifier are very intense and uniform all along the length and are pictorially represented in Fig. 3.3.

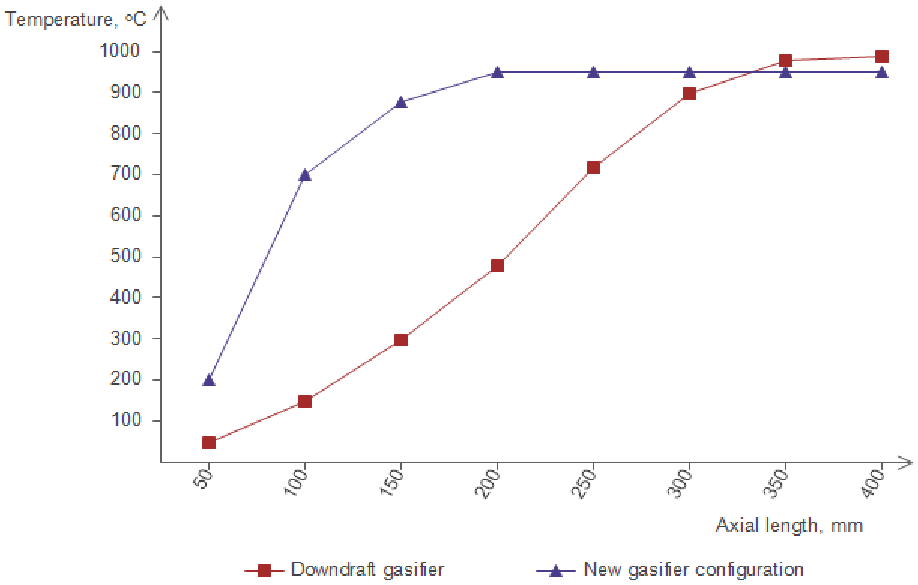

Fig. 3.1 Temperature profile along the axial length of the gasification reactors.

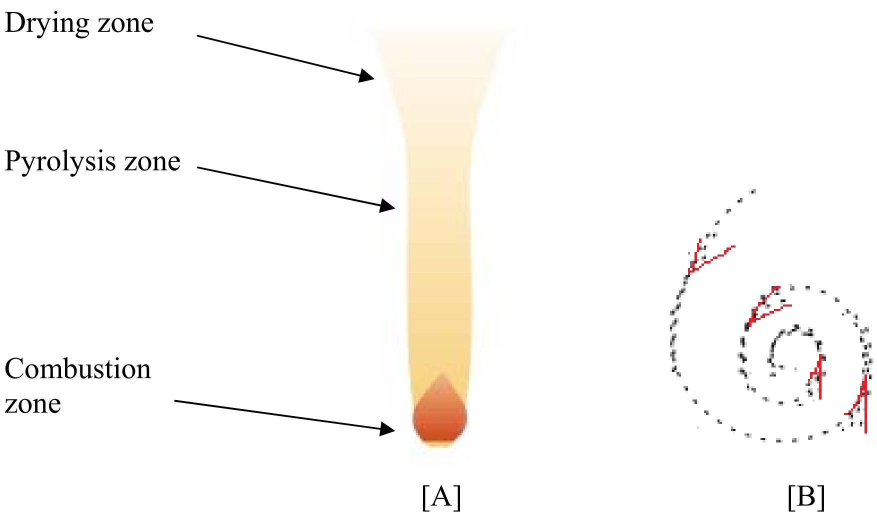

Fig. 3.2 Mixing pattern in downdraft gasification reactor: Pictorial representation [A], Temperature profile view of vertical section [B], mixing pattern (top view)

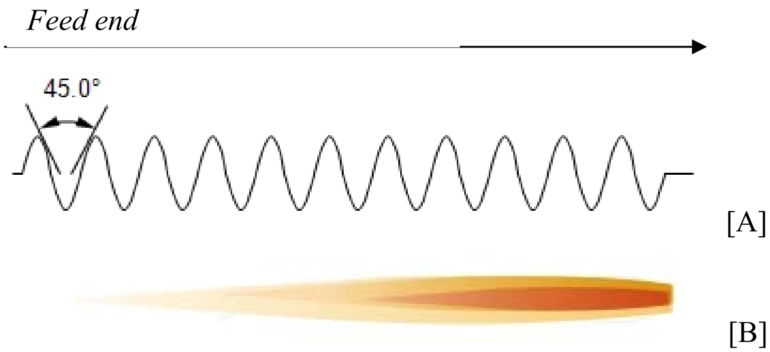

Fig. 3.3 Pictorial representation of mixing pattern in new configuration reactor [A], pictorial representation of temperature profile in new configuration reactor [B]

3.3 Reactor configuration, equipments and procedures

The research scale rotary tubular helical coil gasifier set-up was designed and fabricated for a temperature of 1000°C and pressure of 10 bar(g). All necessary accessories including helical coil conveyor, double valve lock-open type continuous biomass feeding system, vaporizer and feed pump for superheated steam generator, solid char collection bottle, gas liquid separator were also integrated with the experimental system for gasification.

A schematic of the experimental set-up is given below (Fig. 3.4). Demineralized water is pumped at specific flow rate through a vaporizer to generate superheated steam at 300°C. The superheated steam is then fed to the rotary tubular helical coil gasifier. Pulverized biomass is fed to the gasifier from a hopper at specific feed rate adjusted with the help of a double valve arrangement. A helical coil conveyor made of SS 316 was fixed inside the gasifier tube (Fig. 3.6). Rotation of the gasifier tube can be adjusted with the help of a motor. The residence time of the biomass can be varied with the help of motor rpm control. The total heated length of the gasifier is 1540 mm and has inner diameter of 70 mm and outer diameter of 80 mm.

The dimensions of the gasifier tube was chosen based on sizing calculations used for a conventional throat-less downdraft gasifier. The sizing calculations are enclosed in Appendix-II A.

The temperature of the gasifier tube is maintained by means of an electrically heated 3.4 kW external split-furnace heater mounted over the tube in such a way that the tube can rotate freely inside the furnace. The furnace is equipped with three zone control and tilting device for height adjustment. There are three equidistant thermocouples attached to the furnace, which measure the skin temperatures of the tube. The photograph of the reactor set-up is given in Fig. 3.5.

The downstream of the gasifier tube is fitted with a char collection bottle immediately at the end of the gasifier and a gas-liquid separator for separation of liquid and vapor. The separator is equipped with a 7 micron SS fine filter in its dip leg, which can be easily dismantled for removal of solid deposition and clean-up. This helps in separation of fine particles from the product gas under hot condition. The uncondensed gaseous product is driven out by a vacuum pump and the product gas from vacuum pump vent at positive pressure is routed into a second stage fixed bed catalytic reactor for further conversion. A gas sample line is taken into online gas analyzer (IR/TCD analyzer for CO, CO_2 and H_2) and refinery gas analyzer for detailed analysis.

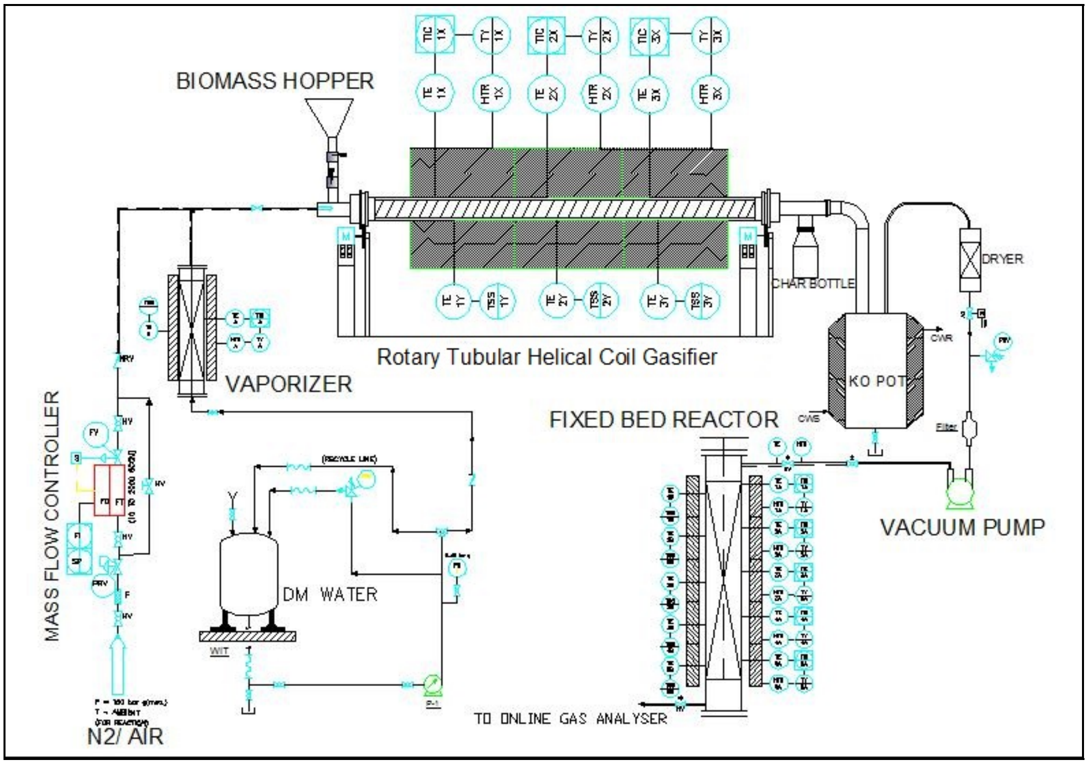

Fig. 3.4 Schematic drawing of the rotary tubular helical coil gasifier experimental set-up

Fig. 3.5 Photograph of the rotary tubular helical coil gasifier experimental set-up

Following are the salient features of the experimental set-up.

Screw conveyor reactor

The screw conveyor reactor consists of the following parts.

- SS reactor tube
- SS coiled conveyor
- 3-zone split furnace (make Nabertherm) with temperature controllers
- Rotary drive
- Rotary joints on both ends
- Jack-tilt arrangement for vertical movement of one side of the furnace

Reactor tube and internals

The reactor tube was made of SS 310 which can go upto 1000°C. The dimensions of the reactor tube are 1540 mm length and 70 mm ID (OD= 80 mm). The SS screw conveyor inside the reactor is a 36 coil-conveyor with a total length of 1540 mm (Fig 3.6). The pitches for each coil is about 4 cm. Tapered ends of the reactor are fitted to the rotary drive assembly. Rotary drive assembly consists of rotary body, sleeves and high temperature o-rings. Once the rotary drives are assembled the tightening of the ends are done with screws. The assembly was then placed on the furnace and the split furnace is locked. The rotary drives were attached with the drive motor. The rotary DC motor drive for the rotation of reactor is fixed on one end of the reactor tube. An RPM controller is also attached with the same so that the RPM can be varied in the range of 5 to 60 during run. Taking the pitch of the conveyor and maximum and minimum RPMs, the reactor can be operated in a range of residence time 0.6 min to 7.2 min. The temperature elements are located on the skin of the reactor tube. Due to complexity of design of rotary joints on both ends of the reactor there are no internal thermocouples. The furnace is equipped with three zone control and tilting device. There are three equidistant thermocouples attached to the furnace, which measure the skin temperatures of the reactor tube. The reactor system has the advantage of easy removal through beltless drive and hinged casing. The furnace is also equipped with an over-temperature limit controller with adjustable cut-out temperature for thermal protection class 2 in accordance with EN60519-2 as temperature limiter to protect the furnace and material.

Fig. 3.6 Photograph of screw conveyor

Biomass and steam feeding system

The biomass is fed through a hopper at 90^o angle to the horizontal reactor. The oxidant superheated steam is supplied axially into the reactor. Intense mixing of biomass and steam was realized by use of a venturi mixing device. When steam is passed through the venture, a low pressure region was created and the biomass is sucked into it and is conveyed very easily through the feed pipe constriction. This also ensures proper mixing of biomass and steam before entering into hot region. Superheated steam is generated by pumping demineralised water through an electrically heated vaporizer followed by a super heater. The steam flow rate is controlled by setting the flow rate on the water feed pump. The biomass feed rate is controlled by loading the hopper with known weight of biomass at fixed intervals. After feeding required quantity of biomass, the hopper is isolated by closing of valve in the feed pipe below the hopper.

Hot gas filtration

The product gas along with residue char exits from the other end of the reactor at very high temperature. The mixture is allowed to pass through a *fin cooling* section in order to reduce the temperature below 300°C. A photograph of the fin cooling mechanism is given in below Fig. 3.7. Following the fin cooling section, there is rotary joint which joins the rotating reactor part and the non-rotating downstream separation part. A char collection bottle is fixed right after the rotary joint, where in the residue char gets collected continuously. This works also as a gas-solid separator. The temperature of this section is kept at above 200°C so that steam doesn't condense and stick to the char collection section. After the char collection bottle, the product gas is cooled by a 2-stage jacketed knock-out pots (gas-liquid separators) having chilled water flow in the jacket. The first knock-out pot is fixed with a fine SS mesh filter (50 micron), which prevents carryover of fine char particles into the gas-liquid separators. The steam along with any condensable hydrocarbon formed from reaction is condensed in the gas-liquid separators. The purified gas flows into a fine fabric filter and then taken to measurement and analysis instruments through a vacuum pump.

Fig. 3.7 Photograph of the fin cooling mechanism

Vacuum control

As there are pressure drops all along the reactor, hot gas filtration system and downstream gas-liquid separators, driving the product gas along with steam is difficult without applying vacuum from the downstream side. Hence, a vacuum pump is used to control vacuum inside the reactor and other equipments so that there is no back flow of product gas. The vacuum also aids in feeding of biomass into the reactor.

The product gas exiting the second knock-out pot is drawn by the vacuum pump and the vacuum discharge is connected to the IR/TCD online analysers for CO, CO_2 and H_2 analysis. Detailed analysis was done by Gas Chromatograph. The gas exiting the analysers are combined and sent to Wet Gas Meter for volumetric gas measurement. The product gas from the vacuum pump vent could be sent to a fixed bed reactor via a demister and a pre-heater section for secondary conversion to produce hydrogen rich gas.

Fixed bed reactor system for secondary conversion

The schematic of the fixed bed reactor used in this reaction system is also shown in Fig.3.1. The reactor is made of Inconel alloy. The reactor was heated externally with a 5-zone tubular furnace, by which the temperatures along the length of the reactor can be varied largely. The total length of the reactor is 90 cm and internal diameter is 20 mm. A thermowell (1/4") consisting of three thermocouples was inserted from the top to exactly determine the bed temperatures at three different locations. The top bed of the reactor is filled with a conventional commercial reforming catalyst and the bottom bed with a commercial CO conversion catalyst. The catalyst details are explained in section 3.7.2. The two catalyst beds were separated by an inert alumina layer. Temperatures of both the catalyst beds are maintained differently by controlled heating of the furnaces.

3.4 Feedstock and Materials

The classification of biomass can be done in four types. They are a) wood and wood wastes like saw dust, b) agricultural crop residues include rice husk, wheat husk etc., c) vegetable oil extraction residues like seed cake, seed husk, seed shell etc., d) cane sugar farm residues. Out of these varieties the agricultural crop residues and vegetable oil extraction residues are the most available ones. Moreover, rice husk and deoiled jatropha cake are available in powder form and in-turn can be used without further grinding. Hence, rice husk and jatropha deoiled cake were chosen as the two types of biomass under the study. Jatropha has one more advantages as this has been considered as non-edible and toxic for living entities. Hence benefit in terms of generating value added products from the jatropha deoiled seed cake contributes to making biodiesel from Jatropha as a profitable proposition. Jatropha deoiled cake residue is obtained after the mechanical extraction of oil from the Jatropha seeds. On extraction, about 30% by weight of seeds is obtained as oil. Remaining 70% left over seed cake is described as waste biomass. Rice husk is one among abundantly available biomass materials in India.

In this work, the feedstock was pulverized into powder and sieved into a specific particle size in the range of 0.20- 0.30 mm. The moisture content of the sample was determined by weight loss measurement after oven drying at 110°C for 24 hrs. The procedure is continued till consistent weight of sample is obtained. The elemental composition of biomass was analyzed by means of CHNO elemental analyzer (Make: Thermo Fisher Scientific; Model: Flash EA 112). Table 3.1 shows the results from elemental composition of rice husk and deoiled Jatropha cake. The density and moisture content of the feed biomass particles are given in table 3.1. A photograph of the pulverized feed biomass is given in fig. 3.8.

Elemental composition of rice husk was determined by CHNO analyser (Table 3.2). Proximate analysis was determined according to ASTM D3172 method, employing the following procedure. Proximate analysis results are given in Table 3.3.

Moisture content (MC): 105 degree C for 2~3 hr using an oven

Volatile content (VC): 925 degree C for 7 min using a furnace

Fixed carbon (FC): 800 degree C for 3hr using a furnace

100 (%) - MC (%) - VC (%) - FC (%) = Ash content (%)

Table 3.1

Physical properties of dried rice husk biomass and Jatropha deoiled cake biomass

Biomass	Density of biomass, gm/cc	Moisture content, wt%
Rice husk	0.431	7
Jatropha deoiled cake	0.820	9

Table 3.2

Elemental composition of dried rice husk biomass and Jatropha deoiled cake biomass

Biomass	% C	% H	% N	% O	% Ash
Rice husk	42.1	5.6	2.2	36.6	13.5
Jatropha deoiled cake	46	5.8	3.0	33.2	12.5

Table 3.3. Proximate analysis of rice husk biomass

Moisture in the biomass = 7%

% Fixed carbon	% volatiles	% Ash
14.5	72	13.5

Fig. 3.8 Images of pulverized biomass samples of jatropha deoiled cake and rice husk

3.5 Product Analysis

The product gas analysis is carried out by means of IR/TCD based online analyser. It has got advantage of fast response for any minor change in composition. The product gas from both the primary gasifier stage as well as the fixed bed reactor were analyzed using rapid online gas analyzer (CO, CO_2 analyzer; make: FUGI; model-ZRJ, measured by non-dispersion infrared method (NDIR); H_2 analyzer; make: FUGI; model-ZAF 3, measured by thermal conductivity technique, which measures change in temperature of a heated platinum wire with change in gas concentration). The detailed component analysis of the gaseous products was carried out by Refinery Gas Analyser (Agilant make: 7890A), equipped with two thermal conductivity detectors (TCDs) with nitrogen as carrier gas for hydrogen detection and helium as the carrier gas for rest of the components. Four packed columns are used for complete analysis. The columns used are 2Ft 20% Sebaconitrile, 30Ft 20% Sebaconitrile, 6Ft Porapak Q 80/100 and 10Ft Molecular Sieve 13X and 4Ft Molecular Sieve 13X were used for the analysis. Oven heating profile was set to increase at a rate of 10 ºC/min, up to temperature of $60^{o}C$. Standard gas mixtures were used for calibration. The tar and coke yields were estimated based on the carbon balance obtained after the experimentation. Each experiment was carried out twice or more in order to ensure repeatability of results and to assure reliable operation of the system.

3.6 Thermodynamic model development

3.6.1 Conceptualization of thermodynamic model in ASPEN Plus

A comprehensive process model was developed for biomass gasification in a screw conveyor reactor using the ASPEN PLUS simulator. The entire steam gasification process is divided into four stages. They are decomposition of the feed, volatile reactions, char gasification, and gas–solid separation.

Decomposition:

The ASPEN PLUS yield reactor- RYIELD, was used to simulate the decomposition of the feed. In RYIELD reactor, biomass is converted into its constituting components including carbon, hydrogen, oxygen, nitrogen and ash, by specifying the yield distribution according to the biomass ultimate analysis.

Volatile Reactions:

The ASPEN PLUS Gibbs reactor- RGIBBS was used for volatile combustion, with the assumption that the volatile reactions are in chemical equilibrium. Biomass consists of mainly C, H, N, O, ash, and moisture. Carbon will partly constitute the gas phase, which takes part in devolatilization, and the remaining carbon comprises part of the solid phase (char) and subsequently results in char gasification. The amount of volatile material can be specified from the biomass proximate analysis. Also, considering the assumption that char contains only carbon and ash, the amount of carbon in the volatile portion can be calculated by deducting the total amount of carbon in char from the total carbon in biomass.

Gasification reactions:

The ASPEN PLUS PLUG FLOW reactor, performs char gasification by using steam reforming and water gas reactions as per given kinetics. The hydrodynamic and kinetic parameters, such as superficial velocity, voidage, and partial pressure of steam are constant in these reactors.

Kinetic parameters used for simulation are given below (Table 3.4). These kinetic parameters were taken from the kinetics data sheet for the respective reforming and shift catalysts supplied by commercial suppliers.

Table 3.4 Kinetic parameters for RPlug reactor in ASPEN Plus simulation

Parameter	Reforming	High temperature CO shift reaction
Pre-exponential factor, k	3.63E-05	8237.01
Exponent, n	0	0
Activation Energy E, MJ/kmol	240.1	43.56
Reference Temperature T_o, K	648	637.1

The stream class selected was *MCINCPCSD,* which includes all mixed conventional streams, conventional solids like carbon, non conventional solids like biomass, ash which can be defined by means of proximate, ultimate analyses, and particle size distribution (PSD).

Heat of combustion was directly calculated from the proximate analysis, ultimate analysis and sulphur analysis. Built-in property models in ASPEN Plus are used for calculating the heat of combustion of BIOMASS as well as the ASH.

In the stream data, the flow rates of biomass and steam were specified. The decomposition is simulated by a RYIELD reactor. For this simulation, the yield distribution is internally calculated by a Calculator block based on the component attributes (proximate analysis, ultimate analysis) for biomass in the feed stream (table 3.2 and 3.3). The calculator block is assigned to run before the RYIELD reactor. The calculator programme is written in FORTRAN. In RYIELD reactor the biomass is broken down into char and elements such as carbon, hydrogen, nitrogen, oxygen and sulphur. ULTANAL is defined as the ultimate analysis on a dry basis. The variable WATER, defined as the percent H2O in the PROXANAL (proximate analysis) for biomass, is used to convert the ultimate analysis to a wet basis. The remaining seven variables (H2O through O2) are defined as the individual component element yields of various species in the RYIELD block. ULT and WATER are then be used to calculate the yield of the individual species in the RYIELD block. The process simulation block diagram is given in Fig. 3.9.

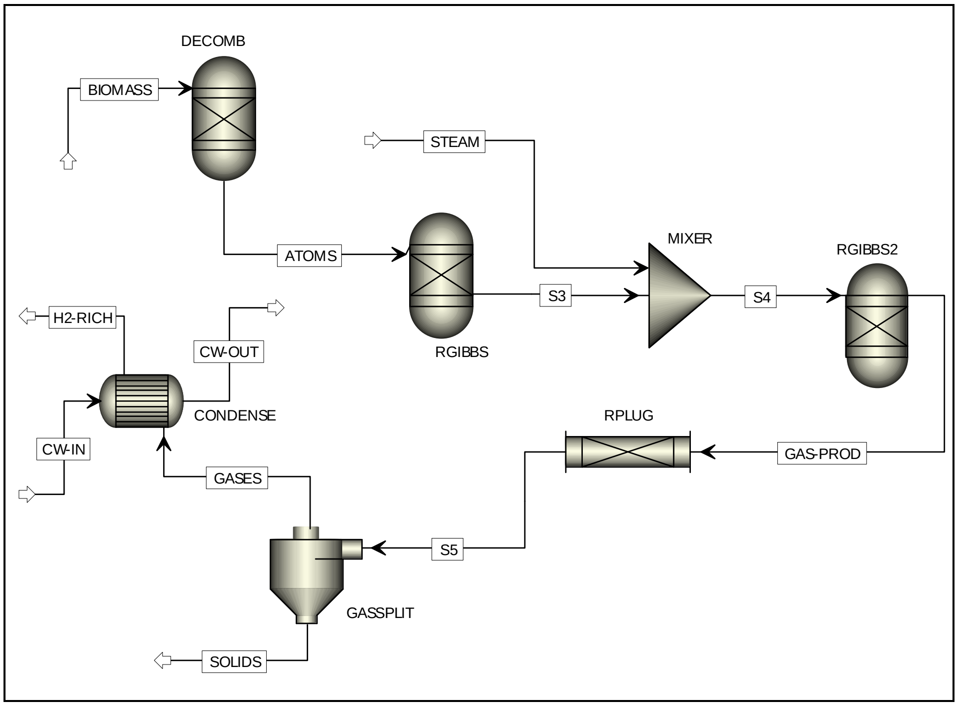

Fig. 3.9 ASPEN Plus simulation block diagram on biomass steam gasification

Table 3.5 Experimental set-up parameters for the simulation

Biomass flow rate	0.25 kg/h – 1 kg/h
Reactor	
Temperature (^{o}C)	700- 900
Pressure (bar)	-0.3 - 2
Reactor heated length	1 metre
Reactor diameter	1.9 cm
Steam	
Temperature (^{o}C)	400
Flow rate (kg/h)	1
Biomass particle size (range)	0.25 mm- 1.45 mm

The FORTRAN programme to convert ultimate and proximate analysis to component yields is given below.

```
C            DENOM IS THE FACTOR TO CONVERT THE ULTIMATE ANALYSIS TO WET BASIS
DENOM = (100 - WATER) / 100
H2O = WATER / 100
ASH = ULT(1) / 100 * DENOM
CARBON = ULT(2) / 100 * DENOM
H2 = ULT(3) / 100 * DENOM
N2 = ULT(4) / 100 * DENOM
SULF = ULT(6) / 100 * DENOM
O2 = ULT(7) / 100 * DENOM
```

The first RGIBBS reactor utilizes Gibbs minimization method to find the equilibrium composition of volatiles and char. All the volatile elements, char are mixed in a MIXER to the second GIBSS reactor. The volatile reactions and gasification reactions take place in the second RGIBBS reactor, wherein the solid char and the volatile components are subjected to steam gasification.

The gasified components from the second RGIBBS reactor along with solid char are subjected to reduction, steam reforming, extended char gasification and Water-Gas-Shift reaction in the RPLUG flow reactor.

3.6.2 Stoichiometric yield determination and model validation

Proximate analysis and ultimate analysis results obtained from lab analysis of rice husk has been used for determining the composition of biomass (Table 3.2, 3.3)

Considering the major elements from the table 3.2, biomass molar formula can be represented as $CH_{1.6}O_{0.65}$. Using steam as oxidizer decomposition of biomass, thermal cracking and reforming reactions take place. The extents of each of these reactions depend on the reaction conditions within the rector. In overall, the following balanced chemical equations can be written.

$CH_{1.6}O_{0.65}N_{0.044} + 0.35\ H_2O \rightarrow CO + 1.15\ H_2 + 0.022\ N_2$ ……..............*(Eq. 3.1)*

$CO + H_2O = CO_2 + H_2$ ……..............*(Eq. 3.2)*

Maximum Hydrogen Yield Potential (MHYP) is defined as the mass of hydrogen which could theoretically be formed by completely reforming the hydrocarbon species derived from unit mass of biomass according to the above equations (1) and (2). For the case of rice husk, the MHYP calculated is 152.33 g/kg (H_2/ moisture-free biomass) or 141.67 g/kgH_2 (raw biomass), where as the innate H_2 content in the biomass is only 56 g/kg (H_2/ moisture-free biomass).

The Gas Yield Potential has been later compared with the Aspen Plus predicted values. The results have been discussed in section 4.2.

3.7 Experimental methodology

3.7.1 Primary gasification stage

The work on the present reactor system was carried out to maximize carbon conversion and tar conversion by control of various process parameters such as temperature, steam-to-biomass ratio and residence time and thereby attain maximum gas yield and lowest residual carbon in biochar.

The experiments are performed in the following sequential manner.

1. Integrity tests
   - Leak check after assembly of all equipment parts
   - Vacuum hold test at -0.5 barg
   - Ramping all the three furnaces at maximum rate of 5°C/min to reach final temperature and ramping of all the steam line heaters, vaporizer and super-heater
   - Rotation test for RPM check and smoothness
   - Dry run with steam to check for any condensation in the feeding and char collection sections
   - Complete condensation before vacuum pump
2. Functionality tests
   - Biomass feeding check and measuring biomass flow rate (manual)
   - Pressure (vacuum) drop in the entire system
   - Attain required steam flow
   - Temperature control and uniformity of temperature profile across the length of the reactors
   - Char collection and fines removal
   - Product gas sampling

After initial system integrity tests and functionality checks, the actual gasification reaction was carried out and the compositions of the product gas and gas yield are determined. Theoretical predictions were matched with the obtained results in order to establish efficiency of the system. Steam to biomass ratio was varied at constant reaction temperature to study the effect of steam. Temperature has the most profound impact on product gas composition since gasification is a temperature controlled reaction.

3. Parametric tests (to study the effect of various parameters on biomass conversion, gas yield and product gas composition)
    - Effect of temperature
    - Effect of steam-to-biomass ratio
    - Effect of residence time

The range of parameters was selected based on the operating ranges available from literature. The operating parameters studied here are given in Table 3.6. The following set of experiments was carried out and the experimental window has been selected based on the initial screening tests. Lower and upper limits for solid residence time could not be stretched beyond 1.8 and 7.2 minutes respectively due to system limitation as the rotating drive frequency could not go beyond the given limits.

Table 3.6 Operating parameters for experiments

Biomass flow rate, kg/h	0.48
Steam-to-biomass ratio (g/g)	0.33, 0.67, 1.0, 1.33, 2.0, 2.5
Temperature,^{o}C	600, 650,700, 725, 750,775 800, 850
Residence time, minutes	1.8, 2.0, 2.4, 3.0, 3.6, …7.2

3.7.2 Secondary conversion of gasifier product in fixed bed reactor

Secondary conversion of the product gases and condensate liquids to hydrogen rich gas is envisaged through a fixed bed reactor.

Steam and dry reforming reactions with the use catalysts have shown to be a promising way to remove the tar components from the gasification product gas at a lower temperature [128-132]. Dolomite and VIII metals such as Ni, Fe, and Co, were the most common catalysts for the tar removing reactions [133-135]. The use of $NiMo/Al_2O_3$ and dolomite could significantly reduce the activation energy of the steam reforming reaction. The decomposition of tar compounds with addition of a dolomite catalyst increased the conversion significantly.

Apart from that, group VIII metals such as Ni, Fe, and Co, Ni/Al_2O_3 and dolomite are supposed to reduce the activation energy of the tar/ ammonia cracking and steam reforming reactions in the gasifier. It was inferred that the higher gas yield was primarily due to combined effect of decarboxylation, depolymerization, thermal cracking reactions and Boudouard reaction. Further experiments on secondary conversion of uncondensed hydrocarbons, CO and condensed hydrocarbons were carried out to obtain a higher hydrogen yield mainly by Water Gas Shift reaction and steam reforming reaction. Similar type experiments on a small scale two stage fixed bed reactor carried out by Waheed et.al., using rice husk as feed, showed maximum hydrogen concentration of 65 vol.% in the product gas [136]. In the present work, a segregated two-catalyst bed reactor system was used to optimize the operating conditions in small scale. Subsequently, combination trials by coupling primary rotary tubular helical coil reactor with secondary fixed bed reactor were carried out.

A lot of work on analysis of biomass gasification based systems has been reported in the literature. The product gas from fixed bed gasification reactors also contains large amounts of contaminants like char, ash and some higher hydrocarbons or tar, primarily due to less contact of oxidants or steam with the biomass particles and inept heat and mass transfer within the system. Xiao et al., reported 15-20% char-carbon production from fixed bed gasification [137]. On the other hand, a fluidized bed reactor system is limited by the size and moisture content of the feed. Also, in fluidized bed reactor system, all the biomass particles are in perfectly mixed equilibrium condition and it would be difficult to compartmentalize the possible reactions, such as decomposition, oxidation and reduction etc., unlike fixed bed configuration. It would also be difficult to control the residence time of the reaction in a fluidized bed reactor system. It has been demonstrated in recent literature on fluidized bed reactor system that it requires to attain a balance between temperature and residence time of reaction when the particle size of the biomass varies over a range [138]. In the rotary tubular helical coil reactor, the residence time can be controlled and devolatilization time for biomass can be increased so as to eliminate the variability in product gas yield due to irregular and large particle sizes.

Model feed for second stage conversion

In order to study the optimum operating conditions of the second stage catalytic reactor, the following gas mixture and model tar compound were used.

1. Gas mixture (CO: 30%, CO_2: 30%, N_2: 15%, H_2: 12.5%, CH_4: 12.5%)
2. Model tar compound (Toluene)

The gas mixture contains all possible gas components from a biomass gasifier. Although the gas mixture doesn't represent the actual product gas composition, it is chosen such that process conditions indicating enhancement of hydrogen yield based on conversion of CH_4 and CO could be optimized based on the known feed gas composition.

Tar is defined as "all organic contaminants with a molecular weight larger than benzene". Here, toluene is chosen as the model tar compound. Also, toluene has got the average molecular size of the hydrocarbon compounds known to be present in the condensate liquid from the primary steam gasification step. The conditions yielding maximum conversion of toluene and minimum CO were considered as optimum for carrying out integrated operation of primary biomass steam gasification and secondary catalytic conversion of gasified vapors.

Catalysts

Commercial steam reforming catalysts, crushed to 4 to 5 mm sieve size are used for secondary conversion.

Catalyst 1: Ni/Al_2O_3 (Catalyst composition: 12 mass% Ni, 65–70 mass% Al_2O_3, 10–14 mass% CaO, and 1.4–1.8 mass% K_2O)

Catalyst 2: Ni/ $CaAl_2O_4$ (Catalyst composition: 23% NiO, supported on Calcium Aluminate, promoted with K_2CO_3).

The catalytic conversion experiments were designed in two parts.

The first set of experiments was conducted in fixed bed catalytic reactor loaded with two types of reforming catalysts to optimize process conditions for conversion of model gasification vapour mixture and heavier (tar) compound to hydrogen rich gas. 100 g each of the two catalysts were loaded. The experimental conditions were given below.

Model gas mixture: 160 ml/min; steam: 1.6 g/min

Model tar compound (toluene): 0.5 g/min and steam 0.2 ml/min (at S/C ratio of 2.0)

Weight hourly space velocity (WHSV) = 1.0 h^{-1} (generally adopted for industrial fixed bed reactors)

Reaction pressure = 1 barg

Temperature of the two catalyst beds were varied in order to obtain optimum CH_4 and CO conversions primarily. The experimental temperature conditions are given in below table 3.7. The bed temperatures are chosen based on the catalyst activity versus temperature data available from literature for both reforming and CO shift catalysts as top and bottom bed catalysts respectively.

Table 3.7 Temperature conditions for experimental studies with segregated catalysts beds in the secondary conversion reactor

Top bed temperature, ^{o}C	Bottom bed temperature, ^{o}C
659	656
657	613
660	553
663	527
662	453
652	430
591	590
591	497

Based on the experimental results, fixed bed reactor conditions were optimized.

The optimized experimental conditions were used for second set of trials (directly coupling the product gas from primary steam gasification stage to fixed bed secondary converter) by coupling both rotary tubular helical coil reactor and the fixed bed reactor.

3.7.3 Pyrolysis of biomass

Fluidized bed, ablative, rotating cone, auger, fixed bed and entrained flow are the various types of reactors used to carry out pyrolysis [139,140]. Fluidized bed reactor, rotating cone and ablative reactors even after demonstrated commercially have poses disadvantages like high energy requirement, high fluidizing gas requirement, complex design, narrow feed size range, high heat carrier requirements and catalyst de-activation [116].

Feasibility of pyrolysis of biomass in the new configuration screw conveyor reactor was studied. The features of the new reactor system such as compact design, control of residence time, flexibility in use of biomass of varied particle size and better separation of solids from vapour makes it suitable for pyrolysis of biomass. Yield of pyrolysis products are also dependant on operating parameters such as temperature, residence time, heating rate and flow rate of sweep gas and steam / biomass ratio [141].

The size of biomass particles should also be minimal so as to ensure uniform biomass heating rate. Here the biomass is ground to less than 2 mm size. The prepared feed is charged into the pyrolysis reactor chamber maintained at the required pyrolysis temperature. The reactor is rotated at highest possible RPM and the vapour generated from the reactor is driven out using vacuum applied through condensation vessels. Effect of sweeping gas like N_2 has been studied by many researchers in the past. It was also reported that higher inert gas flow rates more than an optimum value leads to less bio-oil yield. [142-146].

Also it has been reported by many researchers that a low vapour line temperature ($<400^{o}C$) after pyrolysis leads to secondary condensation reactions which results in low molecular weight compounds and choking of internal surfaces of the vessels. In the present reactor system, the vapor line is maintained at more than $400^{o}C$ followed by abrupt cooling of the reaction vapour to room temperature by jacketed chilled water circulation.

The products obtained are char and ash (solids), pyrolysis-oil also called as bio-oil (liquid), and volatile gases [146, 147]. Reactor configurations also play an important role in the techno-economic feasibility the process.

The distribution of products is highly dependent on the reactor temperature. At lower temperatures the decomposition and primary reactions are initiated thus resulting in high char content. At higher temperatures, secondary reactions and cracking take place resulting in high yield of gaseous products which in turn reduces the bio-oil yield. Thus an intermediate temperature will facilitate optimum primary and secondary reactions to take place, yielding more liquid products [96]. Similar to temperature, residence time is also highly influential in the product distribution. Low residence time favours bio-oil yield as the vapours are quickly removed evading secondary reactions. In contrast, high residence time results in high yield of gases and char. Sweeping gas is used in pyrolysis to provide inert atmosphere and to inhibit secondary reactions. Also, use of sweeping gas is found to reduce the yield of bio-char thus improving the liquid product distribution [148]. Use of steam improves the product quality and also favours vapour yield. Earlier researches on pyrolysis of biomass using steam at various steam-to-biomass ratios and found that increasing the ratio decreases the char yield and increases the gaseous products [149, 150]. Previous researchers have reported that a technique called *Steam Explosion* by which exposure of saturated steam to biomass generally at 5 - 40 barg pressure and 200 - 250^{o}C temperature for some seconds in a sealed vessel followed by sudden depressurization lead to disintegration of biomass structure [150]. Steam explosion causes the breakage of the carbohydrate linkages and also alters the physical properties of lognocellulose, thus changing the behaviour of biomass pyrolysis and product properties. As per the literature, due to steam exposure, degradation of hemicellulose shifted to the low temperature region and became more active. Also, the steam explosion was also reportedly reduced the acid value of the resultant bio-oil from 90 to 64 and viscosity (cSt at 40^{o}C) from 6.5 to 3.9. Decrease of acetic acid content was another advantage envisaged by previous researchers, which lead to stabilization of oils [151]. In the present study, pyrolysis vapour formed is driven out fast by a gas suction pump at the downstream side of the reactor. But the major design related disadvantages of tubular reactors are *low capacity heat exchange and problems with leakage, wear due to presence of rotating parts.* In the present work, the tubular reactor has been designed and fabricated with internal coils such that heat transfer between external heated surface of the reactor and process chamber is high. The downstream of the gasifier tube is fitted with a char collection bottle immediately at the end of the gasifier and a gas-liquid separator pot for separation of liquids from the gasified vapour. In order to address the issues related to wear and tear at the rotary joint, a *gas cooler assembly* fabricated with internal perforations for gas and char passage with external cooling fins has been provided at the end of the tube before the rotary joint [152].

Catalytic reforming of bio-oil by Ni based catalyst in a fixed bed reactor reported fast deactivation of the catalyst. In the current work, the compounds identified to have boiling range above 350^{o}C are eliminated by distillation such that the issues arising out of catalyst deactivation are reduced.

Feedstock

Jatropha seed cake also called as de-oiled cake is the residue obtained after the mechanical extraction of oil from the Jatropha seeds. On extraction, about 30% by weight of seeds is obtained as oil. Remaining 70% left over seed cake is described as waste biomass. The seed cakes are rich in carbon and hydrogen, hence, can be valorized to useful hydrocarbon fuels and chemicals. Biradar et.al., carried out slow pyrolysis of Jatropha seed cake resulting in 18.42 wt % bio-oil yield at a pyrolysis temperature of 500°C [153]. After extraction of oil from the seeds, the cake is oven-dried using a tray drier at 105^{o}C and powdered using jaw crusher and sieved into 200-300 micron size. It was then stored in air-tight plastic containers for subsequent use for pyrolysis experiments. Characterization of Jatropha Curcas de-oiled seed cake was done using ultimate analysis by means of CHNO elemental analyzer (Thermo Fisher Scientific make, Model- Flash EA 112) (Table 3.2).

Experimental

The present work is the first of its kind of work on thermochemical conversion of jatropha deoiled cake followed by catalytic up-gradation. Biomass along with steam of N_2 is fed into the reactor tube maintained at pyrolysis temperatures. The downstream of the reactor tube is fitted with a char collection bottle immediately at the end of the reactor and a vapor-liquid separator pot for separation of liquids from the pyro-vapour. The separator pot is equipped with a fine filter in its dip leg, which can be easily dismantled for removal of solid deposition and clean-up. This helps in separation of fine particles from the product vapour under hot condition. The pyro-vapor is driven out by a gas suction vacuum pump and the product vapour is allowed to condense in a two stage gas-liquid separator.

Catalysts

Ni-based catalysts are extensively applied in the petrochemical industry for naphtha and methane reforming. Meanwhile, a wide variety of Ni-based catalysts are commercially available. Especially, some studies showed that nickel based catalysts help in reduction of biochar, heavy pyrolytic vapour to produce more hydrogen [154]. Compared to the un-promoted catalysts, K_2CO_3 impregnated catalyst significantly suppressed the coke deposited on the catalyst surface, but only had marginal effect on the product selectivity. Earlier reviews on various catalysts suggested Ni supported by dolomite catalyst by its high activity and stability for a long contact time [155, 156]. Moreover, carbon deposition at the Ni/dolomite catalysts surface was negligible. In the present study, the combination of catalysts is chosen such a way that the top bed is filled with catalyst of higher stability and reforming activity and the bottom bed is filled with catalyst of higher selectivity and higher coke deposition resistance. The composition of the catalysts is given under.

Commercial catalysts, crushed to 4 to 5 mm sieve size are used for steam reforming of pyrolysis oil.

Catalyst 1: Ni/Al_2O_3 (Catalyst composition: 12 mass% Ni, 65–70 mass% Al_2O_3, 10–14 mass% CaO, and 1.4–1.8 mass% K_2O)

Catalyst 2: Ni/ $CaAl_2O_4$ (Catalyst composition: 23% NiO, supported on Calcium Aluminate, promoted with K_2CO_3).

3.7.4 Pyrolysis oil upgradation

The uncondensed product gas from gas suction vacuum pump vent at positive pressure is routed into an online gas analyzer (IR/TCD analyzer for CO, CO_2 and H_2) and refinery gas analyzer for detailed analysis. The condensate liquid from the pyrolysis stage is distilled into two fractions, one having boiling point below 100°C to eliminate the water and the second having boiling range above 100°C and below 350°C. The residue left out after the distillation was very little (~ 5 wt%). The sticky residual mass was discarded. The heavier condensate fraction (100- 350°C boiling fraction) was used for steam reforming experiments in the fixed bed reactor.

Experimental set-up for second stage steam- reforming and procedure

The catalysts used in this work are commercial Ni based steam reforming catalysts. The catalyst pellets, (Ni/Al_2O_3 and alkali promoted Ni catalyst) were crushed to 4 to 5 mm sieve size. For optimization of operating conditions for secondary conversion, 100 g each of the crushed catalysts were loaded in the fixed bed reactor in such a way that the commercial Ni/Al catalyst is loaded as top bed and the alkali promoted steam reforming catalyst as bottom bed. Both the beds are separated by one heating zone (178 mm), such that independent control of temperature of both the beds is possible.

The reactor was made of Inconel alloy. The reactor was heated externally with a 5-zone tubular furnace, by which the temperatures along the length of the reactor can be varied largely. The total length of the reactor is 90 cm and internal diameter is 20 mm. A thermowell (1/4”) consisting of three thermocouples was inserted from the top to exactly determine the bed temperatures at three different locations. The two catalyst beds were separated by an inert alumina layer.

The liquid feed section has two sets of feed tanks, pumps and vaporizers. One set of feed tank, pump and vaporizer caters to rotary tubular helical coil reactor and the other set is connected to fixed bed catalytic converter for re-vaporizing the condensate liquid for steam reforming. The second set of experiments was conducted in pilot scale fixed bed catalytic reactor loaded with two types of reforming catalysts to optimize process conditions for conversion of the bio-oil condensate distillate to hydrogen rich gas. 100 g each of the two catalysts were loaded. The experimental conditions were given below in Table 3.8.

Table 3.8 Operating parameters for bio-oil steam reforming

Bio-oil flow rate, g/min	1
Pressure, barg	1
Steam-to-bio-oil ratio, g/g	1.0, 2.0, 3.0
Temperature,^{o}C	600, 650, 700, 750, 800, 850

Product analysis

After the char & condensate separation from the produced vapour, the volumetric flow rate is measured by a wet gas meter. The dry and clean gas was sampled from a slip stream and analysed using rapid online gas analyzer (CO, CO_2 analyzer; make: FUGI; model-ZRJ, measured by non-dispersion infrared method (NDIR); H_2 analyzer; make: FUGI; model-ZAF 3, measured by thermal conductivity technique, which measures change in temperature of a heated platinum wire with change in gas concentration). The detailed component analysis of the gaseous products was determined by Refinery Gas Analyser (Agilant make: 7890A), equipped with two thermal conductivity detectors (TCDs) with nitrogen as carrier gas for hydrogen detection and helium as the carrier gas for rest of the components. Four packed columns are used for complete analysis. The columns used are 2Ft 20% Sebaconitrile, 30Ft 20% Sebaconitrile, 6Ft Porapak Q 80/100 and 10Ft Molecular Sieve 13X and 4Ft Molecular Sieve 13X were used for the analysis. Standard gas mixtures were used for calibration. The liquid and coke yields were estimated based on the mass balance obtained after the experimentation. Each experiment was carried out twice or more in order to ensure repeatability of results and to assure reliable operation of the system. Condensate product analysis was carried out with an Agilent 7000 series triple quadrapole GCMS. The column used is HP5-MS 30 m x 0.25 µm x 0.25 µm with the following program: 2 min at 50^{o}C then ramped at 3^{o}C/min upto 350^{o}C and held at that temperature for 10 min. MS detection was carried out under electron impact (EI) ionization conditions in full scan from m/z 30- 400. Carrier gas used was helium. The left over char and ash collected at the end of the experiment were also analyzed by CHNO analyzer (Thermo Fisher Scientific make, Model- Flash EA 112).

3.8 Conceptualization of continuous process

A continuous mode process was conceptualized based on the lab scale data generated. Operation of this kind of a process in continuous mode could really throw some challenges and that would guide the path for scale-up and possible commercialization of the technology. Hence, the development of the continuous process was divided into four (4) steps. These are, 1) *consistent feeding of biomass* into the reactor without the risk of clogging in the system and efficient mixing of biomass with steam, 2) understanding overall pressure drop in the system and selection of equipments with *minimum pressure drop*, 3) ensuring consistent flow of solid particles by use of an *internal screw in the reactor tube* instead of the externally rotating reactor tube and 4) *coupling or integration* of the gasification reactor and second stage fixed bed reactor for hydrogen maximization.

The consistent feeding of the biomass was realized by use of positive displacement screw feeder in the biomass hopper itself, which displaces biomass into a 2” diameter discharge spout equipped with a sight glass and an automatic choke-sensor which activates on choking of the discharge spout. The discharge spout ends in the main reactor screw conveyor.

Pressure drop in the system is an important parameter for steady state operation of the process as the char, ash or condensate liquid should not be retaining on internal surfaces of equipments leading to pressure drop and eventual shut-down of the unit. The gasification reactor is followed by char gasification and collection vessel at 500^{o}C and a cyclone separator fitted with a fine filter in its discharge. Vapour line from the cyclone to liquid condensate vessel is kept at above 400^{o}C to keep all heavy condensable above the dew point so that there are no sticky materials coating over the internals of the equipments. Condensation is carried out in two stages in two fractional condensate vessels. One vessel is kept at 60°C and the other at room temperature to condense all the unreacted water.

In the lab experiments the flow of biomass through the heated reactor tube was realized by means of a conveyor coil fixed to the internal surface of the tube, and the tube is rotated externally. This has disadvantage of material sticking to the internal surface of the coils, thus it fails to push biomass and char positively through the reactor tube. In the continuous flow reactor, the positive displacement screw rotating inside the reactor tube pushes the biomass material through the reactor. This reduces the left-over material inside the reactor to almost nil.

Coupling of the gasification reactor with the second stage fixed bed reactor was done by means of a vacuum pump driving all the gases and vapour from the gasification stage through the condensate vessels. The un-condensable gas from the vacuum pump vent is routed into the fixed bed reactor along with additional steam to convert hydrocarbons and CO into H_2 and CO_2.

The complete process description along with the process and instrumentation diagram (P&ID) is given in subsequent sections. P&ID of the 3 sections of the plant are given in fig. 3.12- 3.14.

3.8.1 Engineering design of process equipments

Biomass feed hopper, Screw feeder and Screw conveyor reactor

The biomass feed hopper is designed for 10 kg of biomass feed. The screw feeder is fixed inside the hopper horizontally across the biomass hopper such that the biomass flows out of the hopper as per given rotational speed of the screw. The hopper is fitted with a vibrator, which gets on at a certain pre-set frequency once the drive screw motor gets started. The vibrator is set by a timer to come on and off as needed.

Actual feed rates vary in accordance with the material density, material flow characteristics and ambient environmental influences. For accurate results it is important to determine the actual feed rates at different settings of the Variable Frequency Drive. The pictorial view and dimensional data sheet for the biomass feeder, screw conveyor reactor are given below in Fig. 3.10. Screw conveyor reactor consists of the screw conveyor driven from the feeding end by a drive motor. The screw conveyor moves in a tubular reactor of 8 mm ID. The diameter of the reactor was determined considering the mass flow rate of the biomass feed and steam into the reactor. The length of reactor thermal zone and rotation speed range of the screw conveyor are kept the same as 1 metre and 0- 60 rpm respectively. Both skin temperature and internal temperatures are measured at 3 equidistant locations. The design data for the screw reactor, drive motor are also given in Table 3.9. The reactor design basis and sizing calculations are given in Appendix-II B.

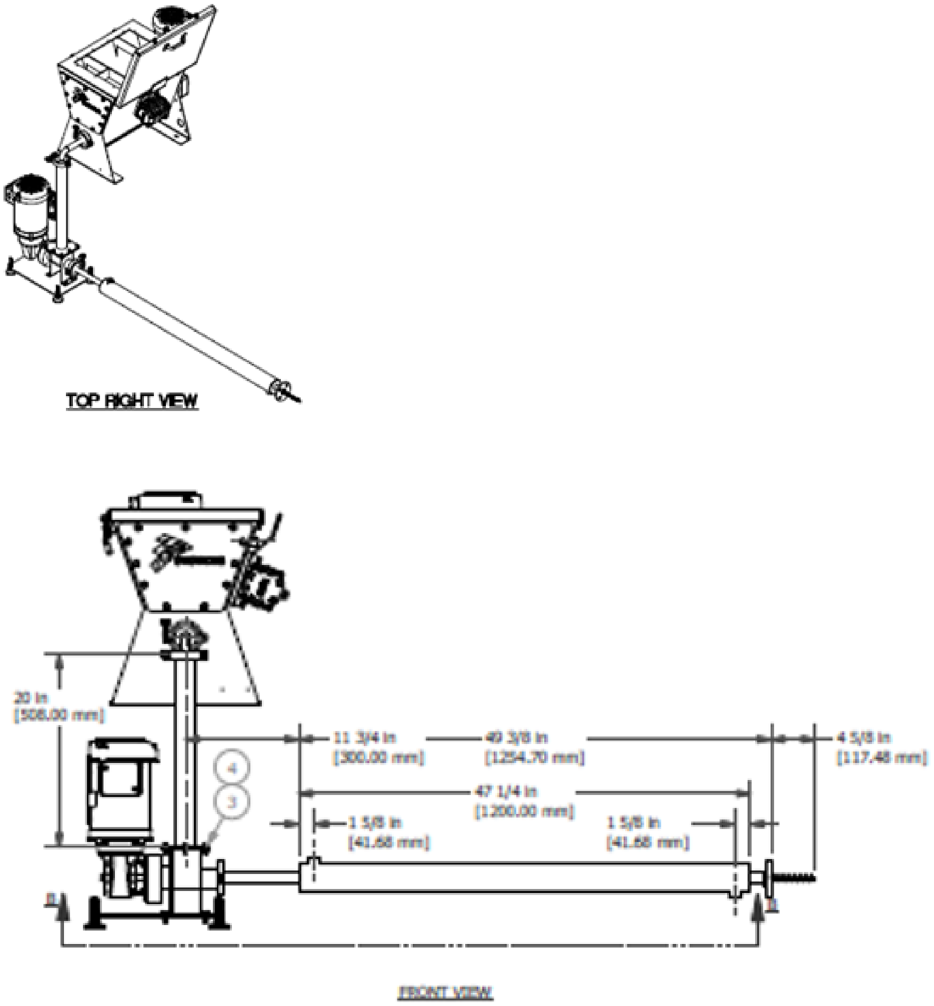

Fig. 3.10 Design drawing and data sheet of screw conveyor reactor system

Gas and steam feed sections:

The screw conveyor drive seal is required to be cooled to keep the seal temperature less than 70°C. Seal cooling has been done by passing nitrogen through the feed spout. Also, H_2 gas is used to activate the secondary conversion catalyst in fixed bed reactor.

Steam is used for both gasification and secondary conversion of product gas. De-mineralized Water (DM Water) is vaporized in sequence by pre-heater, vaporizer and super-heater. Feeding rate is controlled by positive displacement pumps.

Before start of experimentation, the biomass feed rate is manually calibrated for a type of biomass at various frequencies. The biomass feed rate varies from 0.2 kg/h to 2 kg/h depending upon the bulk density of the biomass.

Table 3.9 Specifications of the Biomass Screw feeder and Screw conveyor reactor

Specification	Feed rate @ 50 Hz	Feed rate @ 40 Hz	Feed rate @ 30 Hz	Feed rate @ 20 Hz	Feed rate @ 10 Hz
O.D.	0.6250				
I.D.	0.2500				
Pitch	0.6250				
Motor RPM	1800				
Gear box ratio	20				
Auger RPM	62.25	60	45	30	15
Volumetric flow Rate ft^3/h	0.2785	0.2684	0.2013	0.1342	0.0671

Char gasification and collection vessel

The screw conveyor reactor ends in the extended char gasification reactor-cum-char collector, which serves two purposes. One is collection of the gasified biomass as biochar in the char-collector vessel. In this case, this vessel works as a vapour-solid separator at high temperature above 500°C. Secondly, it's also envisaged that CO_2 present in the product gas reacts with un-reacted carbon in the char to form CO via. Boudard reaction. This vessel can thus be utilized for extended char gasification, which resembles to the reduction section of the downdraft gasifier. There is a double valve arrangement given at the bottom of the vessel in case of char removal. The temperature of the vessel is kept uniform using 3 vertical heaters. The vessel drawing is given in Fig. 3.11.

Cyclone separator

The char carried over from the char gasification vessel is separated out in the cyclone separator. The cyclone separator is designed to settle particles less than 100 micron size. The temperature of the cyclone and the discharge vessels are kept at 450°C so that the vapour is maintained above the tar due point. A fine filter assembly is also provided in the discharge of the cyclone separator to retain fine char particles of diameter less than 25 micron.

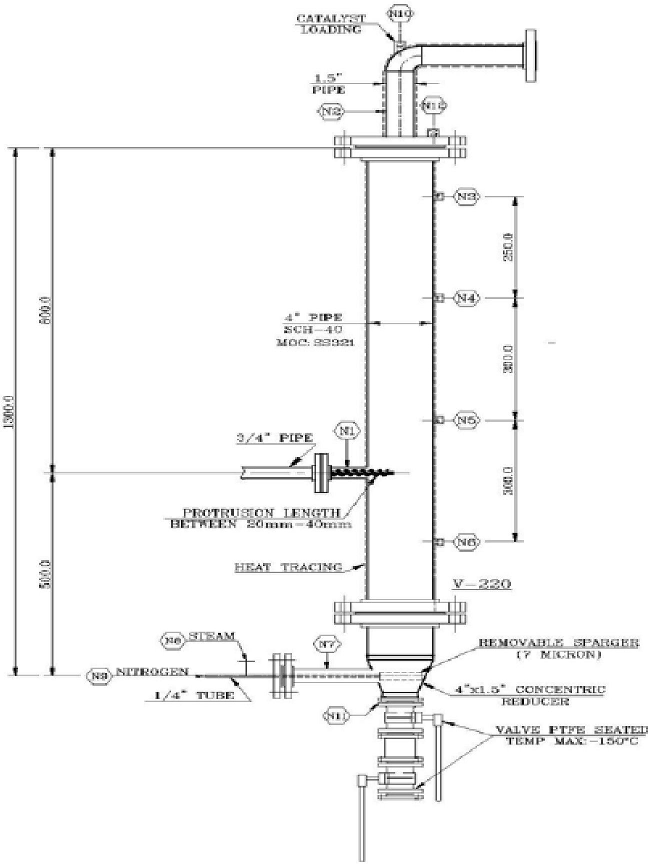

Fig. 3.11 Design drawing for char gasification –cum-collection vessel

Fractional condensate vessels

The vapour from the vessels are condensed from 450°C using two condensate vessels, the vapour line temperature is maintained using a hot oil circulator unit. Hot oil at required temperature is flown through the jacketed vapour line to maintain the vapour temperature. The first stage condensate vessel can also be kept at some cut temperature suitable to separate heavy fractions. Final condensate vessel is kept at room temperature to condense all the liquids.

The pure syngas is then fed to the fixed bed reactor system for secondary conversion.

Fixed bed reactors

The secondary conversion of syngas to H_2 is carried out in a two stage fixed bed reactor. The first stage reactor is filled with commonly used LT reforming catalyst and the second stage reactor is filled with Water Gas Shift Catalyst. The catalyst combinations and their loading details and operating conditions were already mentioned in section 3.7.2.

Volumetric gas flow measurement:

The flow rate of product gas is measured by drum type volumetric gas flow meter. The temperature corrections of the gas flow rate are done to accurately measure the flow rate. The gas samples are tested in IR/TCD detectors followed by Gas Chromatograph for detailed analysis.

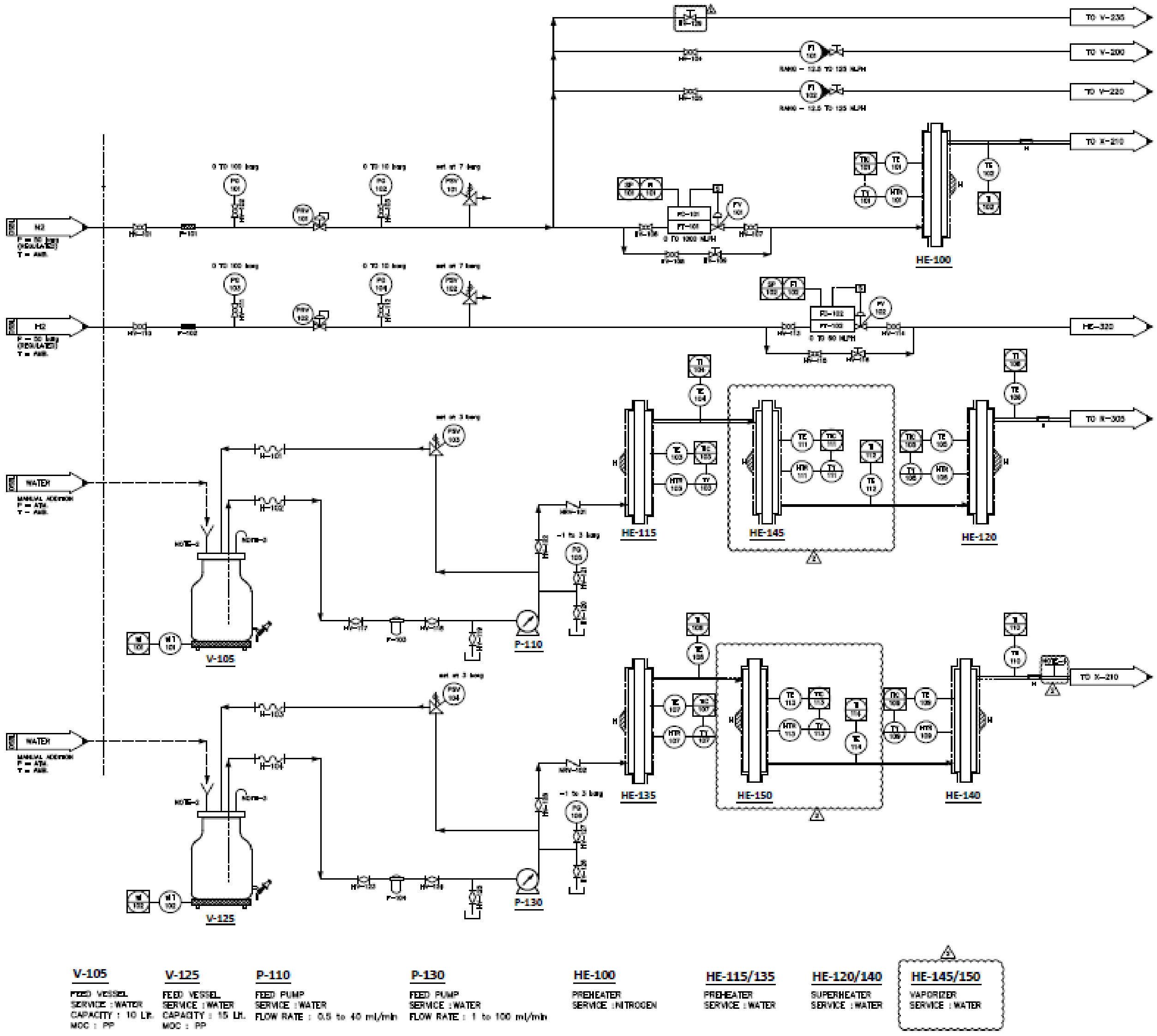

Fig. 3.12 Section-I: P&ID of gas and liquid feed section

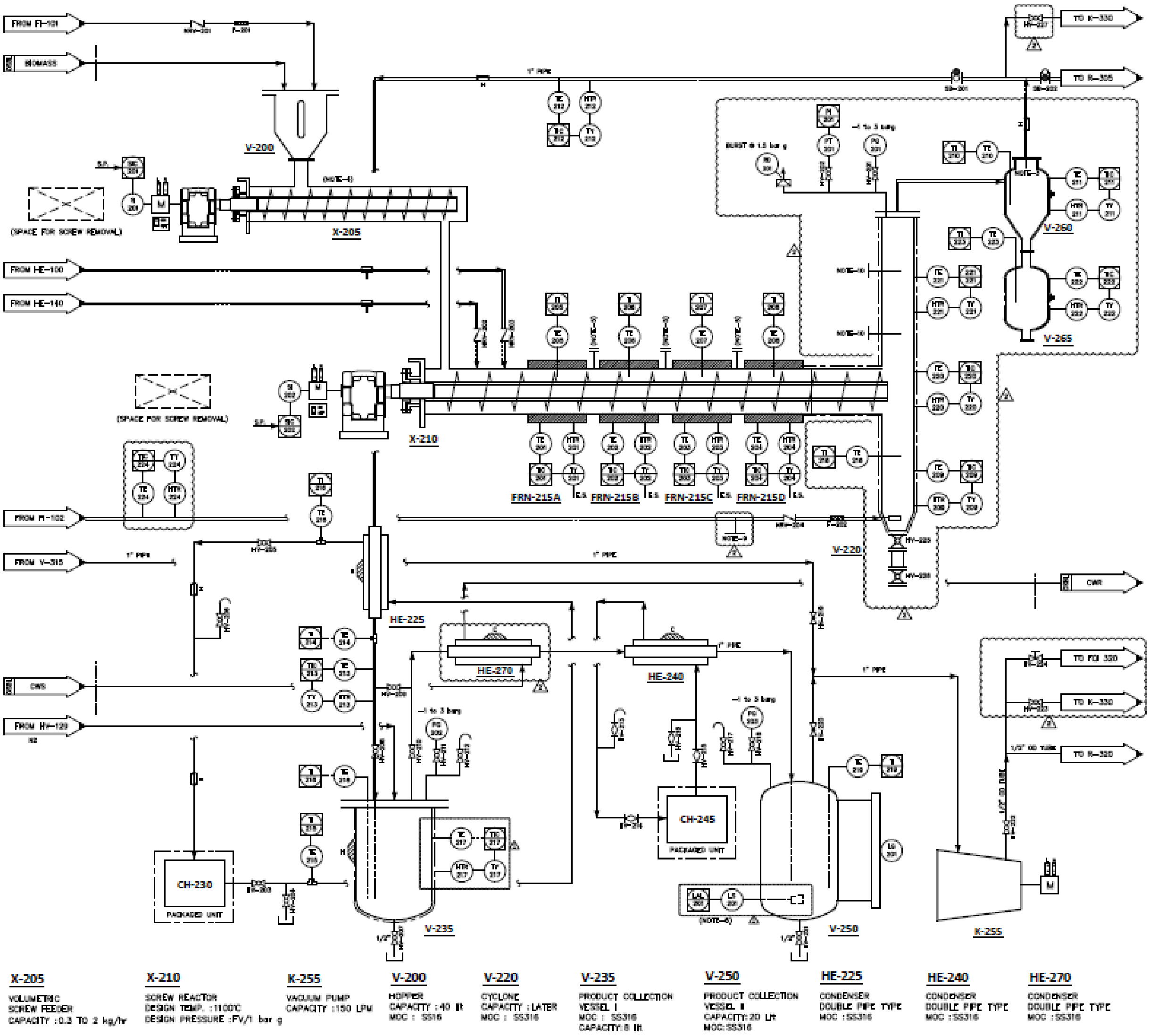

Fig. 3.13 Section- II: P&ID of gasification reactor and gas-solid-liquid separation

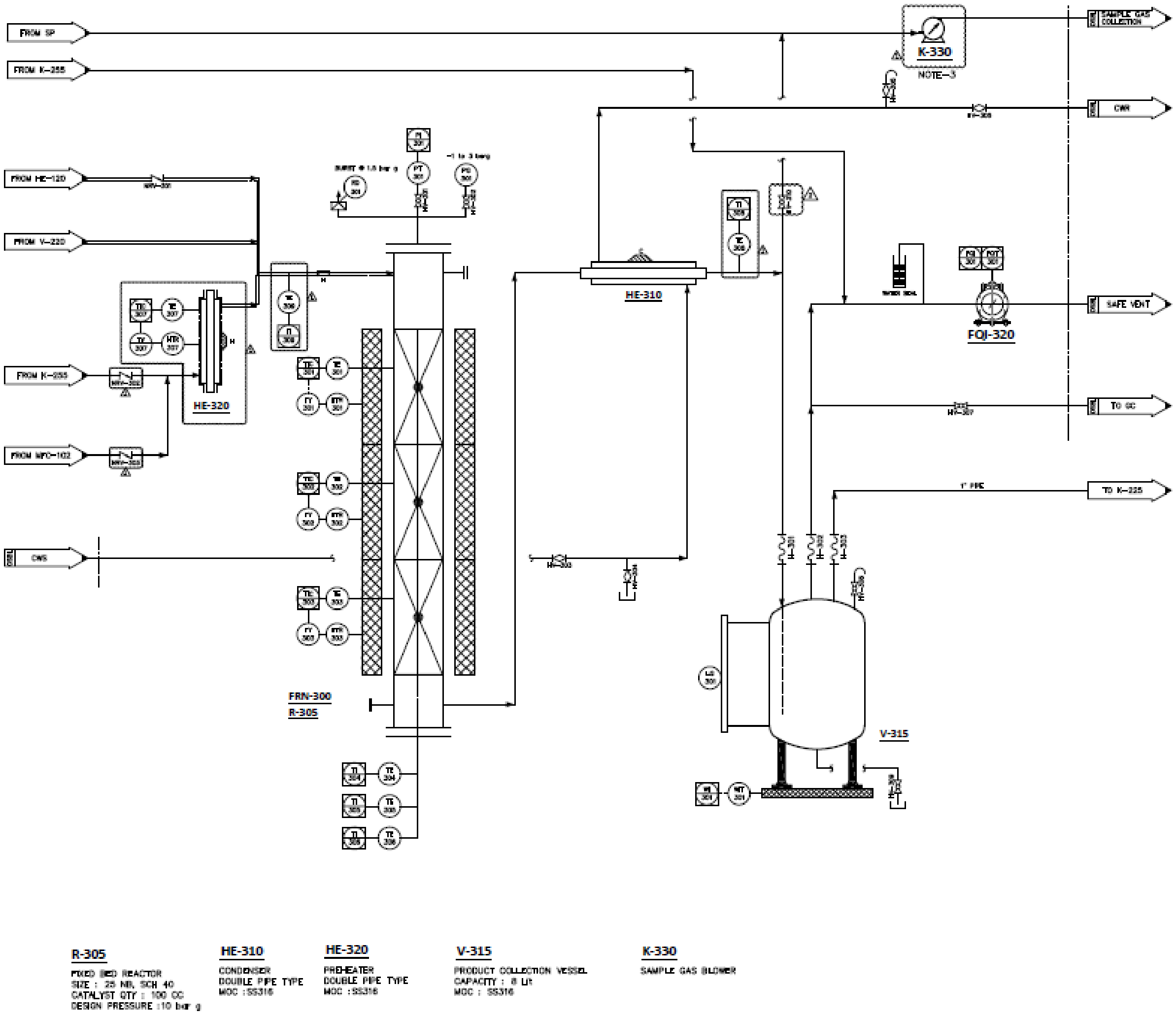

Fig. 3.14 Section-III: P&ID of secondary conversion of un-condensable gases

3.8.2 Key Performance Indicators for scale-up

3.8.2.1 Hydrogen Conversion Efficiency

Hydrogen Conversion Efficiency (HCE) is calculated by the formula;

$(M_{gas} \times X_{H2\ gas})/(M_{feed}\ x\ X_{H2\ feed})x\ 100$

Where, M_{gas} is the mass flow rate of the product gas

$X_{H2\ gas}$ is the mass fraction of hydrogen in the product gas

M_{feed} is the mass flow rate of the feed biomass

$X_{H2\ feed}$ is the mass fraction of hydrogen in the biomass feed

Theoretical hydrogen conversion efficiency calculated from the molecular formula derived from CHNO data, after deducting the moisture content (7 wt%) and ash content (13.5 wt%) from the total mass of biomass fed.

$CH_{1.6}O_{0.65}N_{0.044} + 0.35\ H_2O \rightarrow CO + 1.15H_2$

$CO + H_2O \rightarrow CO_2 + H_2 + 0.022N_2$

Theoretical HCE = **140%**

The HCE is high in case of Steam Methane Reforming (SMR) process, where the theoretical efficiency is as high as 200% as 2 moles of hydrogen each from methane and steam contribute to overall hydrogen production.

Conventional SMR reaction: $CH_4 + 2H_2O \rightarrow CO_2 + 4\ H_2$

But due to limitation in equilibrium conversion (~ 85%) and recovery from purification stage (PSA ~ 85%), the actual efficiency goes down to **145 -150%.**

The actual hydrogen conversion efficiency was calculated from the experimental data and results obtained from gasification reactions. The calculations and results are given in Section 4.5.3.

3.8.2.2 Overall Energy Efficiency

The overall energy efficiency of a process is calculated based on the energy output from a process divided by the total energy input in terms of energy associated with the feed biomass, energy in the feed steam and the total processing energy required for heating and operation of various process equipments like pumps and motors in the process. The simplified formula is given under.

Energy Efficiency = $(M_{gas} \times HHV_{gas}) / (M_{feed}\ x\ HHV_{feed} + H(_{heating + Utilities}) + M_{steam} x\ \Delta H_{steam})$

Where, HHV_{gas} is the Higher Heating Value of the product gas calculated

HHV_{feed} is the Higher Heating Value of feed

$H(_{heating + Utilities})$ is the energy consumption in terms of heating, operation of motors and pumps.

ΔH_{steam} is the enthalpy of the steam

For conventional SMR reaction: $CH_4 + 2H_2O \rightarrow CO_2 + 4H_2$, as per the well established plants of SMR, apart from 1 mole of methane feed, 0.3 mole of methane is required to be burned as fuel for supply of heat to the furnace. Also, the equilibrium conversion of methane is nearly 85% and the purification stage PSA operates at 85% recovery. Hence, the overall energy efficiency of the SMR process is calculated as

(4x0.85x0.85x2.02x141.85)/(1x16x50 + 0.3x16x50) = 79.6%

Conventional SMR process efficiency ~**80%** (mainly due to highest H/C ratio of methane)

The calculated overall energy efficiency of the new *thermal conveyor reactor* has been calculated based on the experimental results and is given in section 4.5.4.

3.9 Summary

Steam gasification is known for unlocking nearly 100% of the elemental carbon and hydrogen in biomass into hydrogen enriched syngas, but the process is hindered by high energy consumption due to high operating temperatures and requirement of superheated steam. Little information was available on the energy efficiency of the process or the cost of producing hydrogen enriched syngas. It is unknown if the cost of production of hydrogen from biomass is comparable to that of steam methane reforming. An attempt has been made to design a unique moderate temperature pyro-gasification reactor system which would be capable to reduce the energy load per unit weight of biomass processed with less sensitivity over the feed specifications.

The reactor system comprises of a rotating tubular reactor externally heated by electrical furnace, integrated with char, liquid condensate collection vessels and secondary conversion reactor at the downstream side.

Biomass and steam are progressively pushed through the reactor by means of a coiled conveyor with the help of continuous rotational mixing. The solid residence time and heating rate can be controlled by means of rpm control of the rotating drive and high temperature furnaces respectively. A thorough explanation of the experimental facilities used for the study has been done. The experimental methodology adopted for further studies has been detailed. The feed stock speciation and their physical properties were elaborated. Reaction products analysis by online gas analyzers and gas chromatograph were discussed. To accomplish the goal of high carbon conversion and hydrogen conversion efficiency with less processing energy requirement, parametric studies with a range of parameters, such as temperature, steam-to-biomass ratio and residence time were conducted and the detailed experimental results are explained in the subsequent chapters. Experiments on steam gasification of rice husk biomass and pyrolysis of deoiled cake of jatropha were conducted in the laboratory scale unit. In the second stage, the gasification product vapour has been catalytically reformed and converted to hydrogen rich gas.

Feasibility of carrying out pyrolysis of biomass in the new reactor system was also envisaged. Pyrolysis liquid condensate was distilled and the fractional condensate has been catalytically reformed and converted to hydrogen rich gas. The design basis for the novel reactor system has been explained in detail. The new reactor system focuses on uniform heat flux, increased biomass residence time, heat and mass transfer within the reactor system. The process has also been designed to operate on a wide range of biomass feedstock varying in moisture, ash content, bulk density and size.

In order to establish the scalability of the process, a continuous mode process has been conceptualized, designed and assembled. The process was demonstrated at 0.5-1 kg/h scale to obtain scale-up parameters. The experimental results are explained in forthcoming section.

* * *

CHAPTER-4

Results and Discussion

4.1 Chapter Overview

For hydrogen production, gasification of biomass is more sustainable and environment friendly as compared to other conventional fossil fuel based processes. Hydrogen is an attractive energy carrier that can be used as an excellent alternative fuel as well as a raw material for several value-added chemical products. In the current work, a screw conveyor reactor with a rotating furnace was designed and made to work as a thermo-chemical reactor. The gasification media used was superheated steam.

The gasification and pyrolysis characteristics of two of the available biomass materials- rice husk and deoiled cake of Jatropha were determined experimentally using superheated steam as oxidant. The un-catalysed steam gasification followed by CO conversion was modelled in ASPEN Plus to determine the thermodynamic hydrogen yield and overall gas yield potential with the system.

The experiments were conducted on an indigenously designed and assembled lab scale reactor system. Initially the reactor system was tested for its integrity and efficiency in terms of carbon conversion and overall gas yield. The preliminary experimental results were compared with the thermodynamic yield data at various operating conditions.

After the system integrity tests, parametric effects of the operating parameters have been studied in the lab scale reactor system. Experiments were performed under both gasification and pyrolysis conditions to assimilate the optimum conditions for both modes of operation. The gasified vapour from the gasification reactor was converted to hydrogen rich gas by steam reforming of the residual hydrocarbons and methane in a fixed bed reactor system.

The overall mass balance for the reactor system was also carried out to confirm consistent performance and reliability of data generated.

The steam gasification process was optimized for operating parameters such as temperature, steam-to-biomass ratio, and residence time and biomass type. After that, secondary conversion of the gasification products into hydrogen rich gas was carried out. Here, the gasification products are fed to a secondary fixed bed reactor containing reforming and CO-shift catalysts. Overall biomass carbon conversion of 90% (and above) was achieved.

Increase in gasifier temperature from 650^{o}C to 750^{o}C improves the decomposition of biomass, thermal cracking and reforming reactions; but further increase in temperature has resulted in decrease in product gas yield, reducing the efficiency. Also, a higher steam- to-biomass ratio of 2.0 has significantly increased the gas yield as it helps Water Gas Shift reaction and reforming of carbonaceous matter and carbon. A residence time greater than 3.0 min resulted in extensive devolatilization, cracking of heavier compounds and intermediates and reduction of carbon into carbon monoxide and hydrogen.

During secondary conversion of gasified vapour in the fixed bed reactor, highly active Ni catalyst and presence of alkali (K) promoter has enhanced the overall performance by improving the hydrogen yield as well as reducing the concentration of CO and lighter hydrocarbons in the product gas. Under optimized conditions, an overall gas yield of 1.46 Nm^3/ kg biomass (~1.9Nm^3/kg moisture-free and ash-free biomass) was obtained. Recent literature on rice husk gasification for hydrogen production in a fixed bed 2-stage catalytic reactor reported a maximum H_2 yield of 64.28 g/kg (H_2/ moisture-free biomass) [136]. Similarly a previous work on steam pyrolysis of rice husk in a moving bed screw conveyor reported H_2 yield of 65 g/kg of biomass [163]. Whereas in the current process, superior hydrogen yield of 70.1 g/kg of neat biomass is obtained.

Followed by steam gasification of rice husk, pyrolysis of deoiled cake of Jatropha was carried out in the laboratory scale unit. The operating conditions varied are temperature and carrier media (steam, nitrogen). Bio-oil yield (pyrolysis condensate) and gas yields were determined. Bio-oil was analyzed for its constituents. In order to find out the total hydrogen yield, the bio-oil was subjected to steam reforming in the secondary fixed bed reactor. H_2 yield from bio-oil reforming was found to be 245 gH_2/ kg bio-oil. Considering the bio-oil yield of 43wt% from biomass, the overall hydrogen yield from the integrated process is 105.35 g/ kg biomass. However, the long duration tests indicated gradual catalyst deactivation, which could be attributed to the high nitrogen and oxygen content in the bio-oil. Hence, scale-up of this process in continuous mode requires periodic regeneration of catalysts by a reactor-swing operation (two reactors operating in parallel; one undergoing reaction while the other undergoing regeneration).

A continuous mode process was conceptualized and the plant was designed, fabricated and assembled based on the laboratory scale steam gasification and pyrolysis data generated. Continuous runs at steady state established efficient biomass conversion upto 90% (on ash-free basis). Scalability parameters such as hydrogen production efficiency and overall energy efficiency were determined.

4.2 Thermodynamic model results

Parametric studies carried out with the help of the developed process model revealed influence of various process parameters such as temperature, steam-to-biomass ratio on biomass conversion and product gas yield. Later on, simulation results were compared with the experimental yields.

The ASPEN Plus model: Steam gasification

For ease of devolatilization modelling, decomposition of biomass into constituent elements using RYILED reactor has been done. The steam gasification model developed in ASPEN Plus consists of two equilibrium stages and one kinetic stage. Devolatilization of biomass and gasification of char and volatiles were represented by two equilibrium RGIBBS reactor models. Pyrolysis reactions to produce volatiles and char were simulated by the first RGIBBS reactor followed by the steam gasification of char and volatiles in second RGIBBS reactor. Subsequent to the initial pyrolysis (devolatilization) and gasification stages, kinetic approach was used to model the extended char gasification, reduction, steam reforming and Water Gas Shift reactions. Both un-catalyzed and catalyzed reactions were assumed to occur at this stage. The kinetic parameters used for simulation are given in table 3.4.

ASPEN Plus Simulation results

The developed ASPEN Plus model was used as the guiding tool for obtaining equilibrium gas yield and hydrogen yield with steam gasification of given biomass. An equilibrium molar yield of 0.07 kmol/h of hydrogen could be obtained from one kg of biomass. This corresponds to 141.4 g H_2/ kg of biomass as against stoichiometric yield of 141.67gH_2/kg calculated as per the theoretical steam gasification reactions. The simulated maximum hydrogen concentration in the product gas obtained from rice husk steam gasification is 67.31%. The biomass conversion was found to be 96% with an overall gas yield of 2.3Nm^3/kg biomass.

The following results were obtained from the simulation (table 4.1).

Table 4.1 Simulation results on product gas yields at various stages of steam gasification process at conditions T= 750°C, Steam-to-Biomass ratio (S/B)= 2.0

	Stage-1 (Gasification) kmol/h	Stage-2 (Water Gas Shift) kmol/h	Gas composition Stage-1 (% vol)	Gas composition Stage-2 (% vol)
H_2	0.022	0.07	28.94	67.31
CO	0.045	0	42.11	0.00
CO_2	0.021	0.033	27.63	31.73
N_2	0.001	0.001	1.32	0.96
O_2	0	0	0.00	0.00
SUM	**0.089**	**0.104**	**100**	**100**

Parametric studies carried out on ASPEN Plus generated the following results.

Here, the parameters varied are temperature and steam-to-biomass ratio. In the first stage, product gas yields from gasification above 750°C temperature showed only marginal increase (Fig 4.1). Similarly, the product gas yields reached a plateau above steam-to-biomass ratio (S/B) of 2.0 (Fig. 4.2). In the second stage conversion, the leftover CO got converted into H_2 and CO_2 almost completely (Fig. 4.3- 4.4). These results indicate the thermodynamic feasibility for a two stage process scheme comprising of steam gasification and catalytic conversion.

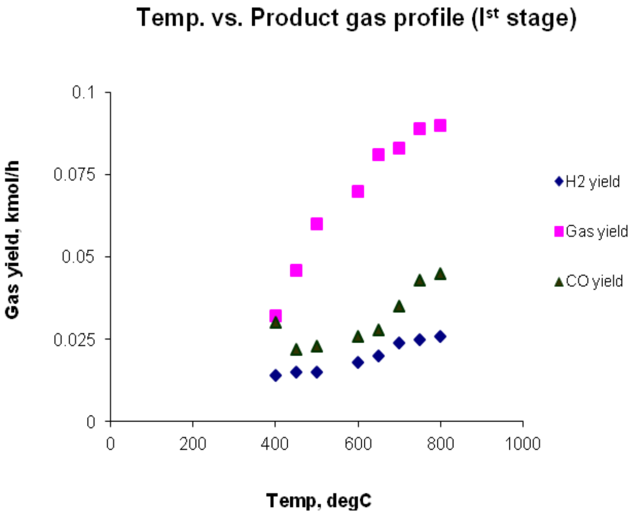

Fig. 4.1 Effect of reaction temperature on the primary stage product gas, CO and H_2 yields.

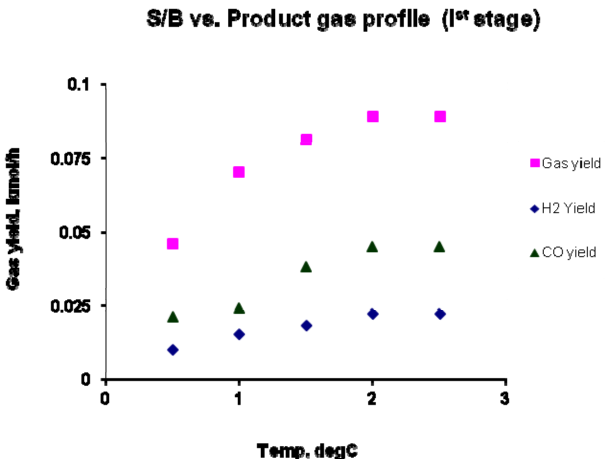

Fig. 4.2 Effect of steam-to-biomass ratio on the primary stage product gas, CO and H_2 yields.

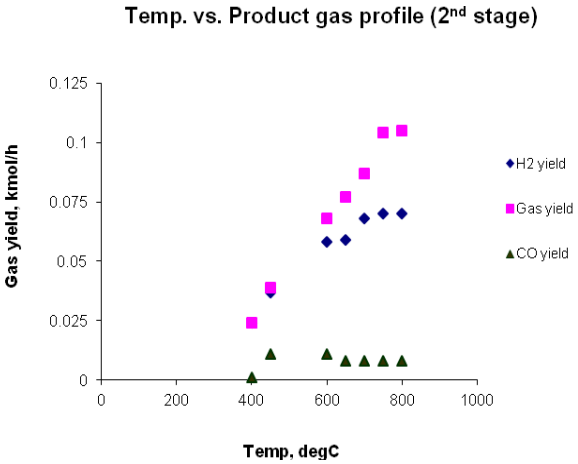

Fig. 4.3 Effect of temperature on the second stage product gas, CO and H_2 yields.

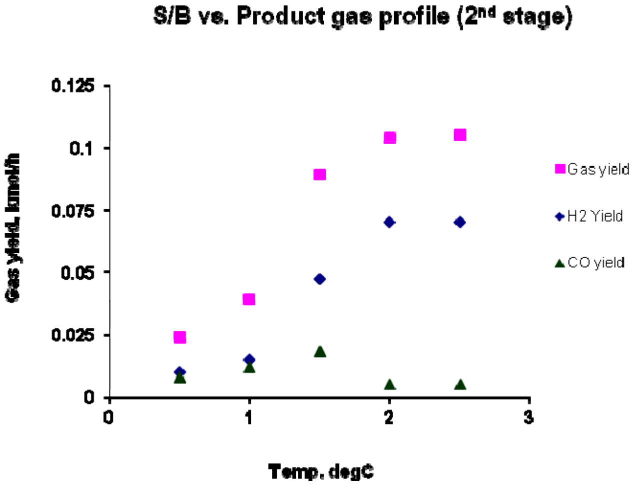

Fig. 4.4 Effect of steam-to-biomass ratio on the second stage product gas, CO and H_2 yields

Results from both ASPEN Plus simulation as well as the stoichiometric calculations yield (refer section 3.6.3) are showing similar yield patterns. This work was mainly used as process optimization tool for obtaining the maximum possible product gas yield and hydrogen concentration in the product gas. The operating parameters and corresponding ranges adopted for experiments are given in table 3.3. Simulation results show that the overall product gas yield and hydrogen concentration that can be achieved are 141.4 g H_2/ kg of biomass and 67.31% respectively.

4.3 Experimental validation

This section attempts to discover the range of operating conditions that maximize thermal conversion of biomass into high calorific value gaseous products. This also validates the simulation results obtained by the model developed in ASPEN Plus.

4.3.1 Effect of gasification temperature

The results from the experiments showed that the biomass conversion is most influenced by temperature of gasification. The effect of temperature was studied from 600°C to 850°C at a biomass residence time of 2.4 minutes and a steam-to-biomass ratio of 2.0 (weight basis). A few literature studies have reported higher temperature, such as 1000°C [157, 158], yield high hydrogen yield and lower tar formation. In the present work, high product gas yields were achieved when temperature was increased in the range of 600 – 850°C. The result is shown in Fig. 4.5. H_2 content reached maximum at 750°C whereas CO content reached maximum at 775°C. Both CO and H_2 started decreasing with further increase in temperature beyond 800°C. A higher reaction temperature favors endothermic reforming and subsequent Water-Gas Shift reaction. But as the temperature increases further, CO_2 concentration started increasing at the expense of CO and H_2. This may be attributed to complete oxidation of CO, H_2 and char (carbon) formed during reaction by the presence of innate oxygen in the biomass and air trapped along with biomass during feeding. This is in full agreement with earlier researches [159]. The product gas yields were also plotted in Nm^3/kg of moisture-free biomass in order to study the effect of gas yields with respect to temperature (Fig. 4.1). There was a marked increase in the gas yield upto 750°C (1.25 Nm^3/kg) due to extensive steam aided gasification of biomass, corresponds to a maximum calorific value of product gas (2169 kCal/Nm^3). Although the product gas yield showed marginal increasing trend above 750°C, majorly due to secondary char gasification, the calorific value of product gas started decreasing beyond 750°C. Left-over char was analyzed for its elemental composition, which contained only 16% carbon. Elemental analysis data for the biochar residue is shown in table 4.2. The low carbon content in the biochar residue obtained at 750°C confirms that gasification reactions approach completion. The data obtained show that in steam gasification, the reaction temperature in the range of 725- 750°C, thermal cracking and steam reforming probably play a significant part. Above 750°C, the char gasification and complete oxidation reactions seems to be the stronghold and more CO_2 is produced and the overall production of valuable product gas (CO and H_2) decreases. The innate oxygen from biomass would also be contributing to the oxidation reactions. The product gases from primary stage (rotary tubular helical coil gasifier) obtained from runs at 750°C and 775°C were analyzed by GC for detailed composition (table 4.3). The corresponding hydrogen yields at an average product gas flow rate of 0.51 Nm^3/h was 18.19 g/ kg (H_2/ moisture- free biomass). On a carbon balance carried out on the basis of weight of biomass charged and weight of biochar residue obtained (19 g Carbon in 120 g biochar residue), carbon conversion efficiency to the tune of 90.5% was obtained.

The calculated Hydrogen Yield Potential taking into account catalytic conversion of hydrocarbons and CO in a secondary reactor is 86.08 g/kg (H_2/ moisture-free biomass) or 80.05 gH_2/kg raw biomass.

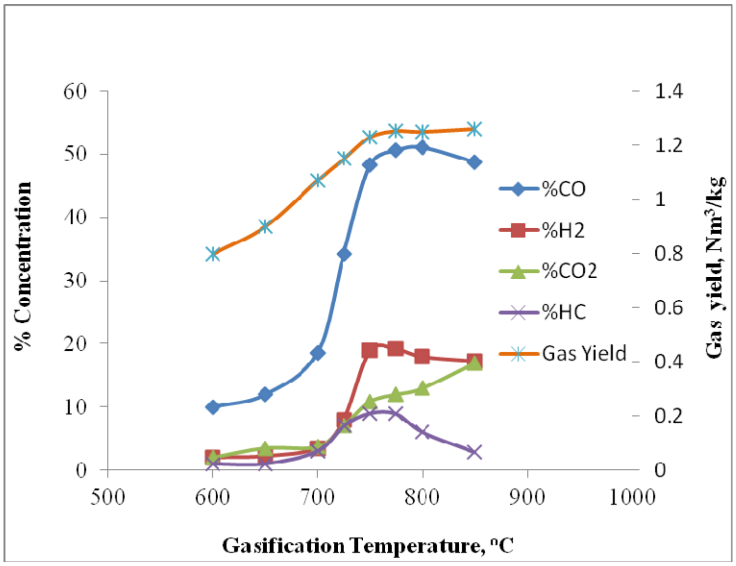

Fig. 4.5 Effect of gasification temperature on gasifier product gas composition and product gas yield (experimental data)

Table 4.2 Elemental composition of biochar residue from gasification of rice husk at different temperatures

Temperature, ^oC	% C	% H	% N	% O	% Ash
650	56	2.1	0.21	7.5	34.19
750	16	1.1	0.17	N.D.	82.73
850	15.5	1.0	0.1	N.D.	83.4

Table 4.3 GC analysis data from experimental runs at 750 ^oC and 775^oC.

Temp. ^oC	% CO	% H_2	% CO_2	% CH_4	% C_2H_6	% C_2H_4	% C_3H_8	% iC_4H_8	% C_4H_{10}	% N_2	% O_2
750	48.4	19	10.9	4.5	2.2	1.4	1.1	0.8	0.7	8.8	0.8
775	49.8	19	12	4	2.0	0.8	0.5	0.3	0.2	10.7	0.7

4.3.2 Effect of steam-to-biomass ratio (S/B)

Steam has a strong influence on overall product gas yield. At temperatures above 600^oC, water is a strong oxidant and reacts with carbonaceous matter and releases CO, CO_2 and H_2. In the present work, six different steam-to- biomass ratios were used (0.33, 0.67, 1.0, 1.33, 2.0 and 2.5). The runs were conducted at gasification temperature of 775^oC and residence time of 3.0 min. At low values of steam-to-biomass ratio, carbon conversion was comparatively less. At higher steam-to-biomass ratios above 1.33, the hydrogen and overall gas yield have increased (Fig. 4.6). At higher steam to biomass ratios, 1.33 to 2.0, product gas yield as well as the hydrogen yield have shown an increasing trend and maximum gas yield of 1.25Nm^3/kg with a net calorific value of product gas 2491 kCal/kg was obtained at steam-to-biomass ratio of 2.0. Above a steam-to-biomass ratio of 2.0, the hydrocarbon content has slightly decreased with an equivalent increase of CO and H_2. This could be attributed to enhanced steam reforming of carbonaceous matter and carbon at the prevailing equilibrium reaction conditions. The product gas from primary stage (rotary tubular helical coil gasifier) under best conditions was analyzed by GC for detailed composition. The GC analysis data is shown in below table 4.4. CHNO analyses of the biochar residue obtained from the experiments showed marked increase in the carbon conversion efficiency of biomass to the tune of 92% with increase in steam-to-biomass ratio (Table 4.5). The corresponding hydrogen yields at an average product gas flow rate of 0.52 Nm^3/h was 18.74 g/kg (H_2/

moisture-free biomass). The calculated Hydrogen Yield Potential taking into account catalytic conversion of residual hydrocarbons and CO in a secondary reactor is 76.81 g/kg (H_2/ moisture-free biomass). The slight decrease in HYP could be attributed to reduced lighter hydrocarbons in the product gas due to high steam-to-biomass ratio.

Table 4.4 GC analysis data from experimental runs at steam-to-biomass ratio of 2 and 2.5

Steam to biomass ratio	% CO	% H_2	% CO_2	% CH_4	% C_2H_6	% C_2H_4	% C_3H_8	% iC_4H_8	% C_4H_{10}	% N_2	% O_2
2.0	48.4	19	10.9	4.6	2.5	2.8	1.8	1.1	0.7	7.4	0.8
2.5	49	19.2	11	4.3	2.5	2.5	1.6	0.3	0.2	8.0	1.4

Table 4.5 Elemental composition of biochar residue from gasification of rice husk at different S/B ratios

Steam-to-Biomass ratio.	% C	% H	% N	% O	% Ash
1.33	16.5	1.4	0.17	N.D.	81.93
2.0	15.7	1.0	0.17	N.D.	83.13
2.5	14.0	0.9	0.1	N.D.	85.0

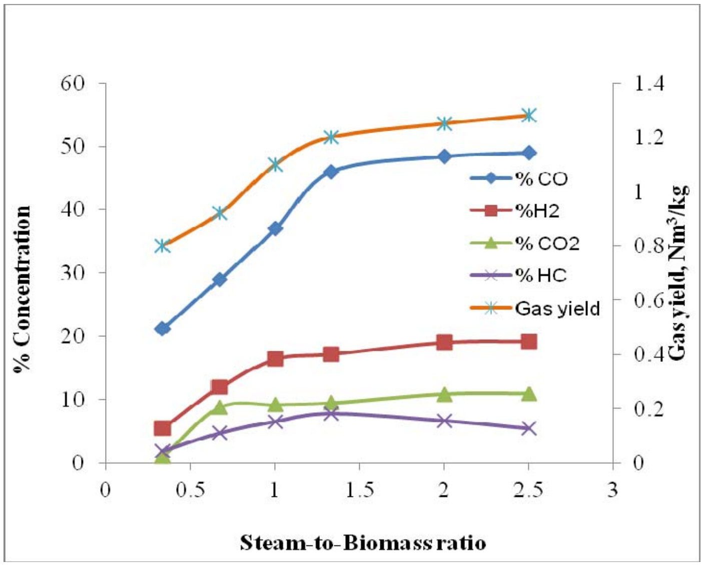

Fig 4.6 Effect of steam-to-biomass ratio on gasifier product gas composition and gas yield (experimental data)

4.3.3 Effect of solid residence time

As per earlier researchers, the effect of biomass residence time on gasification efficiency is actually evident when large biomass particles were used [160-162]. In the present work, biomass particles of very small size, 0.20 to 0.30 mm having large surface area are used. These particles in turn offer high heat and mass transfer. As the residence time of the reactor is controlled externally by the rpm of the rotor, the largest residence time possible with the present experimental set-up was 7.2 min (achieved at 5 rpm of the rotor). Also during the selection of residence time range, it was observed that at residence time beyond 3.6 minute, wetting of biomass by contact with steam was more and hence char particles collected at the end of the run were big in size due to agglomeration and both gas yield and H_2 yield were considerably less. The effect of biomass residence time on product gas composition and gas yield were studied at 750°C and at a steam-to-biomass ratio of 2.5 (Fig. 4.7). The detailed analysis of the gaseous products is enclosed in Table 4.6. The maximum average concentration corresponds to the highest calorific value (2315 kCal/Nm^3) of valuable gases H_2, CO and lighter hydrocarbons obtained at biomass residence time of 3 minute was 19.2%, 49% and 10.5% respectively. The corresponding H_2 yields at an average product gas flow rate of 0.52 Nm^3/h was 18.74 g/kg (H_2/moisture-free biomass). It was observed that the yield of product gas has shown an increasing trend with increase in residence time initially and became constant above a residence time of 3 minute. Also from the graph, it can be concluded that the pyrolysis, decomposition, cracking, steam reforming and Water Gas Shift reactions take place instantaneously, provided the particle size of biomass is very small so that diffusion resistance associated with the particles doesn't affect the overall gasification efficiency. The vapor residence time calculated based on the prevailing conditions and reactor working volume of 5.9 lit was 30 seconds. The biochar collected at the end of the experiments were analyzed for carbon content and the results are reported in table 4.7.

Influence of residence time on carbon conversion and product gas yield is dependent on the type of biomass also. The study was limited to one type of biomass with one particular size range. From table 4.7, it can be observed that an increase in residence time lead to increase of CO_2 content and decrease of hydrocarbon content in the product gas and hence the calorific value of the product gas has gone down beyond a residence time of 3 minute. This could be attributed to extensive steam reforming reactions taking place towards the end of the reactor. The corresponding hydrogen yields at an average product gas flow rate of 0.51 Nm^3/h was

18.19 g/kg (H_2/ moisture-free biomass). The calculated Hydrogen Yield Potential taking into account catalytic conversion of residual hydrocarbons and CO in a secondary reactor is 86.08 g/kg (H_2/ moisture-free biomass).

Table 4.6 GC analysis data from experimental runs at residence time of 3 min and 3.6 min

Residence time, min	% CO	% H_2	% CO_2	% CH_4	% C_2H_6	% C_2H_4	% C_3H_8	% iC_4H_8	% C_4H_{10}	% N_2	% O_2
3.0	49	19.2	10.9	4.2	2.6	1.8	1.2	1.1	0.7	8.5	0.8
3.6	48.6	18.2	13.5	4.1	1.2	1.6	1.9	0.8	0.4	9	0.7

Table 4.7 Elemental composition of biochar residue from gasification of rice husk at different residence times

Residence time, min.	% C	% H	% N	% O	% Ash
2.4	16	1.1	0.17	N.D.	82.73
3.0	15.1	1.0	0.17	N.D.	83.73
3.6	14.6	0.9	0.1	N.D.	84.4

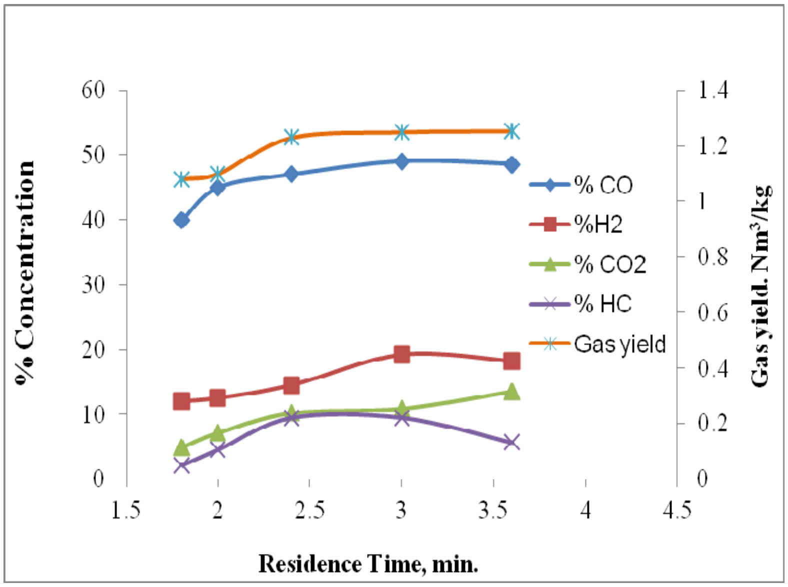

Fig. 4.7 Effect of residence time on gasifier product gas composition and product gas yield (experimental data)

4.3.4 *Gasification experimental summary*

An accurate mass balance was carried out with the help of wet gas metering mechanism. The char and liquid condensates were weighed at the end of the experiments. The mass balance is obtained upto 97.7%. The mass balance is given in table 4.8.

The steam gasification run data and the mass balance closure shows a carbon conversion efficiency of 92%, considering the fact that the carbon in the biomass is lost only through biochar residue.

Although the reactor resembles to plug flow type, each particle in the reactor is subjected to move radially due to the rotation of the tubular furnace and this enhances the heat and mass transfer within the system. Critical process parameters such as temperature, steam-to-biomass ratio and residence time have been studied with the purpose to get the optimum conditions for maximum product gas yield and hydrogen yield. At optimum conditions, the highest product gas yield was 1.252 Nm^3/ kg moisture-free biomass and the Hydrogen Yield Potential calculated based on the results was 86.08 g/kg (moisture-free biomass) compared to a Maximum Hydrogen Yield Potential (MHYP) of 152.33 g/kg (H_2/ moisture-free biomass) and an inherent H_2 content of 56 g/kg moisture-free biomass. This shows enhanced conversion of biomass to H_2 by superheated steam in the reactor system as compared to fixed bed or other gasification configurations reported in literature for hydrogen production. Recent literature [136] on rice husk gasification for hydrogen production in a fixed bed 2 stage catalytic reactor reported a maximum H_2 yield of 64.28 g/kg (H_2/ moisture-free biomass). Similarly a previous work on steam pyrolysis of rice husk in a moving bed screw conveyor reported H_2 yield of 65 g/kg of biomass [163].

Table 4.8 Mass Balance from steam gasification of rice husk biomass

Biomass flow rate, kg/h	0.48
Steam flow rate, kg/h	0.96
Total mass flow of feed, kg/h	**1.44**
Product gas flow rate, Nm^3/h	0.52
Product gas composition	H_2: 19-20% ; CO: 48-50%; CO_2: 10-

	12%; N_2: 7-8%; CH_4:4-5% ; C_2+C_3+C_4: 7-8%: O_2: 0-1%
Biochar residue collected (including solid hold-up inside reactor), kg/h	0.120
Total condensate liquid, kg/h	0.710
Total gas flowing out, kg/h	0.570
Total mass flow out, kg/h	**1.400**
Carbon in the biochar residue, g	16.8
Carbon conversion efficiency, %	92

Water content in the condensate liquid is found to be 87%. A GC-MS analysis data of the condensate liquid is given in table 4.9. The approach in the current work was to carry out extensive biomass and char gasification in the primary gasification stage and enhance overall efficiency of the process by revaporizing and converting the condensate liquid and gaseous hydrocarbons through a fixed bed catalytic converter.

Table 4.9 GCMS analysis data of the organic portion of the condensate from rice husk gasification

Components	Wt%
Dimethylamine	13.4
Ammonium acetate	34.5
Ethyl acetate	18.7
Phenol	9.48
6-nonynoic acid	1.50
Butanoic acid,3-methyl-	01.33
Hexanoic acid,2-methyl-	0.58

2-Furanmethanol	5.63
Mequinol	4.51
2,2-Dimethyl-3-vinyl-bicyclo[2,2,1]Heptane	1.45
d-Glycero-d-ido-heptose	0.89
17-Octadecynoic acid	0.70
5,7-Octadien-3-ol,2,4,4,7-tetramethyl-,(E)-	0.47
Ethanol,2-nitro-,propionate	2.80
2-Isobutyl-3-methylpyrazine	1.355
N-.alpha.,N-.omega,-Di-cbz-L-arginine	0.58
Phenol,3-methyl-	0.40
P-cresol	0.75
11-(2-Cyclopenten-1-yl)undecanoicacid,(+)-	0.77

4.3.5 *Secondary conversion of gasification products*

Secondary fixed bed conversion of lighter residual hydrocarbons was studied by using a model feed with composition as mentioned in section 3.7.2. At high top bed temperature such as 660^{o}C, CH_4 conversion was predominant, which resulted in very low residual CH_4 concentration in the product gas. Due to low activity of reforming catalyst at low temperatures conversion of CH_4 got reduced drastically to 49% when top bed temperature was decreased to 590^{o}C. This effect is also substantiated by the catalyst activity profile with respect to reaction temperatures for Ni based catalysts [164].

The bottom bed catalyst is composed of Water Gas Shift catalyst which aid conversion of CO into CO_2 and H_2 in presence of steam. Due to slightly exothermic nature of this reaction, when temperature of the bottom bed was decreased from 656^{o}C to 430^{o}C, CO conversion has increased from 75% to 99%.

Although very minimal in quantity, in order to study mitigation of tar and heavy hydrocarbons generated from primary gasification stage, secondary fixed bed conversion with model feed Toluene was carried out. Toluene is chosen as the model compound by many researchers in past [165-167]. In order to investigate secondary conversion of tar compounds, independent reactions with toluene have been conducted under various top bed and bottom bed temperatures. The flow rate of Toluene was 0.5 g/min and the steam/C ratio was 2.0. Result on influence of temperature on % conversion is shown in Table 4.10. With the increase of temperature at the top bed, the CO and H_2 concentrations increased, whereas that of CO_2 and CH_4 concentrations decreased in the product gas. A decrease in temperature in the lower bed has resulted in enhanced CO conversion which resulted in an outlet CO concentration of 0.1%. Based on the experiments, a top zone temperature of 655-660°C and a bottom zone temperature of 430-450°C found as optimum conditions for desired H_2 yield and CO conversion. Conversion of toluene and CO conversion achieved 75% and 98% respectively under optimized top bed and bottom bed temperatures. All the experiments were carried out twice to ensure reproducibility of results.

Table 4.10 Optimized temperatures for segregated catalyst beds in the secondary conversion reactor

Top bed temperature, °C	Bottom bed temperature, °C	% CH_4 conversion	% CO Conversion	% Toluene conversion
659	656	76	75	72
657	613	74	84	70
660	553	74	85	72
663	527	74	86	72
662	453	75	98	72
652	430	73	99	72
591	590	49	83	53
591	497	48	92	48

4.3.6 Determination of gas yield from secondary conversion of biomass

Based on the results obtained from the experiments conducted with simulated gas mixtures and model tar compound- toluene, conditions for carrying out secondary conversion of biomass gasification vapors were identified. The conditions adopted in the secondary conversion reactor are, temperature of 660°C at top to 450°C at the bottom and the Steam/CO molar ratio of 2.0. The hot vapor stream from the gasification reactor is inducted into the secondary conversion reactor. CO content in the product gas was reduced to about 0.7 mol%. The Water Gas Shift reaction is favored at relatively low temperature for steady formation of H_2. In the combination trials, by taking gasifier and the second stage catalytic converter in series, product gas contained 0.7% CO, 53% H_2, 40% CO_2, approx. 4-5% nitrogen and its oxides and 2% CH_4 and lighter hydrocarbons. An accurate mass balance was carried out with the help of wet gas metering mechanism (Table 4.11). The mass balance is obtained upto 98% taking into consideration of the material hold-up in the system. The losses are again attributed to the char carryover from char collector and fines deposition in downstream separators. GCMS analysis of the condensate liquid collected after secondary conversion showed no presence of hydrocarbons. At optimum conditions, the highest product gas yield obtained 1.46 Nm^3/ kg of moisture-free biomass at a hydrogen yield of 70.1 g/kg biomass and carbon conversion efficiency of 92%.

Table 4.11 Final mass balance

Biomass flow rate, kg/h	0.48
Steam flow rate, kg/h	0.96
Total mass flow of feed, kg/h	**1.44**
Product gas flow rate, Nm^3/h	0.70
Product gas composition	H_2: 53% ; CO: 0.7%; CO_2: 40%; N_2: 4%; CH_4:2% ; C_2+C_3: 0.3%
Mass flow of product gas, kg/h (A)	0.62
Hydrogen yield, g/kg biomass	70.1
Residue (char and ash) collected, kg/h (B)	0.120
Total condensate liquid, kg/h (C)	0.72
Total mass flow out, kg/h	**1.44**

4.3.7 Experimental summary: Two stage steam gasification of biomass

Steam gasification experiments have been carried out in a rotary tubular helical coil gasifier with rice husk as biomass feed. In order to eliminate the causes that hinder development of rotary tubular reactors for large scale steam gasification of biomass, a novel concept of integrating the rotary tubular reactor with a coiled-conveyor inside was adopted. This has not only helped in achieving high degree of heat transfer but also enhanced mass transfer among biomass particles and vapours. This combines the advantages of both fixed bed and fluidized bed configurations. The plug flow configuration of the reactor enhances char reforming and Water Gas Shift reactions, which in-turn increases the overall gas yield. Although the reactor resembles to plug flow type, each particle in the reactor is subjected to move radially due to the rotation of the tubular furnace and this enhances the heat and mass transfer within the system. In the gasification stage, critical process parameters such as temperature, steam-to-biomass ratio and residence time have been studied with the purpose to get the optimum conditions for maximum biomass conversion, product gas yield and calorific value of gas. Hydrogen-rich gas production from the gasified vapors was also achieved by appropriate process integration with a second stage fixed bed catalytic converter. The approach of conducting extended char gasification in the primary steam gasification step and enhance overall conversion by catalytically converting the lighter hydrocarbons and permanent fuel gases separately in a fixed bed catalytic reactor was found to be superior as compared to other two-stage processes reported in literature, in terms of overall carbon conversion efficiency (92%) and hydrogen yield (70.1 g/kg biomass).

4.4 Pyrolysis of biomass

Pyrolysis is one of the thermochemical processes, to convert biomass into liquids with gases and char at moderate temperatures from 400- 600^{o}C. In the present work, pyrolysis of jatropha seed cake was studied in the screw conveyor reactor designed and developed in-house. The effect of temperature vs. steam and nitrogen was studied in detail to analyze the distribution of pyrolysis products. Further, the effect of steam-to-biomass ratio was also studied in order to check the enhancement in % conversion and H_2 yield.

4.4.1 Effect of steam vs. nitrogen on distribution of pyrolysis products with temperature

A comparative study between the yields from pyrolysis of Jatropha seed cake using steam and nitrogen was carried out. The effects of carrier medium and temperature on yields of the pyrolysis products are shown in fig. 4.8, where both yields of biochar and bio-oil condensate were obtained by weight measurement.

With increase in temperature from 400^{o}C onwards, the pyrolysis liquid yield found to have steadily increased. At elevated temperatures above 550^{o}C, secondary cracking reactions of volatile fractions started taking place, which decreased the bio-oil yield and increased the lighter hydrocarbon fraction in the product gas. The mass flow of non-condensable gases was determined based on the volumetric flow rate measured by wet gas meter and detailed gas analysis result from GC. The bio-oil condensate liquid was distilled to get rid of heavy residue. The distillate (between 100 and 350^{o}C) yield was 34.3 wt% in presence of steam, whereas the same was observed to be 31.25 wt% in presence of nitrogen. On the contrary, the biochar yield has decreased continuously from 58wt% at 400^{o}C with increase in temperature to 9.81% at 600^{o}C in presence of steam. Though both follow similar trends of product yields, there was marked difference in the yield of products. The trends of the products in this study were found in agreement with previously published literature [168-170].

It was observed that the pyrolysis media is crucial for the production of bio-oil, gas and char from biomass pyrolysis in a rotary tubular coiled-flow reactor. The result has shown that the yields of bio-oil, biochar and gases are affected primarily by temperature, when varied from 400 to 600^{o}C under N_2 atmosphere. Temperature has significant influence on the distribution of products also. Devolatilization of volatile matter followed by cracking of the heavier molecules to lighter hydrocarbons is directly dependant on pyrolysis temperature [171, 172]. But the same degree of char reduction was not observed when steam was used as carrier. This is explained as follows. When the temperature is low, the volatile matter slowly evaporates and the carbonization reaction dominates and thus more char yield is obtained. The release of volatile matter begins quickly at higher temperatures. Also, by use of superheated steam, the volatilization of the matter gets enhanced and fast release of gases take place even at low temperatures. From fig. 4.8, one could visualize increase in bio-oil yield when temperature is increased from 400 to 550^{o}C, irrespective of the carrier. This could be attributed to sudden release of volatile matter at higher heating rate resulting in increased bio-oil yield. When temperature was increased beyond 550^{o}C, cracking of unstable components in the volatile matter resulted in a decrease in bio-oil yield. This is in agreement with literature information [173]. At higher temperatures, at or above 600°C, the reactions of thermal cracking gives rise to the formation of permanent gases.

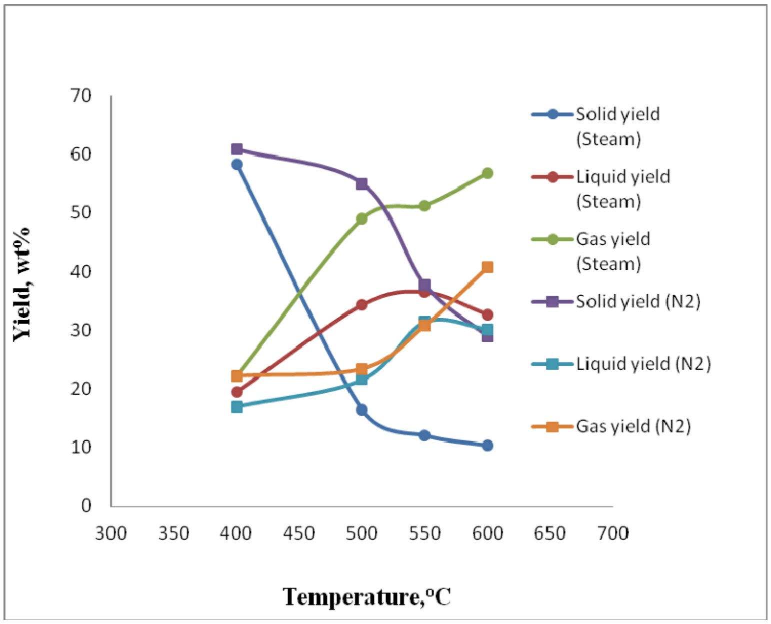

Fig. 4.8 Distribution of pyrolysis products with reference to temperature of pyrolysis

4.4.2 Effect of steam/biomass ratio on steam pyrolysis of Jatropha deoiled cake

The experiments were carried out at temperature of 550° using a steam/ biomass ratios of 1:1, 2:1, 3:1. The quality and yield of bio-oil obtained is plotted against the steam/ biomass ratio. It was observed that mixing of steam and biomass at the feeding section and excess concentration of steam in the gas phase throughout the reactor length is critical to ensure high carbon conversion and bio-oil yield.

In the present experimentation, an innovative mixing technique has been employed such a way that the superheated steam and biomass travel through a venturi constriction, which enhances the mixing pressure for a small fraction of time and the sudden depressurization leads to disintegration of biomass into its constituents in the bio-oil. It was inferred that the conditions leading to formation of lighter and less viscous bio-oil could be produced with the help of superheated steam. The effect of amount of steam on bio-oil distillate yield was studied. The bio-oil distillate yield has increased from 34 wt% to 43% when steam-to-biomass ratio was increased from 1:1 to 3:1 (Fig. 4.9).

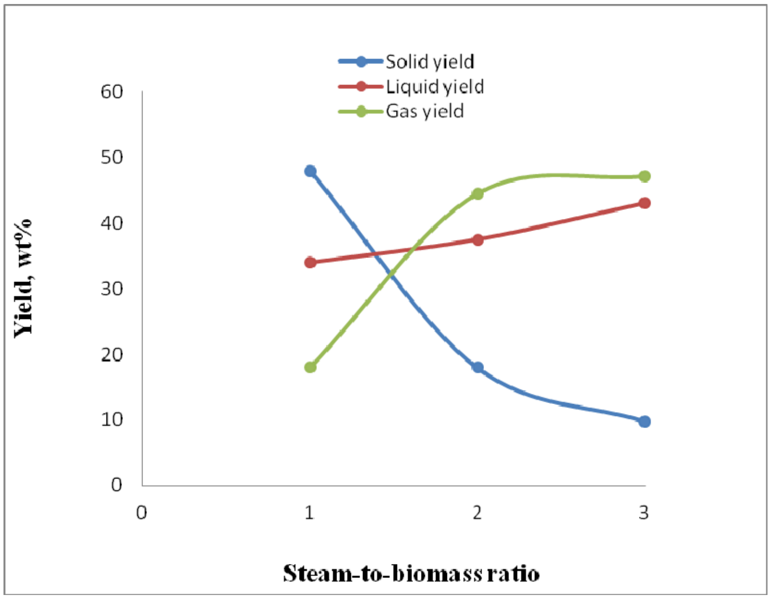

Fig. 4.9 Effect of steam-to-biomass ratio on the pyrolysis product yields

4.4.3 *Effect of residence time on the product yield*

The experiments on the effect of biomass residence time were carried out at temperature of 600°C in presence of superheated steam. The generation of non-condensable gases during thermal pyrolysis of deoiled jatropha cake is strongly dependant on the biomass feedstock. The gases like CO, CO_2, CH_4, C_2H_4, C_2H_6 and H_2 continued to form in the same manner when the biomass residence time was increased from 48 seconds to 120 seconds. During the slow pyrolysis run at 240 seconds, the overall yield of gases came down at the expense of increase of solid char. The percentage composition of gases obtained are 29% CO, 12% CO_2, 15% CH_4, 8-10% other hydrocarbons 26% N_2 and 7-8% H_2. The formation of permanent gases could be attributed to cracking of cellulosic (cellulose and hemicellulose) and sugar contents of the deoiled cake due to the breaking of glycosidic bonds or opening and reforming of pyranoid rings, which produced pentoses and glucoses and followed by C-C bond cleavage of these compounds to form the above gases.

As the residence time increases, the char and gas yields increases. Higher residence time aids the secondary reactions to take place which leads to the formation of gases and char. This is also equally compensated by the decrease in bio-oil condensate yield with increasing residence time. This phenomenon conforms well to the literature as depicted by previous researchers [172]. Thus, it is inferred that the least residence time in the experiment is taken as the optimum residence time (Fig. 4.10). Experiment with lesser residence time is limited by the maximum rotation speed of the coiled conveyor. Maximum yield of char is obtained at the highest residence time and maximum bio-oil yield is obtained at the least residence time.

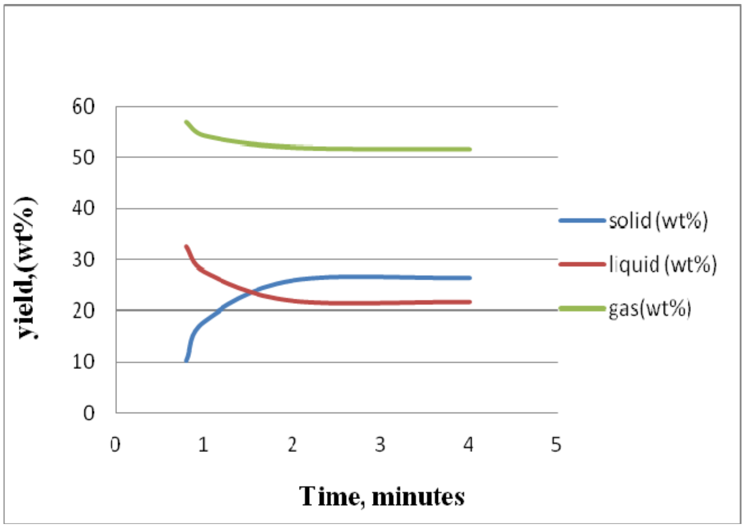

Fig. 4.10. Distribution of product yields at 600°C at different residence times

4.4.4 Bio-oil product distribution

The distribution of pyrolysis products are majorly dependant on process parameters such as temperature, type of carrier media (N_2/steam). Out of the trials conducted, four representative samples based on the highest yielding trials were taken for further analysis. These samples were designated as SPL-1 (N_2 pyrolysis at 550°C), SPL-2 (N_2 pyrolysis at 600°C), SPL-3 (Steam pyrolysis at 550°C) and SPL-4 (Steam pyrolysis at 600°C).

All these samples were investigated with the objective of evaluating the main products of pyrolysis such as organic acids, phenols, alcohols, ester and nitrogenates and were quantified (Table 4.12). The organic acids and oxygenates were known to be products of cellulose portion of the biomass. The phenols are mainly formed from the Lignin portion of the biomass. Pyrolysis of protein content in the Jatropha deoiled cake resulted in nitrogenous compounds. While the analysis of the pyrolysis products gave insight to relationship of yield with process parameters, the study could eventually break pathway or strategy for reduction of O and N in the condensed vapours by a natural and non-catalytic route. The aim of this work was to broadly assess the feasibility of production of hydrogen from the pyrolysis products of Jatropha Curcas using steam reforming catalysts. Although many group researchers have studied the conversion and selectivity of steam reforming of pyrolysis products (REF), the current research focuses on effect of the percentage of O and N (in the pyrolysis products) on the conversion, selectivity for H_2 production and more importantly the deactivation profile of the catalyst.

From table 4.13, it can be deduced that the percentage of Oxygen in the bio-oil condensate reduced with respect to increase in temperature as well as by introduction of steam. This not only reduces the load on secondary processing but also increases the net calorific value of the product. Literature says reduction of yields of nitrogenous compounds is the most difficult and less accomplished task regardless of the process with or without catalyst [174]. At 550°C, under nitrogen atmosphere, all the nitrogen compounds have almost completely converted. On the other hand, the oxygen content was the highest in the product, which decreased gradually with increase in temperature and with introduction of more steam as well.

Table 4.12. Bio-oil condensate analysis

S. N	Pyrolysis products	Molecular Formula	Molecular wt, g/gmol	SPL-1 [N2 Pyrolysis (550°C)]	SPL-2 [N2 Pyrolysis (600°C)]	SPL-3 [Steam Pyrolysis (550°C)]	SPL-4 [Steam Pyrolysis (600°C)]
1	(2-aziridinylethyl)amine	$C_4H_{10}N_2$	86		22.51		
2	Dec-9-en-6-oxo-1-ylamide	$C_{10}H_{17}NO_2$	183		1.05		
3	2-isobutyl-3-methyl pyrazine	$C_9H_{14}N_2$	150		0.40	1.56	2.23
4	Deoxyspergualin	$C_{14}H_{38}ClN_7O_3$	423		0.37		
5	4-Pyridinamine, 2-6-dimethyl-	$C_7H_{10}N_2$	122	0.6			
6	2-Pyridinemethanamine, N-methyl-	$C_7H_{10}N_2$	122				8.82
7	Benzeneethanamine, 2,5-difluoro-.beta.,3,4-	$C_9H_{11}F_2NO_3$	219	0.99			

	trihydroxy-N-methyl-						
8	Methyl N-(N-benzyloxycarbonyl-beta-I-aspartyl)-beta-d-glucosaminide	$C_{19}H_{26}N_2O_{10}$	442	1.09			
9	4-Aminobutyramide, N-methyl-N-[4-(1-pyrrolidinyl)-2-butynyl]-N'-aminoacetyl	$C_{15}H_{26}N_4O_2$	294	1.29			
10	Imidazole-2-methanol	$C_4H_6N_2O$	98				
11	4-Amino-1-.beta.-d-robofuranosylpyrazolo[3,4-d]-pyrimidine 5'-phosphate	$C_{10}H_{14}N_5O_7P$	347	0.28			
12	2,4-Dimethylfuran	C_6H_8O	96				10.03
13	Furan, 2-ethyl-5-methyl	$C_7H_{10}O$	110				2.96
14	6-Methyl-bicyclo[4.2.0]octan-7-one	$C_9H_{14}O$	138				2.25
15	5-[2-(4,5,5-Trimethyl-cyclopent-1-enyl)ethylidene]pyrimidine-2,4,6(1H,3H,5H)-trione	$C_{14}H_{18}N_2O_3$	262	0.49			
16	Tetraacetyl-d-xylonic nitrile	$C_{14}H_{17}NO_9$	343				
17	N.-alpha.,N.-omega.-Di-dicarbobenzoxy-L-arginine	$C_{22}H_{26}N_4O_6$	442			0.68	
18	2-Cyclopenten-1-one, 2,3-dimethyl-	$C_7H_{10}O$	110				2.30
19	Spiro[4.5]dec-6-en-8-one, 1,7-dimethyl-4-(1-	$C_{15}H_{24}O$	220	0.38			

	methylethyl)-						
20	2-Heptanol	$C_7H_{16}O$	116		3.66		
21	Acetic acid	$C_2H_4O_2$	60	73.44	51.40		
22	Propanoic acid	$C_3H_6O_2$	74	6.03			
23	Butanoic acid, 3-methyl-	$C_5H_{10}O_2$	102			1.54	4.21
24	Hexanoic acid, 2-methyl-	$C_7H_{13}O_2$	129			0.67	2.19
25	9-Hexadecenoic acid	$C_{16}H_{32}O_2$	256	0.62			
26	9-Octadecenoic acid, (2-phenyl-1,3-dioxolan-4-yl)methyl ester,cis-	$C_{28}H_{44}O_4$	444				
27	17-octadecynoic acid	$C_{18}H_{32}O_2$	280		0.46	0.82	
28	Pentanoic acid	$C_5H_{10}O_2$	102	1.83			
29	Pentanoic acid, 3-methyl-	$C_6H_{11}O_2$	115	2.82	1.81		
30	6-Nonynoic acid	$C_9H_{14}O_2$	154			1.72	
31	Butanedioic acid, 2,3-bis(acetyloxy)-,[R-(R*,R*)]-	$C_8H_{10}O$	122				
32	11-(2-cyclopenten-1-yl)undecanoic acid, (+)-	$C_{16}H_{28}O_2$	252			0.90	
33	11-Hexadecyn-1-ol	$C_{16}H_{30}O$	238	0.52			
34	2-furanmethanol	$C_5H_{12}O_2$	98	4.75	2.48	6.48	1.22
35	2- Cyclopentene-1-methanol	$C_6H_{10}O$	98				2.95
36	Mequinol (4-methoxy Phenol)	$C_7H_8O_2$	124			5.20	6.18
37	p-Cresol	C_7H_8O	108			0.86	3.70
38	m-Cresol (Phenol, 3-methyl-)	C_7H_8O	108			0.46	3.01
39	Phenol	C_6H_6O	94	1.19		10.91	4.08
40	5,7-Octadien-3-ol,	$C_{12}H_{22}O$	182			0.55	

	2,4,,4,7-tetramethyl-,(E)-						
41	Cyclopropanetetradecanoic,2-octyl,methylester	$C_{26}H_{50}O_2$	394		3.96		
42	Cyclopropanedodecanoic acid,2-octyl,methylester	$C_{24}H_{46}O_2$	366				
43	N,N'-Bis (Carbbenzyloxy)-lysine methyl (ester)	$C_{13}H_{28}N_2O_6$	428		0.42		
44	Acetic acid, 2-[2-methyl-4-(1-piperidylmethyl)-1,3-dioxolan-2-yl]-, ethyl ester	$C_8H_{14}O_4$	174	2.25			
45	[1,1' -Bicyclopropyl]-2-octanoic acid, 2'-hexyl-,methyl ester	$C_{21}H_{38}O_2$	322		0.88		
45	Ethanol, 2-nitro-,propionate (ester)	$C_5H_9NO_4$	147			3.23	21.71
46	Ethyl Acetate	$C_4H_8O_2$	88			21.55	19.78
47	Ammonium Acetate	$C_2H_7NO_2$	77			39.72	2.27
48	d-mannose	$C_6H_{12}O_6$	360		1.99		
49	d-Glycero-d-ido-heptose	$C_7H_{14}O_7$	210		7.68	1.03	
50	Phenyl-.beta.-D-glucoside	$C_{12}H_{16}O_6$	256		0.93		
51	I-Gala-I-ido-octose	$C_8H_{16}O_8$	240	1.42			
52	2,2-Dimethyl-3-vinyl-bicyclo [2.2.1]heptane	$C_{11}H_{18}$	150			1.67	
	Total			100	100	100	100

Table 4.13 Elemental composition of bio-oil obtained from product characterization

% in Bio-oil (w/w)	SPL-1 [N2 Pyrolysis (550°C)]	SPL-2 [N2 Pyrolysis (600°C)]	SPL-3 [Steam Pyrolysis (550°C)]	SPL-4 [Steam Pyrolysis (600°C)]
%C in bio-oil (w/w)	44.64	47.87	50.04	60.68
%H in bio-oil (w/w)	7.30	8.52	9.01	8.13
%N in bio-oil (w/w)	0.62	7.60	7.91	4.92
%O in bio-oil (w/w)	47.55	34.99	33.22	26.31

4.4.5 *Catalytic conversion of pyrolysis oil by Steam Reforming*

This section discusses the results obtained in the catalytic steam reforming of different biomass pyrolysis oils (bio-oils) varied in chemical composition in terms of their nitrogen and oxygen contents. The experiments were done with a combination of two types of reforming catalysts varying in terms of their stability, activity, selectivity and coke resistance. Comparison was made between the bio-oils due to the well known rapid deactivation of catalysts by the various fractions present in bio-oils. High catalytic activity and stability for long term use are important for steam reforming of bio-oil. Presence of sulphur could act as a poison for the active sites in the Ni-based catalyst. Although the biomass pyrolysis oil doesn’t contain any sulphur, presence fairly large amount of oxygen and nitrogen might reduce the catalytic activity. On the other hand cracking of large sized and thermally unstable molecules such as carbohydrates, furans, phenols, cresols etc. contained in the bio-oil could lead to carbon deposition on the catalyst surface, and reduce catalytic activities. Hence in this study, reusability of the catalyst was also examined after every run by repeatedly reusing the same catalyst after regeneration under steam at 750°C for 4 hrs.

The overall reforming reaction can be theoretically represented as:

$$C_nH_mO_k + (2n-k)\ H_2O \xrightarrow{(Catalyst)} CO_2 + (2n + m/2 - k)\ H_2 \qquad \text{............(Eq 4.1)}$$

In the case of bio-oils obtained under different process conditions, the overall molecular formula can be written as shown in Table 4.14. From eq. 4.1, the calculated maximum hydrogen yields from pyrolytic bio-oils are also shown in Table 4.14.

Table 4.14 Empirical molecular formula obtained for bio-oils

% in Bio-oil (w/w)	SPL-1 [N2 Pyrolysis (550°C)]	SPL-2 [N2 Pyrolysis (600°C)]	SPL-3 [Steam Pyrolysis (550°C)]	SPL-4 [Steam Pyrolysis (600°C)]
Moles of C	3.72	3.99	4.17	5.06
Moles of H	7.23	8.43	8.92	8.05
Moles of N	0.04	0.54	0.56	0.35
Moles of O	2.97	2.19	2.08	1.64
Molecular Formula	$CH_{1.94}N_{0.01}O_{0.80}$	$CH_{2.11}N_{0.14}O_{0.55}$	$CH_{2.14}N_{0.13}O_{0.50}$	$CH_{1.59}N_{0.07}O_{0.32}$
Max H_2 yield	2.17	2.505	2.57	2.475
Max H2 yield (g H2/g bio-oil)	0.163	0.203	0.246	0.254

Bio-oil can be reformed to produce H_2 and CO_2 only. However, in fact the H_2 yield is lower than this theoretical value due to some accompanied side reactions, such as the thermal decomposition (Eq. 4.2) and methanation reactions (Eqs. 4.3 and 4.4).

$$C_nH_mO_k/C_xH_yO_z \rightarrow H_2, CO, CO_2, CH_4, C_2H_4, C_3H_6 + coke \quad \text{.............}(Eq.\ 4.2)$$

$$CO + 3H_2 \rightarrow CH_4 + H_2O \quad \text{.............}(Eq.\ 4.3)$$

$$CO_2 + 4H_2 \rightarrow CH_4 + 2H_2O \quad \text{.............}(Eq.\ 4.4)$$

4.4.6 Effect of temperature on product distribution

In case of vapour phase catalytic up-gradation of pyrolysis oil by steam reforming in a fixed bed reactor, temperature is the most critical parameter. The bio-oil sample no.4 (SPL-4) obtained under N_2 at 550°C was chosen for the study on effect of temperature. At WHSV = 0.5 h^{-1}, Steam/Bio-oil ratio = 3.0, the reaction temperature ranges from 600°C to 850°C, gaseous products distribution versus reaction temperature is shown in Fig. 4.11. The hydrogen yield and the bio-oil conversion versus reaction temperature are shown in Fig.4.12. Furthermore, the increase of temperature causes a marked increase in conversion of bio-oil from 26% at 600°C to 96.4% at 850°C and increase of hydrogen yield from 0.066 gH_2/g bio-oil at 600°C to 0.245 gH_2/g bio-oil at 850°C. The average hydrogen purity was of 82.5 vol% with very less percentage of lighter hydrocarbons and CO. This has been confirmed by many researchers [175, 176].

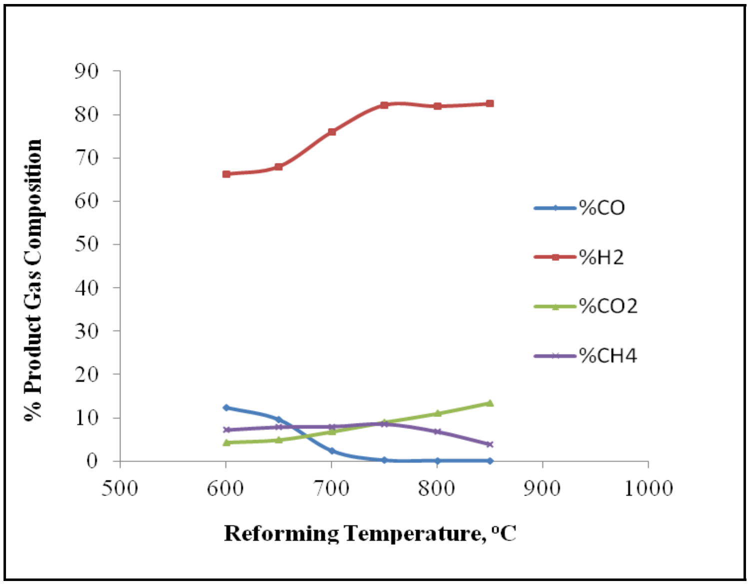

Fig. 4.11 Effect of reforming temperature on product gas distribution

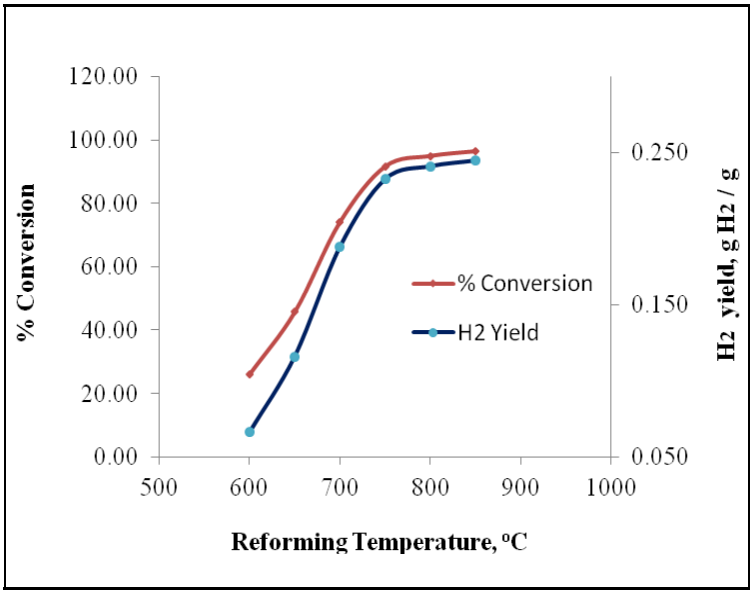

Fig. 4.12 Effect of reforming temperature on bio-oil conversion and hydrogen yield

4.4.7 Effect of steam-to-bio-oil ratio

The effect of steam/ bio-oil ratio was studied from 1:1 to 3:1 at 750°C using the bio-oil sample no-4 (SPL-4). The % conversion was very high at all the steam/ bio-oil ratios and attained plateau at steam/ bio-oil ratio of 2.0. Fig. 4.13 shows the effect of steam/bio-oil ratio on % conversion and H_2 yield at 750 °C. The yields of H_2 and CO_2 increase notably with the steam-to-bio-oil ratio upto 2:1 (Fig 4.14). Above this value, increase of % conversion and H_2

yields were less relevant. Concurrently, there is a marked decrease in CO yield because the WGS reaction is enhanced due to the higher water content in the reaction medium. The obtained results are in agreement with the literature [177].

In steam reforming, adsorption of hydrocarbons on the metal sites (Ni is commonly used) is followed by dehydrogenation and cracking. This results in smaller $C_nH_mO_k$ adsorbed fragments which can polymerize to unwanted intermediates and form coke. These reactions compete with reactions with adsorbed water species. The catalyst must supply enough adsorbed H_2O-derived species, mainly OH and H, to overcome the coke formation reactions. This implies that the adsorbed OH and H must have sufficient surface mobility to reach the adsorbed hydrocarbon derived species and react with them. The steam adsorption capability can be significantly improved by promoting the classical Ni-alumina or Ni-silica/alumina formulations with Ca and/or K.

The sulphur content in biomass is nil. Therefore, a desulfurization prior to the reformer may not be necessary for bio-oil feedstocks. However, because of the oxygenated nature of the pyrolysis oil, the catalyst to be used in the reforming process must be able to handle high percentages of oxygen-containing functional groups [178]. Apart from an increase in H_2 yield, the Water Gas Shift reaction (Eq. (4) and (5)) promoted by higher steam/ bio-oil ratio would be accompanied by an increase in CO_2 yield and a decrease in CO and C_nH_m yield. These trends have been reported by several researchers [179, 168].

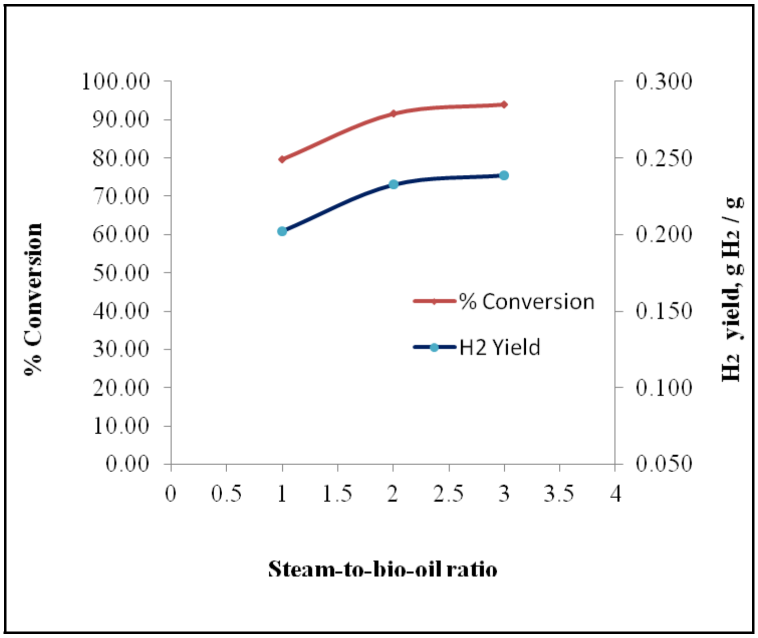

Fig. 4.13 Effect of steam-to-bio-oil ratio on bio-oil conversion and hydrogen yield

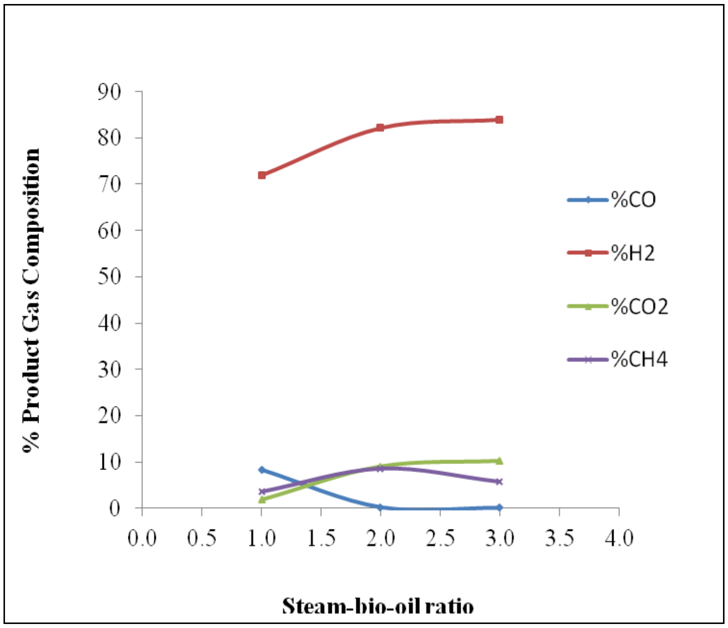

Fig. 4.14 Effect of steam-to-bio-oil ratio on product gas distribution

4.4.8 Effect of nitrogenates and oxygenates on conversion and hydrogen yield

As shown in Fig. 4.13, H_2 yields, mole fractions of H_2, CO, CO_2, and CH_4 changed gradually with the time on stream, which means that the steam reforming of bio-oil is not quite stable. In order to study the catalyst deactivation, the reactions were carried out for all samples starting with sample no.1 (SPL-1) over a long duration of 4 hr steady state time under the optimum reaction conditions of 750^{o}C, S/F of 3.0, 1 barg pressure and WHSV of 0.5 h^{-1} and catalyst of 120 g, to investigate the variation of the catalyst activity with time on stream. H_2 yields decreased slightly with the time on stream, which means that the catalyst activity gradually reduced. However, the H_2 yield and % conversion decreased gradually, and finally, the values reached 68% and 0.09 gH_2/g bio-oil respectively. Also, the decrease of H_2 concentration is accompanied by increase of CH_4 and CO_2, which suggests that the steam reforming reactions are less predominant, but cracking reactions, methanation reactions as depicted by Eq. 4.2 to 4.4. The product gas composition at various steam/ bio-oil ratios is given in Fig 4.14.

This decrease in H_2 yield could be attributed to temporary loss of catalyst activity by blockage of pores of the catalyst by carbon deposition. In order to quantify the deactivation due to nitrogenates content as well as oxygenates content, all the four samples were independently run on fresh catalysts. The deactivation profile has been depicted in terms of the Hydrogen yield over time. It was observed that deactivation was slow in case of sample-1 (SPL-1; low in N) and sample- 4 (SPL-4; moderate N and moderate O contents) (Fig. 4.15-4.19).

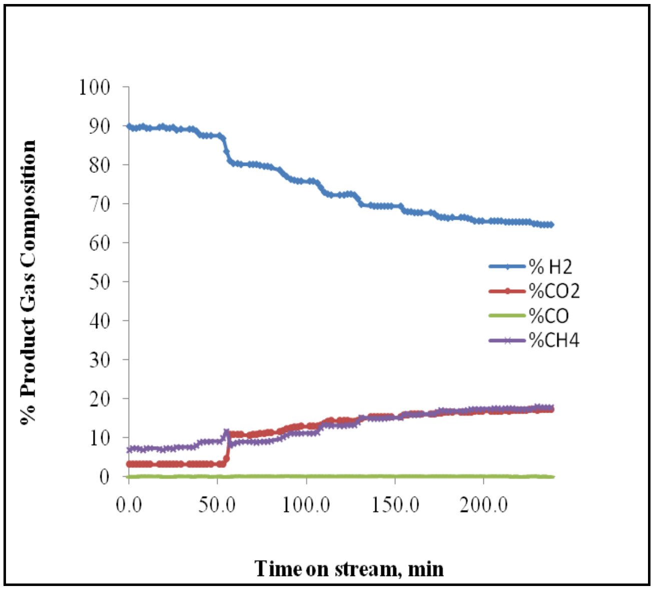

Fig. 4.15 Product gas distribution vs. time on stream in fixed bed conversion of bio-oil

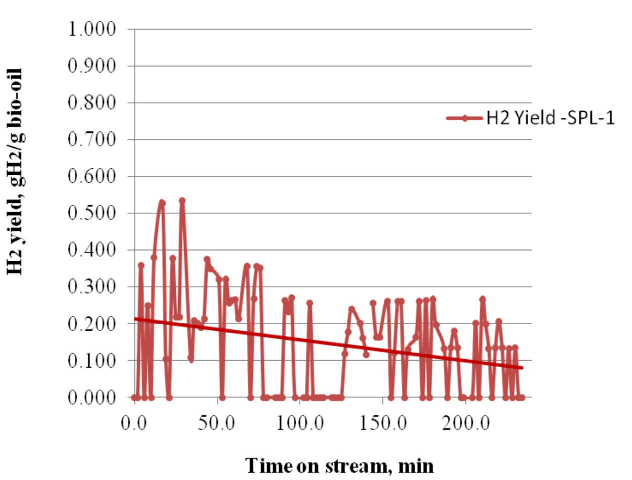

Fig. 4.16. H_2 yield profile for extended reforming of bio-oil distillate SPL-1

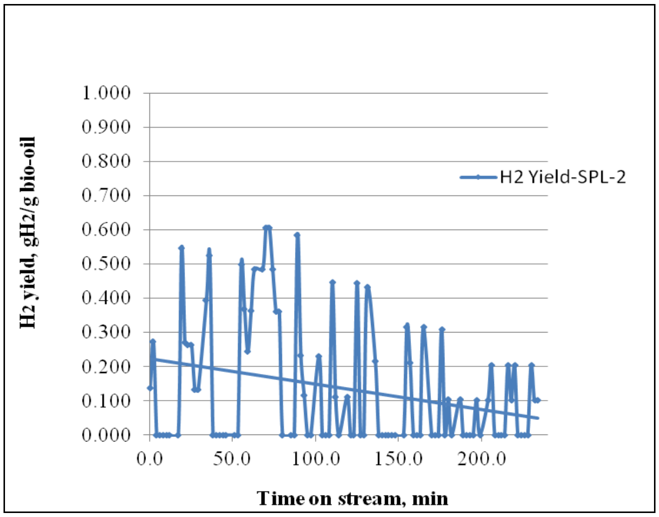

Fig. 4.17 H_2 yield profile for extended reforming of bio-oil distillate SPL-2

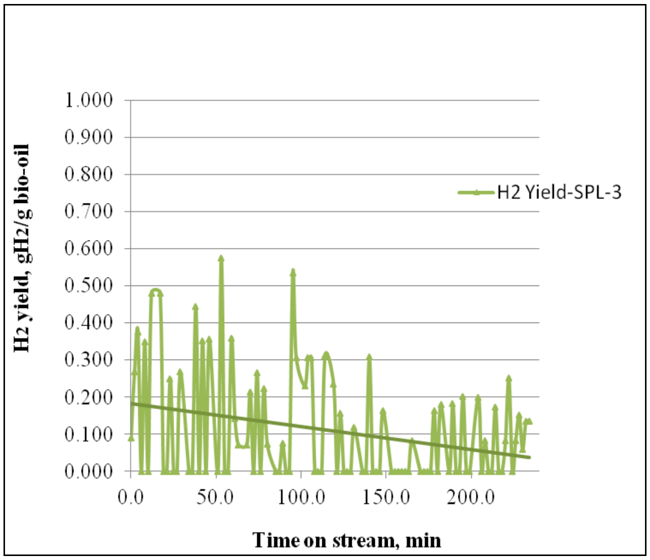

Fig. 4.18 H_2 yield profile for extended reforming of bio-oil distillate SPL-3

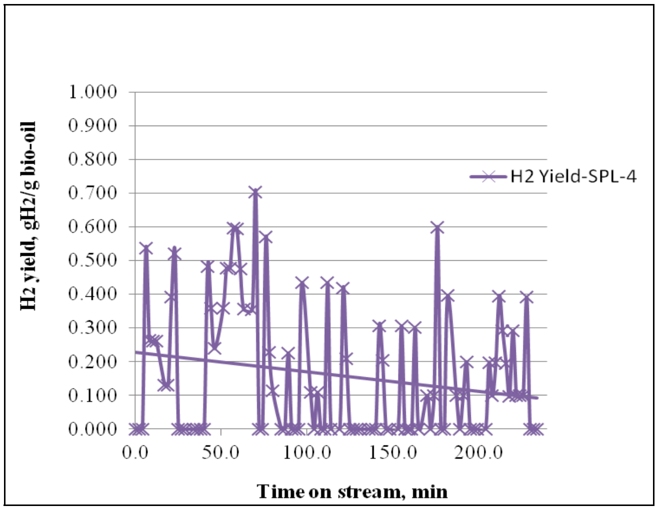

Fig. 4.19 H_2 yield profile for extended reforming of bio-oil distillate SPL-4

4.4.9 Regeneration, reproducibility and cyclic strength of the catalyst

In order to analyse the carbon deposition content of reacted catalysts, after the steady state run the reactor was flushed with nitrogen and superheated steam at the reforming reaction conditions. During the steam activation process, evolution of CO, CO_2 and H_2 has been observed. This corroborates the fact that the carbon deposited during the bio-oil reforming reaction reacted with steam to produce CO, CO_2 and H_2. After the activation process, the second batch of bio-oil was taken in for reforming at the same conditions as that of previous run. The same hydrogen yield profile could be observed this time also. The reaction and regeneration runs were carried out in between each run and it was observed that the average concentration of the product gas and H_2 yield remains constant throughout the runs. Fig. 4.20 shows the H_2 yield profile for regenerative reforming runs carried out with bio-oil sample SPL-4.

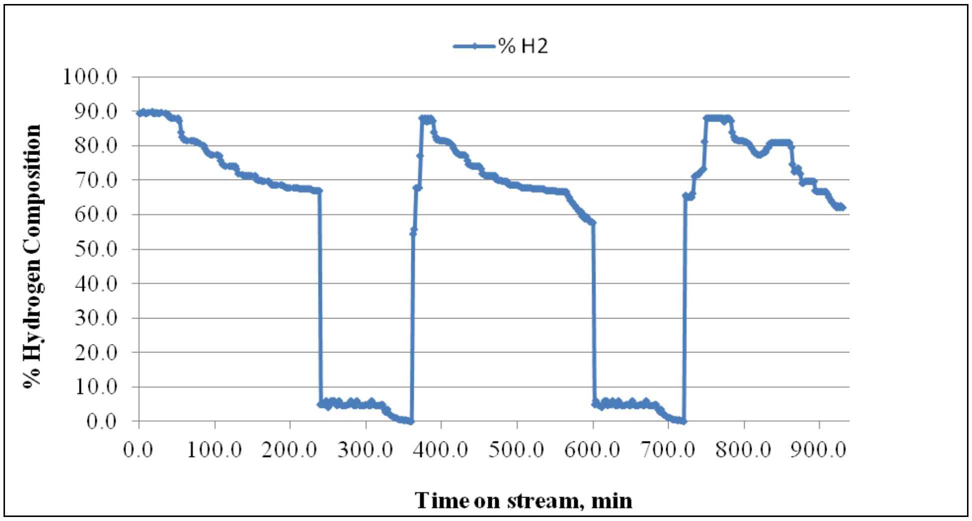

Fig. 4.20 H_2 yield profile for multiple regenerative steam reforming of bio-oil distillate SPL-4

4.4.10 Conclusions

Pyrolysis of *Jatropha* deoiled cake was carried out in an in-house *Pyrolyser* in presence of N_2 and steam. It gave a highest bio-oil liquid yield of 43wt%. The pyrolysis products were analyzed and characterized based on their C, H, N, O content. The steam reforming of bio-oil resulted in H_2 yield of 0.245 g H_2/g bio-oil at % conversion more than 95%. The overall hydrogen yield from biomass was calculated to be 105.35 g H_2/kg of biomass. The long duration tests indicated decrease of the H_2 yield due to temporary loss of catalytic activity by coke deposition from cracking of heavier nitrogenous and oxygenated molecules of bio-oil. Repeated regeneration and reforming runs indicated stable performance.

4.5 Continuous mode operation

The present section shows the results of parametric studies carried out in the continuous mode pilot scale process plant by varying the following process parameters: temperature, steam-to-biomass ratio and residence time. The continuous process has been demonstrated on a completely automated plant, operated with standard operating protocol (SOP is given in Appendix-III)

Table 4.15 Effect of skin temperature of reactor on biomass conversion and product gas composition in the primary gasification stage

Parameters		**Temperature (T) at constant steam to biomass ratio of 2.5 and residence time of 3 minute**		
Skin temperature		**T= 800°C**	**T= 900°C**	**T= 950°C**
Internal temperature		**T_{int}= 630°C**	**T_{int} = 680- 690°C**	**T_{int} =730-750°C**
% Conv. (1- char fraction) x 100 on ash-free basis		79	91.3	95
% Gas Composition (by volume)	$\%H_2$	7.5-9	10-12	14-19
	%CO	27- 32	29- 34	34- 38
	$\%CO_2$	8- 9.6	6- 7	4.6 – 5.5
	$\%CH_4$	3-4	4-7	6-8
	$\%(N_2+ C_2 + C_3)$	Balance	Balance	Balance

Table 4.16 Effect of S/B ratio on biomass conversion and product gas composition in the primary gasification stage

Parameters	**Steam to biomass ratios (S/B) at constant temperature 950°C (T_{int} =740-750°C) and solid residence time of 3 min**			
	S/B= 1.0	**S/B = 1. 3**	**S/B =2.0**	**S/B =2.5**
% Conv. (1- char fraction) x 100 on ash free basis	82%	87%	94%	95.9%

% Gas Composition (by volume)	%H_2	9	11-14	14-16	14-19
	%CO	26- 30	34- 37	32- 36	34- 38
	%CO_2	8-9	7-10	4.8 – 7	4.6 – 5.5
	%CH_4	3-4	8-10	6-8	6-8
	%(N_2+ C_2 + C_3)	Balance	Balance	Balance	Balance

Table 4.17 Effect of residence time on biomass conversion and product gas composition

Parameters		**Residence times at constant temperature (950°C; T_{int} =740-750°C) and steam to biomass ratio (2.0)**		
		Solid residence time = 1.8 min	**Solid residence time = 3**	**Solid residence time = 3.6**
% Conv. (1- char fraction) x 100 on ash-free basis		88	94%	95.9
% Gas Composition (by volume)	%H_2	14-16	14-19	14-17
	%CO	30- 34	34- 38	34- 36
	%CO_2	4.8 – 5.8	4.6 – 5.5	4.6 – 6.5
	%CH_4	6-8	6-8	6-8
	%(N_2+ C_2 + C_3)	Balance	Balance	Balance

A sensitivity study was carried out by first varying the reactor skin temperature from 800°C to 950°C, followed by steam to biomass ratio and solid residence time from 1 to 2.5 and 0.5 min to 5 min respectively. The influence of gasification parameters on the biomass conversion and gas yield are deduced.

Increase in steam to biomass ratio above 2.0 has no large effects on the gas produced and gas composition. Moreover, tar and lighter hydrocarbons are very low. The increase in steam in the reactor causes a dilutive effect in the reaction mixture and the temperature tend to reduce. Thus higher S/B ratio tends to reduce biomass conversion and gas yield. The effect of various parameters on the conversion and gas composition is given in table 4.15- 4.17.

4.5.1 Steady state data analysis

To understand the gasification characteristics under steady state over a period of time, recorded data of gasifier process parameters were plotted historically over time. The steady state plots of reactor skin temperatures, reactor internal temperatures, absolute vacuum levels, steam flow (water feed tank weighing balance), cumulative product gas flow are shown below (Fig 4.21- 4.25). The skin temperatures of the reactor were quite uniform throughout the process, except the slight offset during biomass introduction to the system (Fig. 4.21). The internal reactor temperature also showed a similar effect during introduction of biomass into the system and it maintained at 730°C during the steady state run (Fig 4.22). The vacuum level in the system was maintained at -0.70 mbar during the course of steady state run (Fig. 4.23). Another important parameter governing the steady product gas flow is steam flow rate (Fig 4.24). It was also evident that a constant flow of steam maintained the system *'spike-free'* and yielded steady product gas flows (Fig. 4.25).

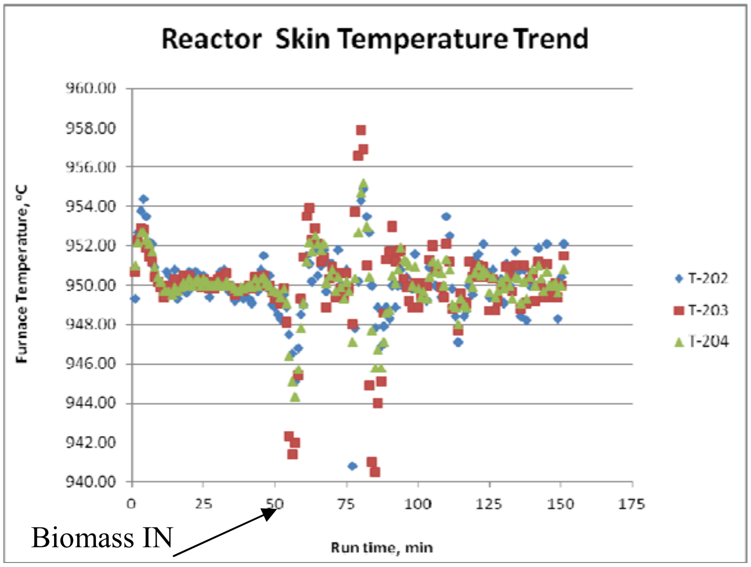

Fig 4.21 Reactor skin temperatures (first zone T202, second zone T203, third zone T204) record over run-time.

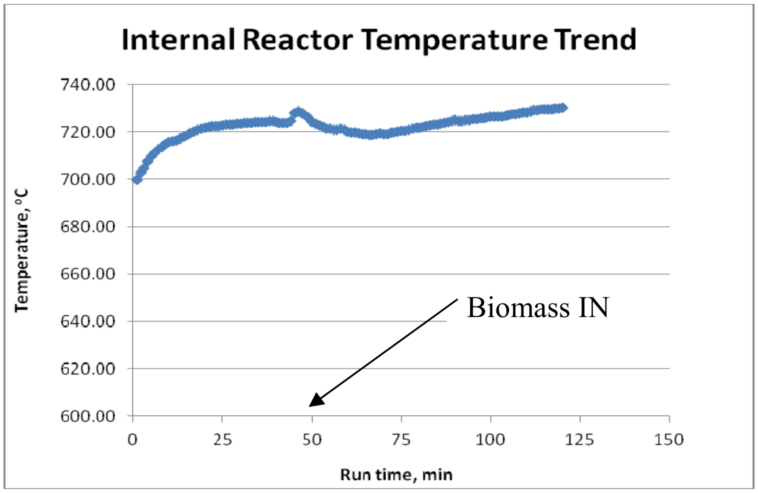

Fig 4.22 Reactor-internal temperature trend

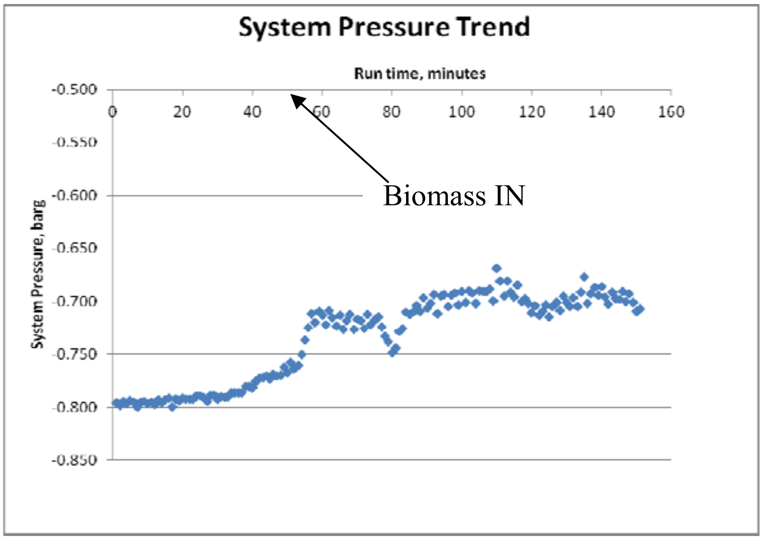

Fig 4.23 System pressure trend over the period of run

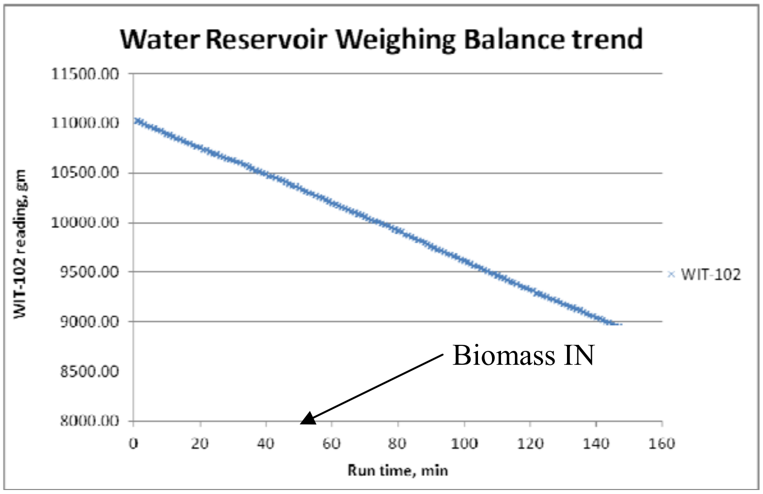

Fig 4.24 Water feed tank weighing balance trend over period of continuous run

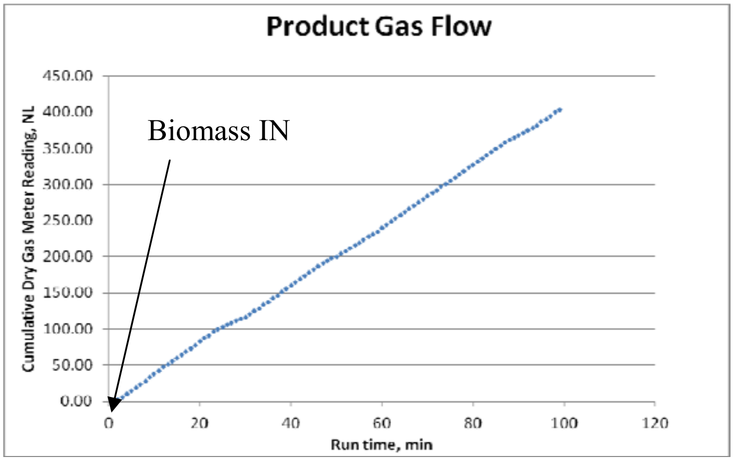

Fig 4.25 Cumulative dry product gas flow over period of continuous run

Contrary to a conventional downdraft reactor, the modified reactor configuration offered a constant product gas flow rate, which is indicated by the linear relationship between cumulative product gas flow rate and the reaction time (Fig. 4.25). As discussed above, the new reactor system can be operated under optimized process conditions at suitable temperature, steam-to-biomass ratio and residence time with excellent contact between metal surface and the particles and mass transfer.

Secondary conversion of the biomass gasification product yielded in a hydrogen rich product gas containing very less amount of impurities. The product gas concentration after secondary conversion is given in table 4.18.

Table 4.18 Product gas yield from continuous integrated run after secondary stage conversion

Product Gas	mol%	mol% (- N_2)	Normalized mol fr.	wt. fr.	moles after CO shift	Normalized mol% after CO shift	wt fr. after CO shift
H_2	20.72	20.72	0.27	0.026	0.81	0.52	0.053
CO_2	4.63	4.63	0.06	0.126	0.59	0.39	0.859
I-C_{4-}	0.57	0.57	0.01	0.020	0.01	0.00	
C_3-	0.05	0.05	0.00	0.000	0.00	0.00	
C_3=	0.2	0.2	0.00	0.000	0.00	0.00	
C_2=	2.35	2.35	0.03	0.041	0.03	0.00	
C_2-	0.42	0.42	0.01	0.008	0.01	0.00	
N_2	23.77	0.00	0.00	0.00	0.00	0.00	
CH_4	6.66	6.66	0.09	0.066	0.09	0.06	0.046
CO	40.64	40.64	0.53	0.704	0.00	0.02	0.029
Total	100	76.24	100.000	0.991	1.53	1.00	1.00

4.5.2 Mass balance

For mass balance the steady state data collected in every minute interval was integrated over the reaction run time. The biomass consumption was found out by subtracting the weight of left over biomass from the initially loaded weight of biomass. The mass of condensate water was also taken into consideration for end-to-end water balance. Below given are the details of the mass balance table (Table 4.19). The product gas concentration was obtained at regular intervals by GC analysis. The average molecular weight of the product gas was obtained from the product composition obtained from GC analysis.

Table 4.19 Mass balance from primary gasification stage of continuous process

Biomass unloaded after the steady state run (g)	3836	
Biomass reacted = biomass loaded – biomass unloaded (g)	5000- 3836 = **1164**	(A)
Total duration of run (min)	220	
Biomass feed rate (g/hr)	317	
Cumulative product gas flow during steady state	968	
Total N_2 fed during Steady state run (NL) for seal cooling	88	
Weight of N_2 fed, g	88/22.414*28= **109.93**	(B)
Net product gas obtained (NL) Product gas yield (Nm^3/kg)	880 880/ (1164*0.865) = 0.88	
No. of moles of gas obtained	=880/22.414= 39.26	
Avg. MW of gas during Steady State run (g/mole)	22.77 (calculated from GC analysis of product gas; calculation given in Appendix-IV)	
Wt. of net gas obtained (g)	39.26 * 22.77 =**894 g**	(C)
Gas Yield (wt%)	= 894/ 1164 *100 = **76.8%**	
Gas Yield (wt% on ash free basis) @ ash% 13.5	= **88.8 wt%**	
Gas Yield (wt% on ash free and moisture free basis)	= **95.5 wt%**	
Biochar obtained (g)	210	(D)
Biochar / biomass feed ratio	210/ 1164 *100= **18%**	
CHNO of Biochar	C: 24.658; H: 2.048; N: 0.0397; O: Not detectable	
Ash content in Biochar	= 73.25%	

% Biomass carbon conversion =(0.421*1164–0.247*210)/(0.421*1164)x100 = **89.4%**

Total Steam fed to reactor during steady state (g)	2325	(E)
Steam feed rate (g/hr)	607	
Steam/Biomass ratio	**1.91**	
Condensate obtained from fractional condensate vessel V-235 (g)	391	
Condensate obtained from final condensate vessel V-250 (g)	1930	
Total condensate obtained (g)	2321	(F)
Total Mass in (g) (Biomass + N_2 + Steam) = (A + B + E)	3599	
Total Mass out (g) (Product gas + N_2+ Biochar + Condensate)= (C + D +F)	3535	
Mass balance / Mass imbalance (g)	64	
Mass balance (%)	**98%**	

Secondary stage conversion of the product gas from primary gasification stage in the fixed bed reactor resulted in hydrogen rich product completely eliminating carbon monoxide and residual hydrocarbons. The second stage mass balance is given below in table 4.20.

Table 4.20 Second stage mass balance of the continuous process

Net product gas from first stage gasifier (NL/ g)	880 NL / 894 g
Total duration of run of secondary conversion (min)	220
Cumulative product gas flow from the secondary converter during steady state (NL)	1346
Moles of product gas, mole	60.05
Avg. MW of gas during Steady State run (g/mole)	19.84 (calculated from GC analysis of product gas- Fig. 4.27)
Wt. of net gas obtained (g) Total hydrogen make (based on table 4.18)	**1191.4 g** **63.14 g/kg biomass**
Gas Yield (wt%) based on stage-1 product gas	= 1191.4/ 894 *100 = **133 %**
Gas Yield (wt% on ash free biomass) @ ash% 13.5	= 1191.4/ (1164*0.865) = **118wt%**
Total Steam fed to reactor during steady state (g)	1760
Steam feed rate (g/hr)	480
Steam/Biomass ratio	**1.9**
Condensate obtained from fractional condensate vessel V-250 (g)	1530

Mass balance (%)	**97.5%**
Overall product gas yield	**1.35 Nm^3/kg**

Typical Gas Chromatographs of the product gas sample from primary gasification stage as well as secondary conversion stage are shown in the Fig 4.26 and Fig 4.27 respectively.

Refinery Gas Analysis

Data File C:\CHEM32\1\DATA\GASIFICATIONRUN\180117 RUN30 SPL1.D
Sample injected on 15:51:30

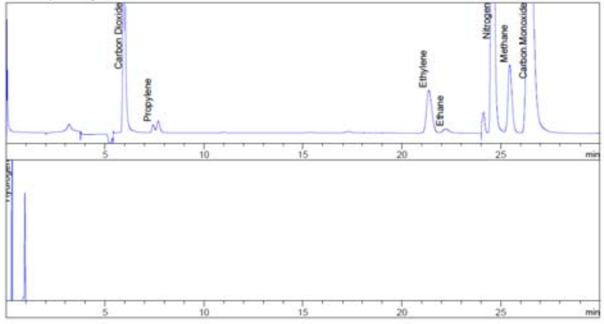

Compound	RT	Area	Mole%
Hydrogen	0.298	13189.4	19.54
Carbon Dioxide	5.958	7853.6	7.87
Propane	0.000	0.0	0.00
Propylene	7.439	300.4	0.21
I-Butane	7.693	518.5	0.34
n-Butane	0.000	0.0	0.00
1-Butene	0.000	0.0	0.00
trans-2-Butene	0.000	0.0	0.00
I-Pentane	0.000	0.0	0.00
cis-2-Butene	0.000	0.0	0.00
n-Pentane	0.000	0.0	0.00
Ethylene	21.356	3345.7	2.61
Ethane	22.200	334.6	0.32
Nitrogen	24.563	25931.0	25.77
Methane	25.444	3999.8	6.20
Carbon Monoxide	26.410	29766.7	34.77

Totals : 97.6257

Fig 4.26 Typical gas chromatograph of the product sample from primary gasification stage

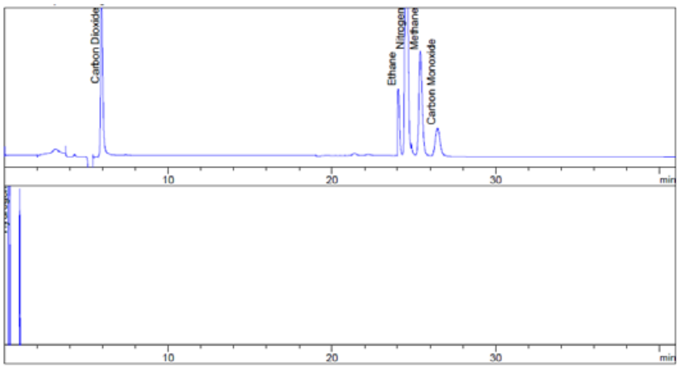

Compound	RT	Area	Mole%
Hydrogen	0.321	41089.1	60.87
Carbon Dioxide	5.939	25614.0	25.62
Propane	0.000	0.0	0.00
Propylene	0.000	0.0	0.00
I-Butane	0.000	0.0	0.00
n-Butane	0.000	0.0	0.00
1-Butene	0.000	0.0	0.00
trans-2-Butene	0.000	0.0	0.00
I-Pentane	0.000	0.0	0.00
cis-2-Butene	0.000	0.0	0.00
n-Pentane	0.000	0.0	0.00
Ethylene	0.000	0.0	0.00
Ethane	24.052	2083.2	1.98
Nitrogen	24.542	11385.6	11.28
Methane	25.405	509.1	0.79
Carbon Monoxide	26.458	2102.6	2.46

Fig 4.27 Typical gas chromatograph of the product sample after secondary stage conversion

4.5.3 Hydrogen Conversion Efficiency (HCE)

The Hydrogen Conversion efficiency was actually determined by the hydrogen yields obtained from the continuous mode process.

From the formula for HCE = $(M_{gas} \times X_{H2\ gas})/(M_{feed} \text{ x } X_{H2\ feed})$x 100

Here, M_{gas} is the mass of product gas yielded

$X_{H2\ gas}$ is the mass fraction of hydrogen in product gas

M_{feed} is the mass of feed biomass

$X_{H2\ feed}$ is the inherent hydrogen concentration in the feed biomass

Based on the product gas yield and mass balance data (Table 4.18- 4.20), the Hydrogen Conversion Efficiency was calculated to be **105%.**

4.5.4 Overall Energy Efficiency

For the current biomass pyrogasification process, the calorific value of biomass (HHV_{feed}) is determined by using Dulong Tillman formula from the composition analysis, which states:

$$HHV\ (BTU/lb) = 146.58C + 568.78H + 29.45 - 6.58\ Ash - 51.53\ (O + N)$$

$$HHV_{feed} = 7302.595\ BTU/lb = 16.96\ MJ/kg$$

In our work, the saturated steam is heated by two super heaters. They increase the temperature of steam to above 400^{o}C before sending into the reactor. The high enthalpy steam is produced by supplying heat continuously to the saturated steam. The temperature-enthalpy diagram for the superheated steam is given in below figure (Fig. 4.28).

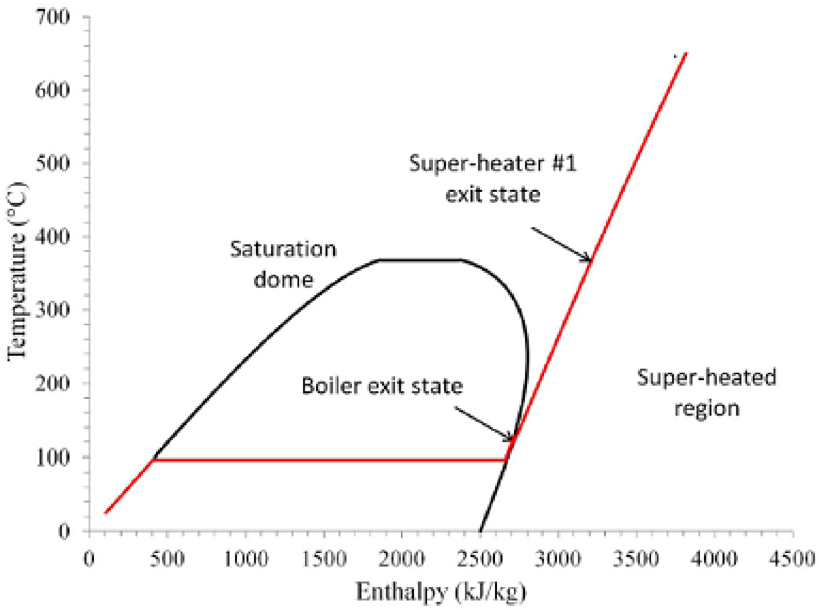

Fig. 4.28 Steam-enthalpy plot (Temperature vs. Enthalpy)

Corresponding to the superheated steam temperature of 400°C, the enthalpy is calculated as 3.2 MJ/kg.

The heat input to the plant is calculated individually for all the furnaces by measuring the resistance of the ceramic heaters and the current flowing into the heaters for maintaining the temperature of the reactor and other vessels.

The electrical energy $=I^2 \times R \times t$; where, 't' is the time that the heater is exposed to the voltage as per the PID controller which controls the heat input to the heaters. The energy input has been cumulatively summed up for the entire run time.

For pumps and motors, the energy consumption was measured directly using load meter.

- Higher Heating Value of product gas = Product gas mass flow (wt fr. H_2* HHV-H_2 + wt.fr.C_2H_4*HHV-C_2H_4 + wt.fr.CH_4*HHV-CH_4) = 1191.5*(0.053*141.8 + 0.029*47.195 + 0.046*50) =13.36 MJ
- Higher Heating Value of feed= mass flow of biomass x weight fraction of biomass which is ash and moisture free x HHV of biomass =1.164*0.795*18.4 = 17.03 MJ
- $H_{(\text{heating + Utilities})}$ = Measured using energy meter = 4.76 MJ
- Enthalpy of steam = mass flow of steam x enthalpy of superheated steam = 1.164*3.2 = 3.73 MJ

Hence **Overall Energy efficiency** = 13.36 / (17.03 +4.76 + 3.73) *100 = **52%**

Here, the external heating of the furnaces are carried out using electric heaters and the efficiency of electric heaters is nearly 85%. Hence, an additional 15% energy loss is accounted for thermal losses. This indicates that the overall efficiency can be as high as 67% or greater depending on the type of biomass being used.

Once the parametric data of the energy efficiency and corresponding elemental hydrogen production data are available, hydrogen production costs can be calculated.
The hydrogen production cost = Processing energy cost/ kg of H_2 produced
In case of steam methane reforming, the production cost per kg of hydrogen production =
Rs. 160/ kg H_2 at a natural gas cost of Rs. 45/kg.

In case of the present work, the cost of hydrogen produced is calculated to be
= Rs. (1.164 x 1.0 + 1.3x3 + 1.164 x 1.5) / (0.053*1.191) kg= **Rs. 203/ kg H_2**
Wherein the biomass cost is assumed as Rs. 1.0/ kg; Heating cost (electricity cost) = Rs. 3/kWh; steam cost is taken as Rs. 1.5/kg.
This cost excludes purification costs required to produce very high pure hydrogen (more than 99% purity) from moderate purity hydrogen product gas.

The below table highlights key experimental results in comparison with theoretical values and that available in literature on corresponding platforms.

Table 4.21 Comparison of rice husk steam gasification experimental results with theoretical values and literature

Particulars	Laboratory scale	Continuous process	Simulation results	Literature results
Biomass carbon conversion efficiency, %	92%	90%- 95%	96%	More than 90%
Gas yield (primary gasification stage), Nm^3/kg	1.25	0.87	--	Not available
Overall Gas yield, Nm^3/kg	1.46	1.35	2.3	1.3 [119]
% Composition in product gas (primary gasification stage)	H_2: 19-20% CO: 48-50% CO_2: 10-12%	H_2: 27% CO: 53% CO_2: 12.6%	H_2: 28.94% CO: 42.11% CO_2: 27.63%	Not available
% Composition in product gas (Final after secondary conversion)	H_2: 53% CO: 0.70% CO_2: 40%	H_2: 52-61% CO: 0.02% CO_2: 39%	H_2: 67.31% CO: 0.00% CO_2: 31.73%	Not available
Overall H_2 yield, g/kg biomass	70.1	63.14	141.4	64.28 [119] 65 [120]

From the above table, it is established that the biomass carbon conversion from the steam gasification platform is found to be at par with the theoretically simulated results. The gas yields and hydrogen yields are superior when the lab scale process results are compared with similar scale lab scale results based on rice husk gasification, reported in literature. The gas yield and hydrogen yield from continuous process of the present work were slightly less as compared to the lab scale process. This is considered to be due to the time-average effect in continuous mode of operation. The yields based on simulation are much higher than the experimental values. This could be attributed to the enhanced extraction of hydrogen from superheated steam at the prevailing gasification and secondary reforming and CO shift conditions; which may not be representative of the physical system.

4.6 Conclusions

Biomass has received more attention in recent years as an alternative source of energy due to its environmental benefits. It has the potential to save fossil fuels and impart energy security in the country. However, widespread implementation of biomass based processes mainly depends on the cost competitiveness of biomass-based fuels and availability of biomass as compared to those produced from conventional fossil sources. Hydrogen is the most pure form of energy which can be used as a fuel. But almost all the commercial processes available for production of hydrogen are based on steam reforming of fossil fuels.

Currently, the most effective method for production of hydrogen from biomass is steam gasification. In the present work, major parameters contributing to maximum thermal conversion efficiency have been studied in detail. This study resulted in identification of optimized conditions leading to higher carbon conversion and gas yield.

The goal of this work was to translate the laboratory scale experimental results to a continuous mode process for production of hydrogen from biomass. The process conditions for steam gasification as well as pyrolysis were optimized at lab scale in the batch experimental unit for primary biomass conversion using two different biomass materials- rice husk and deoiled jatropha cake respectively. Hydrogen rich gas was produced by secondary conversion of gasified vapour from steam gasification stage. In similar pathway, the pyrolytic liquid was also reformed to produce hydrogen rich product gas.

The lab results on steam gasification of rice husk followed by secondary fixed bed catalytic conversion in an integrated operation showed 92% biomass conversion at overall gas yield of 1.46 Nm^3/kg biomass with a hydrogen concentration of 53 vol.%. On the other hand, the bio-oil (pyrolysis oil) yield obtained from steam pyrolysis of jatropha cake biomass was 43 wt%. The bio-oil was then reformed in fixed bed reactor to obtain hydrogen rich product gas.

Further, the continuous mode process was conceptualized, designed, assembled and demonstrated based on the data generated from the lab scale studies.

Optimum biomass conversion at the primary steam gasification stage was more than 90% and was even as high as 95% at high temperatures and high steam/biomass ratios. The product gas yield after the secondary conversion of the gasified vapours was gone upto 118 wt% based on ash-free biomass (or 1.35 Nm^3/kg biomass) with a very high hydrogen concentration of 52 to 61 vol.% in the product gas.

The major highlights of the research work are summarised below;

- A modified biomass gasification system comprising of an externally heated tubular reactor with an internal mixing element or screw conveyor was conceptualized and experimentally validated. Uniform heating rate along the length of the reactor and higher biomass residence time were achieved.
- Biomass conversion more than 90% could be achieved on ash free basis. Left over biochar contained less than 25% carbon.
- In case of steam gasification of rice husk, product gas yield upto 89 wt% and 118 wt% based on the ash free-biomass were obtained in the primary gasification stage and secondary conversion stage respectively. The increase of gas yield in the second stage was above 100% because steam in the water gas shift reaction also contributed to the gas yield. The overall hydrogen make from the integrated steam gasification-and-catalytic conversion was 63.14 g/kg biomass at 61% purity.
- Pyrolysis of deoiled cake of Jatropha in the new reactor system yielded maximum pyrolytic liquid yield of 43 wt%. Pyrolytic oil is subjected to steam reforming to obtain hydrogen rich gas. The bio-oil conversion was 90% in the first hour of reaction. However, decay in the catalyst activity was observed later. But repeated regeneration and reforming runs showed stable performance. Continuous mode operation of this process requires employment of two reactors in parallel keeping one on reaction and the other on regeneration.
- The continuous mode steam gasification plant demonstrated the scalability and efficiency aspects of the process. The continuous mode process was run for a definite steady state period. Reactor skin temperatures at equidistant points, and corresponding internal temperatures, steam flow rate, system pressure and biomass flow rate were maintained constant throughout the runs. The corresponding product gas flow rate and gas concentrations were recorded and found to be invariably constant. Also, feasibility of scale-up of the process has been investigated by the two parameters – Hydrogen Conversion Efficiency and Overall Energy Efficiency. Their values obtained are 105% and 52% respectively, which are satisfactory numbers for an R&D scale process.

Profitability Indicators:

At present, biomass gasification for production of hydrogen would not be as attractive as steam reforming process, but there are few profitability indicators which will work as drivers for future economic implementation of hydrogen energy from biomass. The drivers are given below.

1. Use of biomass rich in carbon and hydrogen
2. Better heat management in the system like, steam generation using waste heat.
3. External heating cost is calculated by electricity cost. In an ideal system, the external heating system can be substituted with biomass generated hot gas energy.
4. Natural Gas price hike could make the biomass based hydrogen competitive.

Selection of appropriate feedstock is important as it accounts for effective utilization of energy spent for conversion of biomass. Agricultural residues having higher calorific value and lower moisture levels will have to be used for obtaining better gas yield.

Electrical heaters are used for heating the reactor and other equipments to required temperature levels. Taking consideration of the losses in electrical heating and reducing the losses encountered in the heating process by better heat management can reduce the processing energy requirement. Also, in the laboratory unit, the product gas from the reactor is directly cooled to room temperature; but in industrial process, with the help of proper heat recovery systems, we can maximize the overall energy utilization.

Although natural gas price volatility is an extraneous factor, the economics of the biomass gasification process is highly dependent on the economics of the parallel competing process of production of hydrogen from reforming of natural gas.

It has been demonstrated that the Auger (screw conveyor) reactors offer high heating rates when they are heated externally. They are compact and robust. They don’t practically require any carrier gas and offer good flexibility in feed stock size and properties, and may have biomass processing capacities from 50 to 100 ton/day. Another advantage is adjustable biomass residence time in terms of length and variable turning frequency of the screw conveyor. Hence, unlike fluidized bed systems, bigger biomass particles (upto 5 mm) can be used and longer biomass residence times and higher steam-to-biomass ratios can be achieved for complete devolatilization and char removal. The research presented in this work provides new information on biomass gasification process design, operating conditions that would result in higher overall efficiency for conversion of biomass into hydrogen via. steam gasification. The unique reactor design enables control of residence time adjustment of rotational speed of the screw conveyor, better heat transfer by continuous stirring and exposure of new solid surfaces to the gasification agent. The disadvantages faced in these type of reactors have been alleviated by improved design such as a) elimination of wear and leakage in the system by incorporating the fin cooling mechanism at the product gas end to cool the rotary joint, b) external seal cooling arrangement in the feeding section to safeguard the motor seal and nitrogen/air for motor seal cooling can be eliminated and c) efficient mixing of steam and biomass immediately at the mixing zone at feed inlet by use of venturi mixers.

Process integration of screw conveyor reactor with down-stream separation equipments like cyclone separator, gas-liquid separator would be comparatively easy as the gas velocity and flow rate are moderate when compared to a fluidized bed reactor system. Thus, the fine char and condensate carry-over in the product gas stream are reduced.

The following are the salient features of the unique steam gasification process developed through the current work.

- Low sensitivity in terms of changes in feed composition, and size of feed. Less requirement of feed preparation
- Uniform reaction temperature, Enhanced mass transfer due to continuous rotational mixing of biomass and steam in the screw conveyor reactor
- Enhanced heat transfer due to better metal-to-metal conductive heat transfer between the reactor body and internal screw conveyor.
- Good ability to control the process parameters like temperature, steam-to-biomass ratio and residence time; uniform process parameters.
- Very low tar concentration in the product gas
- High carbon conversion
- Simple construction and easy start-up
- Reduced investment cost due to reduction in stainless steel material cost
- Reduced operation cost due to less use of inert gas

4.7 Limitations and scope for future research

Gasification technology is a sustainable solution for conversion of residual biomass to syngas. Large scale development of gasification technology has few hindrances. The major problems faced by the technologies are;

- Presence of contaminants/ pollutants in the product gas, like tar, ammonia, chloridic gases etc. For long term sustenance of the plant, it is required to remove all the contaminants to very low level. In this context, ultra fine filters, mist eliminators with moderate pressure drop are required to be used in the product gas lines which will avoid carry-over of these contaminants from product gas.
- High energy efficiency of biomass conversion by way of efficient heat recovery systems (for e.g. Organic Rankine Cycle or heating-cooling cycles) is also the key for success of such a plant.
- Feeding systems that are able to operate under positive pressure but without the complex and failure prone arrangements of lock hoppers and rotary valves would be an important development.
- In-situ separation of hydrogen from gasified product gas by use of high temperature molecular separators like ceramic membranes or composite membranes could reduce the complexity of the process by process intensification.

##

5.0 References

[1] D. Wang, W. Yuan, W. Ji, Char and char-supported nickel catalysts for secondary syngas cleanup and conditioning, Appl. Energy 88(2011)1656–1663.

[2] B. Liu, S. Ji, Comparative study of fluidized-bed and fixed-bed reactor for syngas methanation over Ni-W/TiO_2-SiO_2 catalyst, J. Energy Chem. 22 (2013) 740–746.

[3] Y. Chhiti, M. Peyrot, S. Salvador, Soot formation and oxidation during bio-oil gasification: experiments and modeling, J.Energy Chem. 22 (2013) 701–709.

[4] S. Chopra, A. K. Jain, A review of fixed bed gasification systems for biomass, Agricultural Engineering International: The CIGR Ejournal. Invited Overview no.5, vol IX (2007).

[5] M. A. Adnan, H. Susanto, H. Binous, O. Muraza, M.H. Hossain, Enhancement of hydrogen production in a modified moving bed downdraft gasifier- A thermodynamic study including tar, Int. J. Hydrogen Energy 42 (2017) 10971-985.

[6] Z. Abu El-Rub, E. A. Bramer, G. Brem, Review of catalysts for tar elimination in biomass gasification processes, Ind. Eng. Chem. Res. 43 (2004) 6911-6919.

[7] J. Mazumder, H. De Lasa, Fluidizable Ni/La_2O_3-gAl_2O_3 catalyst for steam gasification of a cellulosic biomass surrogate, Appl. Catal. B (2014) 160- 167.

[8] H. Susanto, A. A. C. M. Beenackers, A moving-bed gasifier with internal recycle of pyrolysis gas, Fuel 75 (1996) 1339-1347.

[9] Y. Matsumura, hydrothermal gasification of biomass, Recent advances in thermochemical conversion of biomass, Ch. 9 (2015) 251-267.

[10] A.A.P. Susastriawana, Harwin Saptoadi, Purnomo, Small-scale downdraft gasifiers for biomass gasification: A review, Renew. Sustain. Energy Rev. 76 (2017) 989–1003.

[11] V. Kirubakaran, V. Sivaramakrishnan, R. Nalini, T. Sekar, M. Premalatha, P. Subramanian, A review on gasification of biomass. Renew. Sustain. Energy Rev. 13 (1) (2009) 179–186.

[12] D. Pawel, M. R. Izadpanah, W. Yang, W. Blasiak, Effect of pressure drop due to grate-bed resistance on the performance of downdraft gasifier, Energy and Fuels 25(2011) 5366-5377.

[13] K. Umeki, K. Yamamoto, T. Namioka, K. Yoshikawa, High temperature steam-only gasification of woody biomass, Appl. Energy 87 (2010) 791–798.

[14] S. D. Ferreira, I. P. Lazzarotto, J. Junges, C. Manera, M. Godinho, E. Osório, Steam gasification of biochar derived from elephant grass pyrolysis in a screw reactor, Energy Convers. Manage. 153 (2017) 163–174.

[15] A.V. Bridgwater, The technical and economic feasibility of biomass gasification for power generation, Fuel 74 (1995) 631–653.

[16] J. Gil, J. Corella, M.P. Aznar, M.A. Caballero, Biomass gasification in atmospheric and bubbling fluidized bed: effect of the type of gasifying agent on the product distribution, Biomass Bioenerg. 17 (1999) 389–403.

[17] W.F. De Groot, G.N. Richards, Relative rates of carbon gasification in oxygen, steam and carbon dioxide, Carbon 27 (2) (1989) 247–252.

[18] S. Turn, C. Kinoshita, Z. Zhang, D. Ishimura, J. Zhou, An experimental investigation of hydrogen production from biomass gasification, Int. J. Hydrogen Energy 23 (8) (1998) 641–648.

[19] C. Pfeifer, S. Koppatz, H. Hofbauer, Steam gasification of various feedstocks at a dual fluidised bed gasifier: Impacts of operation conditions and bed materials, Biomass Conv. Biorefinery 1 (1) (2011) 39–53.

[20] M. Campoy, A. Gómez-Barea, A.L. Villanueva, P. Ollero, Air–steam gasification of biomass in a fluidized bed under simulated autothermal and adiabatic conditions, Ind. Eng. Chem. Res. 47 (2008) 5957–5965.

[21] M. Campoy, A. Gómez-Barea, F.B. Vidal, P. Ollero, Air–steam gasification of biomass in a fluidised bed: process optimisation by enriched air, Fuel Processing Technology 90 (2009) 677–685.

[22] T. Seitarides, C. Athanasiou, A. Zabaniotou, Modular biomass gasification-based solid oxide fuel cells (SOFC) for sustainable development. Renew. Sustain. Energy Rev. 12 (2008) 1251–1276.

[23] A. V. Bridgwater, Renewable fuels and chemicals by thermal processing of biomass, Chem. Eng. J. 91 (2003) 87–102.

[24] H. A. M. Knoef, Handbook of biomass gasification. BTG biomass technologies group, B.V. Meppel, The Netherlands.

[25] F. Mermoud, F. Golfier, S. Salvador, L. Van de Steene, J. L. Dirion, Experimental and numerical study of steam gasification of a single charcoal particle, Combustion and Flame 145 (2006) 59–79.

[26] G. Schuster, G. Löffler, K. Weigl, H. Hofbauer, Biomass steam gasification—an extensive parametric modeling study, Bioresour. Technol. 77 (2001) 71–79.

[27] A. A. Boateng, W. P. Walawender, L. T. Fan, C. S. Chee, Fluidized-bed steam gasification or rice hull, Bioresour. Technol. 40 (1992) 235–239.

[28] J. M. Encinar, J. F. González, J. J. Rodríguez, M. J. Ramiro, Catalysed and uncatalysed steam gasification of eucalyptus char: influence of variables and kinetic study, Fuel 80 (2001) 2025–2036.

[29] J. M. Encinar, J. F. González, J. González, Steam gasification of Cynara cardunculus L.: influence of variables, Fuel Process. Technol. 75 (2002) 27–43.

[30] C. Franco, F. Pinto, I. Gulyurtlu, I. Cabrita, The study of reactions influencing the biomass steam gasification process, Fuel 82 (2003) 835–842.

[31] J.F. González, S. Román, D. Bragado, M. Calderón, Investigation on the reactions influencing biomass air and air/steam gasification for hydrogen production, Fuel Processing Technology 89 (2008) 764–772.

[32] L. Wei, S. Xu, L. Zhang, C. Liu, H. Zhu, S. Liu, Steam gasification of biomass for hydrogen-rich gas in a free-fall reactor, Int. J. Hydrogen Energy 32 (2007) 24-31.

[33] M. Campoy, A. Gómez-Barea, A. L. Villanueva, P. Ollero, Air–steam gasification of biomass in a fluidized bed under simulated autothermal and adiabatic conditions, Ind. Eng. Chem. Res. 47 (2008) 5957–5965.

[34] A. A. Boateng, W. P. Walawender, L. T. Fan, C. S. Chee, Fluidized-bed steam gasification or rice hull, Bioresour. Technol. 40 (1992) 235–239.

[35] C. Franco, F. Pinto, I. Gulyurtlu, I. Cabrita, The study of reactions influencing the biomass steam gasification process, Fuel 82 (2003) 835–842.

[36] A. Kumar, K. Eskridge, D. D. Jones, M. A. Hanna, Steam–air fluidized bed gasification of distillers grains: effects of steam to biomass ratio, equivalence ratio and gasification temperature, Bioresour. Technol. 100 (2009) 2062–2068.

[37] P. M. Lv, Z. H. Xiong, J. Chang, C. Z. Wu, Y. Chen, J. X. Zhu, An experimental study on biomass air–steam gasification in a fluidized bed, Bioresour. Technol. 95 (2004) 95–101.

[38] S. Rapagnà, A. Latif, Steam gasification of almond shells in a fluidised bed reactor: the influence of temperature and particle size on product yield and distribution, Biomass Bioener. 12 (4) (1997) 281–288.

[39] K. Umeki, K. Yamamoto, T. Namioka, K. Yoshikawa, High temperature steam-only gasification of woody biomass, Applied Energy 87 (2010) 791–798.

[40] P. Lv, Z. Yuan, L. Ma, C. Wu, Y. Chen, J. Zhu, Hydrogen-rich gas production from biomass air and oxygen/steam gasification in a downdraft gasifier, Renew. Energy 32 (2007) 2173–2185.

[41] B. Acharya, A. Dutta, P. Basu, An investigation into steam gasification of biomass for hydrogen enriched gas production in presence of CaO, Int. J. Hydrogen Energy 35 (2010) 1582–1589.

[42] G. Gordillo, K. Annamalai, N. Carlin, Adiabatic fixed-bed gasification of coal, dairy biomass, and feedlot biomass using an air–steam mixture as an oxidizing agent, Renew. Energy 34 (2009) 2789–2797.

[43] C. Lucas, D. Szewczyk, W. Blasiak, S. Mochida, High-temperature air and steam gasification of densified fuels, Biomass Bioenerg. 27 (2004) 563–575.

[44] S. Luo, B. Xiao, X. Guo, Z. Hu, S. Liu, M. He, Hydrogen-rich gas from catalytic steam gasification of biomass in a fixed bed reactor: influence of particle size on gasification performance, Int. J. Hydrogen Energy 34 (2009) 1260–1264.

[45] A. Ponzio, S. Kalisz, W. Blasiak, Effect of operating conditions on tar and gas composition in high temperature air/steam gasification (HTAG) of plastic containing waste, Fuel Process. Technol. 87 (2006) 223–233.

[46] J. M. Encinar, J. F. Gnzález, J. J. Rodríguez, M. J. Ramiro, Catalysed and uncatalysed steam gasification of eucalyptus char: influence of variables and kinetic study, Fuel 80 (2001) 2025–2036.

[47] J. M. Encinar, J. F. González, J. González, Steam gasification of Cynara cardunculus L.: influence of variables, Fuel Process. Technol. 75 (2002) 27–43.

[48] V. Skoulou, A. Swiderski, W. Yang, A. Zabaniotou, Process characteristics and products of olive kernel high temperature steam gasification (HTSG), Bioresour. Technol. 100 (2009) 2444–2451.

[49] G. Hu, S. P. Xu, S. G. Li, C. R. Xiao, S. Q. Liu, Steam gasification of apricot stones with olivine and dolomite as downstream catalysts, Fuel Process. Technol. 87 (2006) 375-382.

[50] R. A. Knight, Experience with raw gas analysis from pressurized gasification of biomass, Biomass Bioenerg. 18 (2000) 67-77.

[51] T. M. Ismail, E. A. El-Salam, Parametric studies on biomass gasification process on updraft gasifier high temperature air gasification, Appl. Therm. Eng. 112 (2017) 1460-1473.

[52] V. Minkova, S. P. Marinov, R. Zanzi, E. Bjornborm, T. Budinova, M. Stefanova, L. Lakov, Thermochemical treatment of biomass in a flow of steam or in a mixture of steam and carbon dioxide, Fuel Process. Technol. 62 (2000), 45-52.

[53] L. Garcia, M. L. Salvador, J. Arauzo, R. Bilbao, CO_2 as a gasifying agent for gas production from pine saw dust at low temperatures using a Ni/Al co-precipitated catalyst, Fuel Process. Technol. 69 (2001), 157-174.

[54] V. Pallozzi, A. Di Carlo, E. Bocci, M. Villarini, P. U. Foscolo, M. Carlini, Performance evaluation at different process parameters of an innovative prototype of biomass gasification system aimed to hydrogen production, Energy Convers. Manage. 130 (2016) 34-43.

[55] E. Balu, U. Lee, J. N. Chung, High temperature steam gasification of woody biomass-A combined experimental and mathematical modeling approach, Int. J. Hydrogen Energy 40 (2015) 14104- 14115.

[56] A. D'Orazia, S. Rapagna, P. U. Foscolo, K. Gallucci, M. Nacken, S. Heidenreich, A. Di Carlo, A. Dell'Era, Gas conditioning in H_2 rich syngas production by biomass steam gasification: Experimental comparison between three innovative ceramic filter candles, Int. J. Hydrogen Energy 40 (2015) 7282- 7290.

[57] A. Rapagna, A. Latif, Steam gasification of almond shells in a fluidized bed reactor: the influence of temperature and particle size on product yield and distribution. Biomass Bioenerg. 12 (1997) 281-288.

[58] S. Luo, B. Xiao, X. Guo, Z. Hu, S. Liu, M. He, Hydrogen-rich gas from catalytic steam gasification of biomass in a fixed bed reactor: Influence of particle size on gasification performance. Int J Hydrogen Energy 34 (2009) 1260-64.

[59] P. M. Lv, Z. H. Xiong, J. Chang, C. Z. Wu, Y. Chen, J. X. Zhu, An experimental study on biomass air-steam gasification in a fluidized bed, Bioresour. Technol. 95 (2004) 95-101.

[60] T. B. Reed, MSW gasification principle and technology, Park Ridge, New Jersey: Noyes Data Corporation, 1981.

[61] N. Jand, P. U. Foscolo, Decomposition of wood particles in fluidized beds, Ind. Eng. Chem. Res. 44 (2005) 5079-5089.

[62] S. Rapagna, G. M. Di Celso, Devolatilization of wood particles in a hot fluidized bed: product yields and conversion rates, Biomass Bioenerg. 32 (2008) 1123-1129.

[63] J. J. Hernandez, G. A. Almansa, A. Bula, Gasification of biomass wastes in an entrained flow gasifier: effect of the particle size and the residence time, Fuel Process. Technol. 91 (2010) 681-692.

[64] P.M. Lv, Z. H. Xiong, J. Chang, C. Z. Wu, Y. Chen, J. X. Zhu, An experimental study on biomass air-steam gasification in a fluidized bed. Bioresour. Technol. 95 (2004) 95-101.

[65] N. Nipattummakul, I. Ahmed, A. K. Gupta, S. Kerdsuwan, Hydrogen and syngas yield from residual branches of oil palm tree using steam gasification. Int. J. Hydrogen Energy 36 (2011) 3835-3843.

[66] L. Garcia, A. Benedicto, E. Romeo, M. L. Salvador, J. Arauzo, R. Bilbao, Hydrogen production by steam gasification of biomass using Ni-Al coprecipitated catalysts promoted with magnesium. Energy Fuel 16 (2002) 1222-1230.

[67] A. Demirbas, Hydrogen-rich gases from biomass via pyrolysis and air-steam gasification. Energy Sources, Part A 31 (2009) 1728-1736.

[68] A. Inayat, M. M. Ahmad, M. I. A. Mutalib, S. Yusup, Effect of process parameters on hydrogen production and efficiency in biomass gasification using modelling approach, J. Appl. Sci. 10 (2010) 3183-3190.

[69] H. de Lasa, E. Salaices, J. Mazumder, R. Lucky, Catalytic steam gasification of biomass: catalysts, thermodynamics and kinetics, Chem. Rev. 111 (2011) 5404-5433.

[70] Y. Kalinci, A. Hepbasli, I. Dincer, Biomass-based hydrogen production: a review and analysis, Int. J. Hydrogen Energy 34 (2009) 8799-8817.

[71] M. Ni, D. Y. C. Leung, M. K. H. Leung, K. Sumathy, An overview of hydrogen production from biomass. Fuel Process. Technol. 87 (2006) 467-472.

[72] P. Corte, C. Lacoste, J. P. Traverse, Gasification and catalytic conversion of biomass by flash pyrolysis. J. Anal. Appl. Pyrolysis 7 (1985) 323-335.

[73] L. Garcia, A. Benedicto, E. Romeo, M. L. Salvador, J. Arauzo, R. Bilbao, Hydrogen production by steam gasification of biomass using Ni-Al coprecipitated catalysts promoted with magnesium. Energy Fuel 16 (2002) 1222-1230.

[74] L. Devi, K. J. Ptasinski, F. J. J. G. Janssen, A review of the primary measures for tar elimination in biomass gasification processes. Biomass Bioenergy 24 (2003) 125-40.

[75] D. Sutton, B. Kelleher, J. R. H. Ross, Review of literature on catalysts for biomass gasification, Fuel Process. Technol. 73 (2001) 155-173.

[76] J. Arauzo, D. Radlein, J. Piskorz, D. S. Scott, Catalytic pyrogasification of biomass-evaluation of modified nickel catalyst, Ind. Eng. Chem. Res. 36 (1997) 67-75.

[77] A. Olivares, M. P. Aznar, M. A. Caballero, J. Gil, E. Frances, J. Corella, Biomass Gasification: produced gas upgrading by in-bed use of dolomite, Ind. Eng. Chem. Res. 36 (1997) 5220-5226.

[78] J. Remon, F. Broust, G. Volle, L. Garcia, J. Arauzo. Hydrogen production from pine and poplar bio-oils by catalytic steam reforming. Influence of the bio-oil composition on the process, Int. J. Hydrogen Energy 40 (2015) 5593-5608.

[79] J. Remon, F. Broust, J. Valette, Y. Chhiti, I. AlavaI, A. R. Fernandez-Akarregi, L. Garcia, J. Arauzo. Production of a hydrogen-rich gas from fast pyrolysis bio-oils: Comparison between homogeneous and catalytic steam reforming routes, Int. J. Hydrogen Energy 39 (2014) 171-182.

[80] C. Tianju, W. Ceng, L. Ronghou. Steam reforming of bio-oil from rice husks fast pyrolysis for hydrogen production, Bioresour. Technol. 102 (2011) 9236–9240.

[81] L. Xiao, X. Jun, D. Yuzhao, S. Laihong, Z. Yayun, Experimental study on biomass steam gasification for hydrogen-rich gas in double-bed reactor, Int. J. Hydrogen Energy 39 (2014) 20968-20978.

[82] L. Siyi, X. Bo, H. Zhiquan, L. Shiming, G. Xianjun, H. Maoyun, Hydrogen-rich gas from catalytic steam gasification of biomass in a fixed bed reactor: Influence of temperature and steam on gasification performance, Int. J. Hydrogen Energy 34 (2009) 2191-2194.

[83] K. Zakir, Y. Suzana, M.A. Munri, L.F.C. Bridgid, Hydrogen production from palm kernel shell via integrated catalytic adsorption (ICA) steam gasification, Energy Convers. Manage. 87 (2014) 1224-1230.

[84] W. Fredrik, W. Henrik, H. Henry, W. Jonas, P. Esbjorn, G. Rikard, Influence of process parameters on the performance of an oxygen blown entrained flow biomass gasifier, Fuel 153 (2015) 510–519.

[85] A.M. Reza, Y. Suzana, A. Wan, N. Shahab, T. Ahmad, Investigation on product gas production via biomass conversion through the integration of pyrolysis and air–steam gasification processes, Energy Convers. Manage. 87 (2014) 670-675.

[86] F. Sylvain, B. Sayyed-Mohsen, G. Hojat, S. M. Rasoul, An experimental study on hydrogen-rich gas production via steam gasification of biomass in a research-scale fluidized bed, Renew. Energy 72 (2014) 271-283.

[87] P. Prakash, N. K. Sheeba, Hydrogen production from steam gasification of biomass: Influence of process parameters on hydrogen yield: A review, Renew. Energy 66 (2014) 570-579.

[88] Q. M. K. Waheed, W. Chunfei, P. T. Williams, Pyrolysis/reforming of rice husks with a Ni-dolomite catalyst: Influence of process conditions on product gas and hydrogen yield, J. Energy Institute 89(4) (2015) 657-667.

[89] A. Mohammad, Biomass gasification gas cleaning for downstream applications: A comparative critical review, Renew. Sustain. Energy Rev. 40 (2014) 118-132.

[90] A. Jon, K. Shogo, W. Chunfei, Y. Toshiaki, B. Javier, O. Martin, T. W. Paul, Hydrogen production from biomass and plastic mixtures by pyrolysis-gasification, Int. J. Hydrogen Energy 39 (2014) 10883- 10891.

[91] M. A. A. Mohammed, A. Salmiaton, W. A. K. G. Wan Azlina, M. S. Mohammad Amran, A. Fakhru'l-Razi, Y. H. Tufiq-Yap, Hydrogen rich gas from oil palm biomass as a potential source of renewable energy in Malaysia, Renew. Sustain. Energy Rev. 15 (2011) 1258-1270.

[92] F. Abnisa, W. M. A. Wan Daud, A review on co-pyrolysis of biomass: An optional technique to obtain high-grade pyrolysis oil, Energy Convers. Manage. 87 (2014) 71–85.

[93] M. Guillain M, K. Fairouz K, S. R. Mar, F. Monique, L. D. Jacques, Attrition-free pyrolysis to produce bio-oil and char, Bioresour. Technol. 100 (2009) 6069–6075.

[94] S. Vitolo, M. Seggiani, P. Frediani, G. Ambrosini, L. Politi, Catalytic upgrading of pyrolytic oils to fuel over different zeolites, Fuel 78 (1999) 1147–1159.

[95] A. Oasmaa, S. Czernik, Fuel oil quality of biomass pyrolysis oils-state of the art for the end users, Energy Fuel 13 (1999) 914–921.

[96] A. V. Bridgwater, Review of fast pyrolysis of biomass and product upgrading, Biomass Bioenergy 38 (2012) 68–94.

[97] E. P. Onal, B. B. Uzuna, A. E. Putun, Steam pyrolysis of an industrial waste for bio-oil production, Fuel Process. Technol. 92 (2011) 879−885.

[98] A. V. Bridgwater, Review of fast pyrolysis of biomass and product upgrading, Biomass Bioenergy 38 (2012) 68−94.

[99] M. Sagehashi, N. Miyasaka, H. Shishido, A. Sakoda, Superheated steam pyrolysis of biomass elemental components and Sugi (Japanese cedar) for fuels and chemicals, Bioresour. Technol. 97(11) (2006), 1272−1283.

[100] C. A. Mullen, A. A. Boateng, N. M. Goldberg, I. M. Lima, D. A. Laird, K. B. Hicks, Bio-oil and bio-char production from corn cobs and stover by fast pyrolysis, Biomass Bioenergy 34 (2010), 67−74.

[101] A. E. Pütün, E. Apaydın, E. Pütün, Rice straw as a bio-oil source via pyrolysis and steam pyrolysis, Energy 29 (2004), 2171− 2180.

[102] N. Yi, R. Si, H. Saltsburg, M. Flytzani-Stephanopoulos, Steam reforming of methanol over ceria and gold-ceria nanoshapes, Appl. Catal. B Environ. 95 (2010) 87-92.

[103] S. A. C. Carabineiro, A. M. T. Silva, G. Drazic, P. B. Tavares, J. L. Figueiredo, Gold nanoparticles on ceria supports for the oxidation of carbon monoxide, Catal. Today 154 (2010) 21-30.

[104] E. Aneggi, J. Llorca, M. Boaro, A. Trovarelli, Surface-structure sensitivity of CO oxidation over polycrystalline ceria powders, J. Catal. 234 (2005) 88-95.

[105] Z. Y. Yuan, V. Idakiev, A. Vantomme, T. Tabakova, T. Z. Ren, B. L. Su, Mesoporous and nanostructured CeO2 as supports of nano-sized gold catalysts for low-temperature water-gas shift reaction, Catal. Today 131 (2008) 203-10.

[106] Y. Shen, S. Zhu, T. Qiu, S. Shen, A novel catalyst of CeO_2/Al_2O_3 for selective catalytic reduction of NO by NH_3, Catal. Commun. 11 (2009) 20-23.

[107] J. Zhu, F. Gao, L. Dong, W. Yu, L. Qi, Z. Wang, Studies on surface structure of $MxOy/MoO_3/CeO_2$ system (M¼ Ni, Cu, Fe) and its influence on SCR of NO by NH_3. Appl. Catal. B Environ. 95 (2010) 144-152.

[108] B. Valle, B. Aramburu, C. Santiviago, J. Bilbao, A. G. Gayubo, Upgrading of Bio-Oil in a Continuous Process with Dolomite Catalyst, Energy Fuels 28 (2014) 6419−6428.

[109] S. Czernik, R. French, C. Feik, E. Chornet, Hydrogen by catalytic steam reforming of liquid byproducts from biomass thermoconversion processes. Ind. Eng. Chem. Res. 41 (17) (2002) 4209–4215.

[110] C. Rioche, S. Kulkarni, F. C. Meunier, J. P. Breen, R. Burch, Steam reforming of model compounds and fast pyrolysis bio-oil on supported noble metal catalysts. Appl. Catal., B. 61 (1-2) (2005) 130–139.

[111] A. C. Basagiannis, X. E. Verykios, Steam reforming of the aqueous fraction of bio-oil over structured $Ru/MgO/Al_2O_3$ catalysts, Catal. Today. 127 (1-4) (2007) 256–264.

[112] P. N. Kechagiopoulos, S. S. Voutetakis, A. A. Lemonidou, I. A. Vasalos, Hydrogen production via steam reforming of the aqueous phase of bio-oil in a fixed bed reactor, Energy Fuels 20 (2006) 2155–2163.

[113] D. Wang, S. Czernik, D. Montane, M. Mann, E. Chornet, Biomass to hydrogen via fast pyrolysis and catalytic steam reforming of the pyrolysis oil or its fractions, Ind. Eng. Chem. Res. 36 (1997) 1507–1518.

[114] J. D. Martinez, A. Veses, A. M. Mastral, R. Murillo, M. V. Navarro, N. Puy, Copyrolysis of biomass with waste tyres: upgrading of liquid bio-fuel, Fuel Process. Technol. 119 (2014) 263–271.

[115] M. Dinesh, U. P. Charles, H. S. Philip, Pyrolysis of wood/biomass for bio-oil: A critical review, Energy and Fuels 20 (2006) 848-889.

[116] J. N. Brown, Development of a lab-scale auger reactor for biomass fast pyrolysis and process optimization using response surface methodology, Graduate Theses and Dissertations Paper (2009) 10996.

[117] Y. Güray, R. Frederik, D. Rubenvan, P. Wolter, Challenges in the design and operation of processes for catalytic fast pyrolysis of woody biomass, Renew. Sustain. Energy Rev. 57 (2016) 1596–1610.

[118] R. Maximino, Pyrolysis of biomass residues in a screw reactor, Technical Report, https://fenix.tecnico.ulisboa.pt/downloadFile/395146017998/artigo_ricardo.pdf.

[119] H. Li, Q. Xu, H. Xue, Y. Yan, Catalytic reforming of the aqueous phase derived from fast-pyrolysis of biomass, Renew. Energy, 34 (12) (2009) 2872–2877.

[120] S. Czernik, R. Evans, R. French, Hydrogen from biomass production by steam reforming of biomass pyrolysis oil, Catal. Today 129 (2007) 265–268.

[121] C. Rioche, S. Kulkarni, F. C. Meunier, J. P. Breen, R. Burch, Steam reforming of model compounds and fast pyrolysis bio-oil on supported noble metal catalysts, Appl. Catal., B. 61 (2005) 130–139.

[122] A. C. Basagiannis, X. E. Verykios, Steam reforming of the aqueous fraction of bio-oil over structured Ru/MgO/Al_2O_3 catalysts, Catal. Today. 127 (2007) 256–264.

[123] P. N. Kechagiopoulos, S. S. Voutetakis, A. A. Lemonidou, I. A. Vasalos, Hydrogen production via steam reforming of the aqueous phase of bio-oil in a fixed bed reactor, Energy Fuels, 20 (2006) 2155–2163.

[124] D. Wang D, S. Czernik, D. Montane, M. Mann, E. Chornet, Biomass to hydrogen via fast pyrolysis and catalytic steam reforming of the pyrolysis oil or its fractions. Ind. Eng. Chem. Res. 36 (1997) 1507–1518.

[125] E. Chornet, S. Czernik, D. Wang, C. Gregoire, M. Mann, Biomass to hydrogen via pyrolysis and reforming, Proceedings of the DOE/NREL Hydrogen Program Review. Livermore, CA (1994).

[126] V. Pallozi, A. Di Carlo, E. Bocci, M. Villarini, P.U. Foscolo, M. Carlini, Performance evaluation at different process parameters of an innovative prototype of biomass gasification system aimed to hydrogen production, Energy Convers. Manage. 130 (2016) 34-43.

[127] E. Balu, J. N. Chung, System characteristics and performance evaluation of a trailer-scale downdraft gasifier with different feedstock, Bioresour. Technol. 108 (2012) 264-273.

[128] G. Guan, M. Kaewpanha, X. Hao, A. Abudula, Catalytic steam reforming of biomass tar: Prospects and challenges, Renew. Sustain. Energy Rev. 58 (2016) 450–461.

[129] G. Guan, M. Kaewpanha, X. Hao, A. Zhu, Y. Kasai, A. Kakuta, Steam reforming of tar derived from lignin over pompom-like potassium-promoted iron-based catalysts formed on calcined scallop shell, Bioresour. Technol. 139 (2013) 280–284.

[130] P. Kuchonthara, T. Vitidsant, A. Tsutsumi, Catalytic effects of potassium on lignin steam gasification with γ-Al_2O_3 as a bed material, Korean J. Chem. Eng. 25 (2008) 656–662.

[131] S. Zhang, M. Asadullah, L. Dong, H. L. Tay, C. Z. Li, An advanced biomass gasification technology with integrated catalytic hot gas cleaning- PartII: tar reforming using char as a catalyst or as a catalyst support, Fuel 112 (2013) 646–653.

[132] Z. Min, P. Yimsiri, M. Asadullah, S. Zhang, C. Z. Li, Catalytic reforming of tar during gasification- Part-II. Char as a catalyst or as a catalyst support for tar reforming, Fuel 90 (2011) 2545–2552.

[133] N. Laosiripojana, W. Sutthisripok, S. Charojrochkul, S. Assabumrungrat, Development of Ni–Fe bimetallic based catalysts for biomass tar cracking/reforming: Effects of catalyst support and co-fed reactants on tar conversion characteristics, Fuel Process. Technol. 127 (2014) 26-32.

[134] C. P. B. Quitete, M. M .V. M. Souza, Application of Brazilian dolomites and mixed oxides as catalysts in tar removal system, Appl. Catal. A: General 536 (2017) 1-8.

[135] D. Sutton, B. Kelleher, J. R. H. Ross, Review of literature on catalysts for biomass gasification, Fuel Process. Technol. 73 (3) (2001) 155-173.

[136] Q. M. K. Waheed, W. Chunfei, P. T. Williams, Pyrolysis/reforming of rice husks with a Ni-dolomite catalyst: Influence of process conditions on product gas and hydrogen yield, J. Energy Inst. 89 (2016) 657-667.

[137] L. Xiao, X. Jun, D. Yuzhao, S. Laihong, Z. Yayun, Experimental study on biomass steam gasification for hydrogen-rich gas in double-bed reactor, Int. J. Hydrogen Energy 39 (2014) 20968-20978.

[138] F. Sylvain, B. Sayyed-Mohsen, G. Hojat, S. M. Rasoul, An experimental study on hydrogen-rich gas production via steam gasification of biomass in a research-scale fluidized bed, Energy Convers. Manage. 91 (2015) 427-432.

[139] S. Czernik, R. French, C. Feik, E. Chornet, Hydrogen by catalytic steam reforming of liquid by-products from biomass thermoconversion processes, Ind. Eng. Chem. Res. 41 (17) (2002) 4209–4215.

[140] S. Abhishek, P. Vishnu, Z. Dongke, Biomass pyrolysis—A review of modelling, process parameters and catalytic studies, Renew. Sustain. Energy Rev. 50 (2015) 1081-1096.

[141] T. Bhaskar, H. S. Philip, Thermo-chemical Conversion of Biomass, Bioresour. Technol. 178 (2015) 1.

[142] C. Acikgoz, O. Onay, O. M. Kockar, Fast pyrolysis of linseed: product yields and compositions, J. Anal. Appl. Pyrol. 71 (2004) 417–429.

[143] F. Abnisa, W. M. A. Wan Daud, J. N. Sahu, Optimization and characterization studies on bio-oil production from palm shell by pyrolysis using response surface methodology, Biomass Bioenergy 35 (2011) 3604–3616.

[144] A. E. Putun, E. Apaydın, E. Putun, Rice straw as a bio-oil source via pyrolysis and steam pyrolysis, Energy 29 (2004) 2171–2180.

[145] I. Demiral, S. Ensoz, Fixed-bed pyrolysis of hazelnut (Corylus Avellana L.) bagasse: influence of pyrolysis parameters on product yields, Energy Source Part A 28 (2006) 1149–1158.

[146] F. X. Collard, J. Blin, A review on pyrolysis of biomass constituents: mechanisms and composition of the products obtained from the conversion of cellulose, hemicelluloses and lignin, Renew. Sustain. Energy Rev. 38 (2014) 594-608.

[147] N. Shu-Kuang, Benefit assessment of cost, energy and environment for biomass pyrolysis oil, J. Cleaner Production (2013) 141-149.

[148] M. Tripathi, J. N. Sahu, P. Ganesan, Effect of process parameters on production of biochar from biomass waste through pyrolysis: A review, Renew. Sustain. Energy Rev. 55 (2016) 467–481.

[149] E. Kantarelis, Y. Weihong, B. Wlodzimierz, Production of Liquid Feedstock from Biomass via Steam Pyrolysisin a Fluidized Bed Reactor, Energy Fuels, 27 (2013) 4748−4759.

[150] Tao-khan, S. Vladimir, J. E. Tim, Ligno-cellulosic biomass pyrolysis: A review of product properties and effects of pyrolysis parameters, Renew. Sustain. Energy Rev. 57 (2016) 1126-1140.

[151] D. Carpenter, L. Tyler, B. Westover, C. Stefan, J. Whitney, Biomass feedstocks for renewable fuel production: a review of the impacts of feedstock and pretreatment on the yield and product distribution of fast pyrolysis bio-oils and vapors, Green Chem. 16 (2014) 384-406.

[152] A. Renny, D. T. Gokak, S. Pankaj, G. Shalini, Novel hydrogen rich gas production by steam gasification of biomass in a research scale rotary tubular helical coil gasifier, Int. J. Ener. Res. 40 (13) (2016) 1788-1799.

[153] C. H. Biradar, K. A. Subramanian, M. G. Dastidar, Production and fuel quality upgradation of pyrolytic bio-oilfrom JatrophaCurcas de-oiled seed cake, Fuel, 119 (2014) 81–89.

[154] A. Jon, K. Shogo, W. Chunfei, Y. Toshiaki, B. Javier, O. Martin, T. W. Paul, Hydrogen production from biomass and plastic mixtures by pyrolysis-gasification, Int. J. Hydrogen Energy 39 (2014) 10883- 10891.

[155] M. A. A. Mohammed, A. Salmiaton, W. A. K. G. Wan Azlina, M. S. Mohammad Amran, A. Fakhru'l-Razi, Air gasification of empty fruit bunch for hydrogen-rich gas production in a fluidized-bed reactor, Energy Convers. Manage. 52 (2011) 1555–1561.

[156] M. A. A. Mohammed, A. Salmiaton, W. A. K. G. Wan Azlina, M. S. Mohammad Amran, A. Fakhru'l-Razi, Y. H. Taufiq-Yap, Hydrogen rich gas from oil palm biomass as a potential source of renewable energy in Malaysia. Renew. Sust. Energy Rev. 15 (2011), 1258-1270.

[157] A. Mohammad, Biomass gasification gas cleaning for downstream applications: A comparative critical review, Renew. Sustain. Energy Rev. 40 (2014) 118-132.

[158] L. Siyi, X. Bo, H. Zhiquan, L. Shiming, G. Xianjun, H. Maoyun, Hydrogen-rich gas from catalytic steam gasification of biomass in a fixed bed reactor: Influence of temperature and steam on gasification performance, Int. J. Hydrogen Energy 34 (2009) 2191-2194.

[159] Ge Pu, Z. Hu-Ping, H. Gong-tao, Study on Pine biomass air and oxygen/steam gasification in the fixed bed gasifier, Int. J. Hydrogen Energy 38 (2013) 157557-15763.

[160] P. Prakash, N. K. Sheeba, Hydrogen production from steam gasification of biomass: Influence of process parameters on hydrogen yield: A review, Renew. Energy 66 (2014) 570-579.

[161] L. Siyi, X. Bo, H. Zhiquan, L. Shiming, G. Xianjun, H. Maoyun, Hydrogen-rich gas from catalytic steam gasification of biomass in a fixed bed reactor: Influence of temperature and steam on gasification performance, Int. J. Hydrogen Energy 34 (2009) 2191-2194.

[162] F. Sylvain, B. Sayyed-Mohsen, G. Hojat, S. M. Rasoul, An experimental study on hydrogen-rich gas production via steam gasification of biomass in a research-scale fluidized bed, Energy Convers. Manage. 91 (2015) 427-432.

[163] Z. Baofeng, S. Xiaodong, M. Li, M. Guangfan, C. Li, X. Yi, Hydrogen production from biomass combining pyrolysis and the secondary decomposition, Int. J. Hydrogen Energy 35 (2010) 2606- 2611.

[164] J.R. Rolstrup-Nielson, J. H. Bak Hansen, CO_2 reforming of methane over transition metals, J. catalysis 144 (1993) 38-49.

[165] Z. Baofeng, X. Zhang, Lei-Chen, R. Qu, G.Meng, X. Yi, Li-Sun, Steam reforming of Toluene as model compound of biomass pyrolysis tar for hydrogen, Biomass and Bioenergy 34 (2010) 140-144.

[166] D. Swierczynski, C. Courson, A. Kiennemann, Study of steam reforming of toluene used as model compound of tar produced by biomass gasification, Chem. Eng. Process.: Process Intensification 47 (2008), 508-513.

[167] J Tao, L. Zhao, C. Dong, Q. Lu, X. Du, E. Dahlquist, Catalytic steam reforming of Toluene as a model compound of Biomass Gasification tar using Ni-CeO_2/SBA-15 catalysts, Energies 6 (2013) 3284-3296.

[168] G. Chen, J. Yao, H. Yang, B. Yan, H. Chen, Steam gasification of acid-hydrolysis biomass CAHR for clean syngas production, Bioresour. Technol. 179 (2015) 323-330.

[169] D. Y. Chen, D. Liu, H. R. Zhang, Y. Chen, Q. Li, Bamboo pyrolysis using TG-FTIR and a lab scale reactor: analysis of pyrolysis behaviour, product properties, and carbon and energy yields, Fuel 148 (2015) 79-86.

[170] S. Ucar, S. Karagoz, Co-pyrolysis of pine nut shells with scrap tires, Fuel 137 (2014) 85-93.

[171] A. A. Lappas, V. S. Dimitro Poulos, E. V. Antonakou, S. S. Voutetakis, I. A. Vasalos, Design, Construction, and operation of a transported fluid bed process development unit for biomass fast pyrolysis: Effect of pyrolysis temperature, Ind. Eng. Chem. Res. 47 (2008) 742-747.

[172] Q. Tingting, G. Wanjun, S. Lianhong, J. Xiao, K. Zhao, Experimental study of biomass pyrolysis based on three major components: hemicellulose, cellulose and Lignin, Ind. Eng. Chem. Res. 50 (2011) 10424-10433.

[173] C. Branca, C. Di Blasi, Multistep mechanism for the Devolatilization of biomass fast pyrolysis oils, Ind. Engg. Chem. Res. 45 (2006) 5891-5899.

[174] M. E. Bruna, C. D. Chagas, J. S. Michelle, A. M. Charles, A. B. Akwasi, A. F. Marcus, H. A. Carlos, Catalyst pyrolysis-GC/MS of Spirulina: Evaluation of highly protenaceous biomass source for production of fuels and chemicals, Fuel 179 (2016) 124-134.

[175] S. Portofino, A. Donatelli, P. Iovane, C. Innella, R. Civita, M. Martino, Steam gasification of waste tyre: influence of process temperature on yield and product composition, Waste Manage. 33 (3) (2013) 672-678.

[176] E. S. Seyedeyn-Azad, J. Abedi, T. Harding, Biomass to hydrogen via catalytic steam reforming of bio-oil over Ni-supported alumina catalysts, Fuel Process. Technol. 92 (3) (2011) 563-569.

[177] R. Ainger, V. Beatriz, A. T. Aguayo, B. Javier, G. Ana, Gayubo, Steam Reforming of Raw Bio-oil in a Fluidized Bed Reactor with Prior Separation of Pyrolytic Lignin, Energy Fuels 27 (2013) 7549-7559.

[178] D. Wang, S. Czernik, D. Montane, M. Mann, E. Chornet, Biomass to hydrogen via fast pyrolysis and catalytic steam reforming of the pyrolysis oil or its fractions, Ind. Eng. Chem. Res. 36 (1997) 1507–1518.

[179] J. Udomsirichakorn, P. A. Salam, Review of hydrogen-enriched gas production from steam gasification of biomass: the prospect of CaO-based chemical looping gasification, Renew. Sustain. Energy Rev. 30 (2014) 565-579.

Appendix-I

Critical process parameters for efficient design: Pressure drop calculation

The pressure drop across the porous bed of length L can be predicted by the Ergun equation;

$$\Delta P_{bed}/L = \frac{150\,(1-\varepsilon)^2\,\mu . U_g}{\varepsilon^3\ (dp.\phi)^2} + \frac{1.75(1-\varepsilon)\ \rho\ U_g^2}{\varepsilon^3\,(dp.\phi)} \qquad \text{.................. (Eq. 1.4)}$$

For design consideration, the following parameter values were taken for calculation.

ε is the porosity of the biomass bed inside the reactor = 0.5

μ is the viscosity of the product gas = 1.572×10^{-5} kg/(m.s)

Ug is the superficial velocity of the product gas inside the reactor = 0.7 m/s

ρ is the density of the product gas = 1.03 kg/m^3

dp is the biomass particle size = 1.45×10^{-3} m

ϕ is the sphericity = 0.7

$\Delta P_{bed}/L$ is calculated to be = **0.067 bar**;

This pressure drop value of comparatively very small.

The pressure drop due to the mixing element inside the reactor is represented by $\Delta P_{C;}$

$$\Delta P_{C} = k.\ \rho\, U_g^2/2 \qquad \text{.................. (Eq. 1.5)}$$

Here, *k* is the head-loss coefficient corresponding to the mixing element inside the reactor. This loss is considered constant for the designed system.

The total pressure drop across the system,

Considering the value to *k* as 1.0, the system pressure drop is calculated as

This value is very negligible for the screw conveyor reactor system.

$\Delta P_T = \Delta P_{bed} + \Delta P_C$ ***= 0.07 bar***

The design of the reactor system takes care of the total pressure drop across the reactor.

Appendix II A
Sizing calculations of the new reactor design:

1) Lab scale batch gasification system

Sizing calculations of a conventional throat-less gasifier was chosen as the design basis for the new reactor configuration.

For designing the gasifier the first step is to find out the gas production rate with respect to the biomass feed rate.

For a biomass feed of 1-5 kg/h, as per the gasification rate available in literature (1.3Nm^3/kg), the maximum amount of gas (Vg) that can be obtained is 6.5 Nm^3/h

Taking a maximum hearth load (G_H) of 0.5 Nm^3/h/cm^2, cross sectional area can be calculated as

$A = Vg/ G_H = 6.5 / 0.5 = 13$ cm^2

Hearth diameter = $D= \sqrt{(4.A/\pi)} =$ 4 cm

Subtracting area taken by the screw conveyor, the inner diameter works out to be **70 mm.**

Also, the total heated length of the gasifier is calculated based on the solid residence time required for complete gasification. The lab scale thermo gravimetric studies of biomass carried out in presence of steam revealed a residence time to the tune of 4 minutes. This has been considered as the design basis.

The internal helical coiled conveyor pitch is taken same as the hearth diameter, i.e., 4 cm.

The reactor residence time, $t_{reactor} = N_p/ N$

where, N_p is number of screw pitches and N is the screw rotation speed.

The rotational speed of the tubular reactor is limited upto 5 rpm. A 36 pitch coiled conveyor was found to be enough to carry out the steam gasification of biomass and char gasification.

The maximum residence time possible then can be 7.2 minutes.

The minimum heated length of the reactor can be = 36 *4 cm= 1440 mm

Thus, the total heated length of the reactor including the end fittings is calculated to be **1540 mm.**

Appendix-II B

Sizing calculations of the new reactor design:

2) Design Specifics of continuous mode gasification system

The lab scale experiments revealed that the time scales, the heating rates envisaged as per the laboratory design are sufficient for complete gasification of biomass.

In the continuous design, the reactor size was optimized to get a maximum flow rate of 1 kg/h. This has resulted in the reduction of diameter of the gasification unit to 2.5 cm.

The calculation is given below.

For a biomass feed of 1 kg/h, as per the gasification rate available in literature (1.3Nm^3/kg), the maximum amount of gas (Vg) that can be obtained is 1.3 Nm^3/h

Taking a maximum hearth load (G_H) of 0.5 Nm^3/h/cm^2, cross sectional area can be calculated as

$A = Vg/ G_H = 2.6 / 0.5 = 5.2$ cm^2

Hearth diameter = $D= \sqrt{(4.A/\pi)} = 2.5$ cm

All other design parameters including total heated length, number of pitches remain the same.

Appendix-III

Standard Operating Procedure: Continuous mode operation of the pilot plant

The pilot plant was commissioned in a 3 metre X 3 metre space in two floors. The biomass hopper, screw feeder, Screw conveyor reactor, steam vaporizer, super-heater, chiller for circulating chilled water in condensers, hot vapour condensers and cyclone separator are located in the first floor. The char collector vessel stands in two floors. All feed vessels, condensate vessels, gas feed systems, water feed pumps, vacuum pump, volumetric flow meter, fixed bed reactor, heat exchangers, pre-heaters and vaporizer and super-heater for fixed bed reactor are located in the ground floor.

After all utility and feed connections, the plant was commissioned. As per the start-up procedure, the following steps were adopted.

- Calibration of DM water feed pump
- Flow calibration of electronic flow meters (Mass Flow Controllers and Dry Gas Meter) using bubble flow meter
- Biomass (rice husk, deoiled jatropha cake) pulverization and screening of biomass particles in size range 450 micron – 1.45 mm
- Biomass flow calibration at various frequencies (2.5 Hz, 5 Hz, 7.5 Hz, 10 Hz, 15 Hz) with rice husk and deoiled cake
- Performance check for all the heaters and furnaces
- Leak check
- Vacuum check
- Dry run under steam and N_2 flow at real operating conditions

The Biomass gasification runs were carried out as per a standard operating procedure as mentioned below.

	Start-up Procedure
1	Plan the batch as per pyrolysis/gasification operation, Catalyst loading in second stage fixed bed reactor (R-305), Leak-check by N2
2	Check interlocks and alarms in the PC-PLC. Check Emergency shut-off/system start button in the control panel.

3	Check utilties (N_2, H_2, Cooling water) and Feed (graded biomass and process water)
4	Weigh and load biomass in hopper and level it properly above the screw feeder
5	Check line up. Initially bypass R-305
6	Start vacuum pump. Complete Vacuum holding test by closing needle valve at vacuum pump suction
7	Bring the system to atm pressure by starting N_2 at 500NLPH through biomass hopper. Open needle valve at vacuum pump suction and flush the system with N_2 for 5 min.
8	Start vacuum pump till required vacuum level (-0.8 barg in PT 201 & PT202)
9	Shut off N2 valve to hopper & open N2 to discharge spout. Continue N2 at 100 NLPH
10	Start ramps for screw reactor & R-305
11	Start balance heaters. Start N_2/H_2 (90:10) through the R-305 for catalyst activation.
12	Start Chiller and cooling water circulation
13	Start biomass gasification reactor (X210) at required Hz
14	After required T profile across the X210(already running) is attained start P-130 @ 10% stroke and closely monitor TE205 for temperature surge. Increase the stroke to required levels gradually. Start P-110 after the R-305 has attained required T profile
15	Start biomass metering screw (X205) at 2.5 Hz and gradually increase to required Hz. Reset Dry Gas Meter (DGM) flow.
16	Monitor T and P in the system continuously for any surges or excessive pressure drops.
17	Take syngas sample (R-305 bypassed) after system attains steady state.
18	Stop N2/H2 flow through R-305. Based on sample results, adjust the P-110 water flow, and bring R305 in line to maintain required CO and H_2O ratio.
19	Steady State Run. During the run, monitor the process parameters Temps, ΔP, DGM flow. Take gas samples intermittently.
	Pyro Gasification Unit Shutdown
1	Stop Metering Screw X-205
2	Once DGM flow starts dropping down then Stop P-130 and P-110 and close discharge isolation valve.Start N2 through R-305 to flush out process gas.

3	Stop X-210 reactor screw. Stop X210 and R305 heaters and all balance heaters except TIC 217 and TE 201
4	Increase N2 MFC flow to 500 NLPH to keep motor seal temperature under control
5	Stop vacuum system. Open needle valve on V-235 N_2 line 1 turn.
6	Let the system come to atmosphere using N2. Flush N_2 through V-235 and flush the filter assembly in cyclone top
7	Stop TIC-201 and drain V235 after pressurising it with $N_{2.}$ Drain V250.
8	Stop TIC-217 and let the system cooldown.
9	Stope chiller. Stop N2 through R-305 and isolate R-305. Isolate all utilities (H2, N2, cooling water) at battery limit

Safety and operation check

- Check SOP
- Check Utility/ Check process water
- Check Safety equipments
- Ensure continuous system monitoring when biomass is running (No unmanned op.)
- Check alarms, Product gas flow rate

Run Data

	Pre-Startup	Vacuum test	Heat-up (Ramps)	Steam Start (P-130 on)	Biomass in (X205 on)	R-305 Inline/offline	
Time	9.30 AM	9.45 AM	10:05	15:00	15: 35	Offline	
Settings				20% Stroke	5 Hz	Online	

Steady state data

Section-I (Gas Liquid Feed Section)			
Steam for Screw Conveyor Reactor (X-210)			
External- Skin	**Value, °C**	**Location- Internal**	**Value, °C**
TIC 107 (Pre-heater)	95	TE 108	80
TIC 113 (Vaporizer)	125	TE 114	115
TIC 109 (Super-heater)	500	TE 110	405
Steam for Fixed Bed Reactor (R-305)			
External- Skin	**Value, °C**	**Location- Internal**	**Value, °C**
TIC 103 (Pre-heater)	95	TE 104	85
TIC 111 (Vaporizer)	125	TE 112	116
TIC 105 (Super-heater)	500	TE 106	408
Section-II (Pyro-gasification Section)			
Screw Conveyor Reactor (X-210) Furnaces			
External-Skin	**Value, °C**	**Location- Internal**	**Value, °C**
TIC 201 (Ist)	130	TE 205 (Ist)	80

TIC 202 (IInd)	950	TE 206 (IInd)	458
TIC 203 (IIIrd)	950	TE 207 (IIIrd)	720
TIC 204 (IVth)	950	TE 208 (IVth)	756
Fluidized Bed Reactor/ Char Collector Vessel (V-220)			
External-Skin	**Value, °C**	**Location- Internal**	**Value, °C**
TIC 221 (Top)	500	TE 226 (Top)	440
TIC 220 (Mid)	500	TE 227 (Mid)	549
TIC 209 (Bot)	500	TE 228 (Bot)	517
		TE216 (Char bed)	413
Cyclone Separator and cyclone bottom collector (V-260 & V-265)			
External-Skin	**Value, °C**	**Location- Internal**	**Value, °C**
TIC 211 (V-260)	450	TE 210 (V-260)	420
TIC 222 (V-265)	450	TE 223 (V-265)	420
TIC 212 (vapour out line)	450		
Vapour line and fractional condensate vessels			
External-Skin	**Value, °C**	**Location- Internal**	**Value, °C**
TIC 214 (Vapour line)	NA	TE 215 (Vapour line)	NA
TIC 217 (V-235)	0	TE 218 (V-235)	100
TIC 212 (vapour out line)	450	TE 219 (V-250)	28

Section-III (Fixed Bed Reactor)			
External-Skin	**Value, °C**	**Location- Internal**	**Value, °C**
TIC 301 (R305 Top Zone)	400	TE 304 (R305 Top Zone)	350
TIC 302 (R305 Mid Zone)	300	TE 305 (R 305 Mid Zone)	280
TIC 303 (R305 Bot Zone)	200	TE 306 (R 305 Bot Zone)	190
TIC 307 (R305 Preheat)	400	TE 309 (T combined feed)	380
TIC 224 (R-306 Skin)	200		

Other Steady State run Parameters:

X-205 speed: 5 Hz	P-130 Stroke (DM water for X210): 25%
X-210 speed: 10 Hz	P-110 (DM water for R305): 4 ml/min
FT 101 (N_2 feed): 30 -40 NLPH	PT 201 (Vacuum pump discharge): -0.71
FQI 320 (Product gas): 240 -300 NLPH	PT 202 (V-220 O/H): -0.80
	PT 301 (R305 pressure): 0.4 barg

The process schematic from SCADA is enclosed below from Fig. A1- A3.

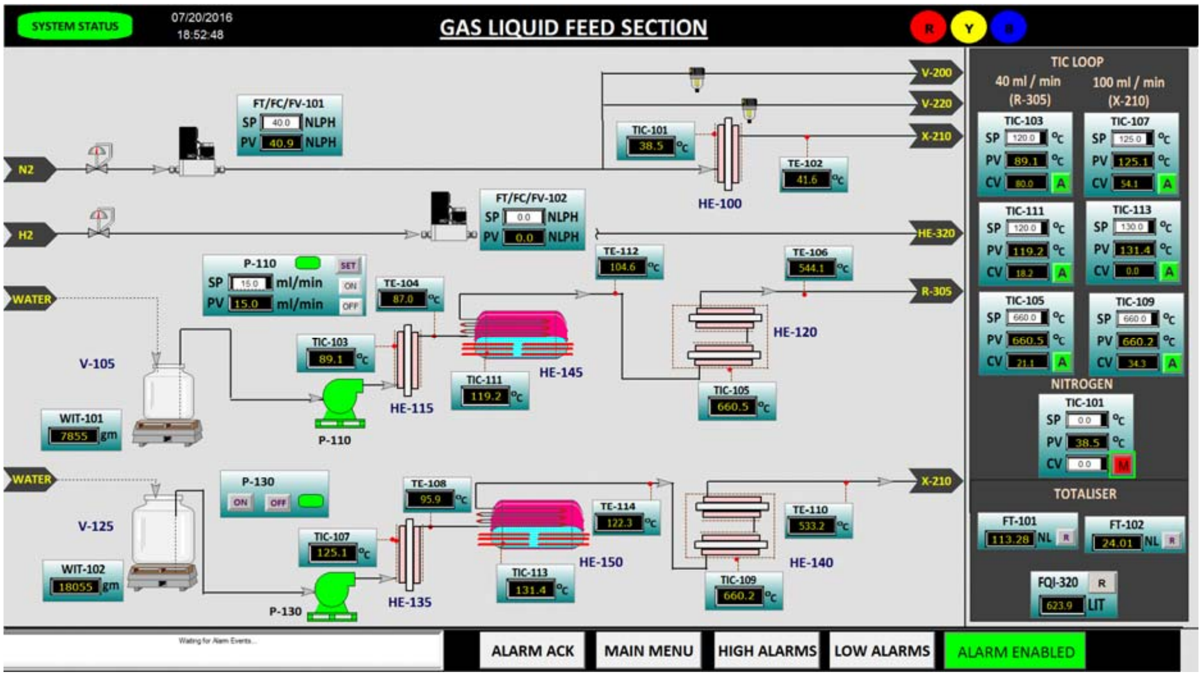
GAS LIQUID FEED SECTION

07/20/2016
18:52:48

FT/FC/FV-101 SP 40.0 NLPH PV 40.9 NLPH

FT/FC/FV-102 SP 0.0 NLPH PV 0.0 NLPH

P-110 SP 15.0 ml/min PV 15.0 ml/min

TIC-101 38.5 °C

TE-102 41.6 °C

TE-112 104.6 °C

TE-106 544.1 °C

TE-104 87.0 °C

TIC-103 89.1 °C

TIC-111 119.2 °C

TIC-105 660.5 °C

WIT-101 7855 gm

TE-108 95.9 °C

TE-114 122.3 °C

TE-110 533.2 °C

TIC-107 125.1 °C

TIC-113 131.4 °C

TIC-109 660.2 °C

WIT-102 18055 gm

TIC LOOP

40 ml / min (R-305)

TIC-103 SP 120.0 °C PV 89.1 °C CV 80.0 A

TIC-111 SP 120.0 °C PV 119.2 °C CV 18.2 A

TIC-105 SP 660.0 °C PV 660.5 °C CV 21.1 A

100 ml / min (X-210)

TIC-107 SP 125.0 °C PV 125.1 °C CV 54.1 A

TIC-113 SP 130.0 °C PV 131.4 °C CV 0.0 A

TIC-109 SP 660.0 °C PV 660.2 °C CV 34.3 A

NITROGEN

TIC-101 SP 0.0 °C PV 38.5 °C CV 0.0 M

TOTALISER

FT-101 113.28 NL

FT-102 24.01 NL

FQI-320 623.9 LIT

Waiting for Alarm Events...

Fig. A1. Section-I: SCADA screenshot of the gas feed section of continuous process for hydrogen production

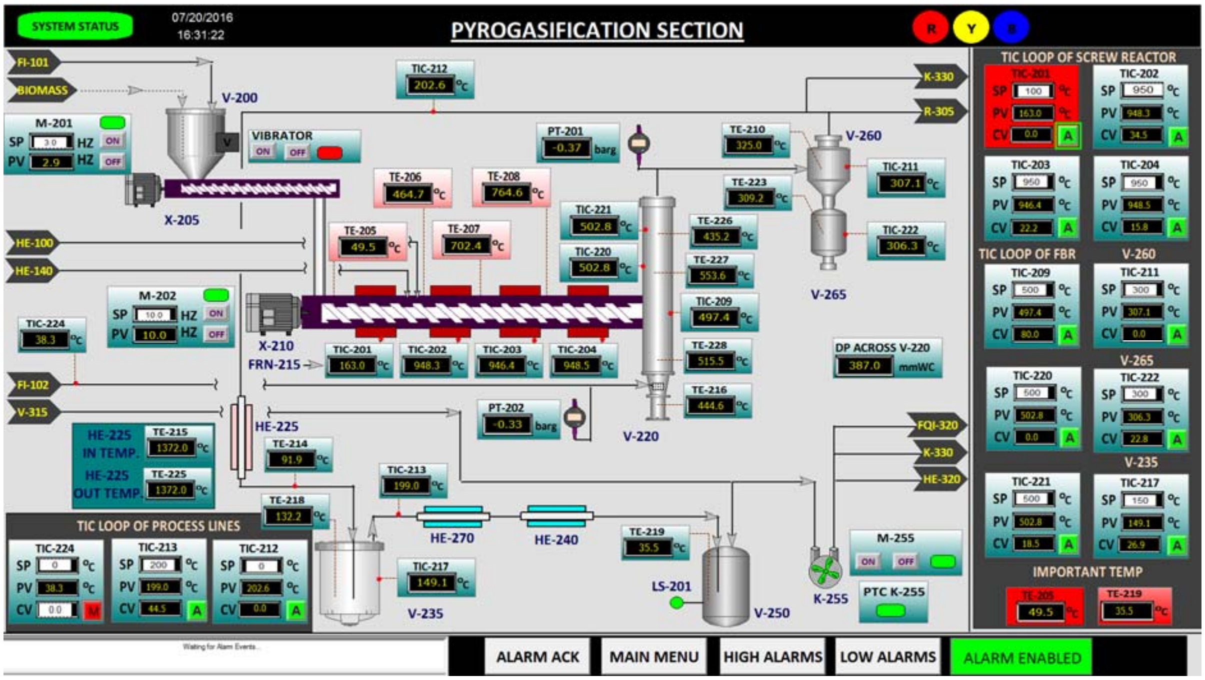

Fig. A2. Section-II: SCADA Screenshot of the gasification reactor section of continuous process for hydrogen production

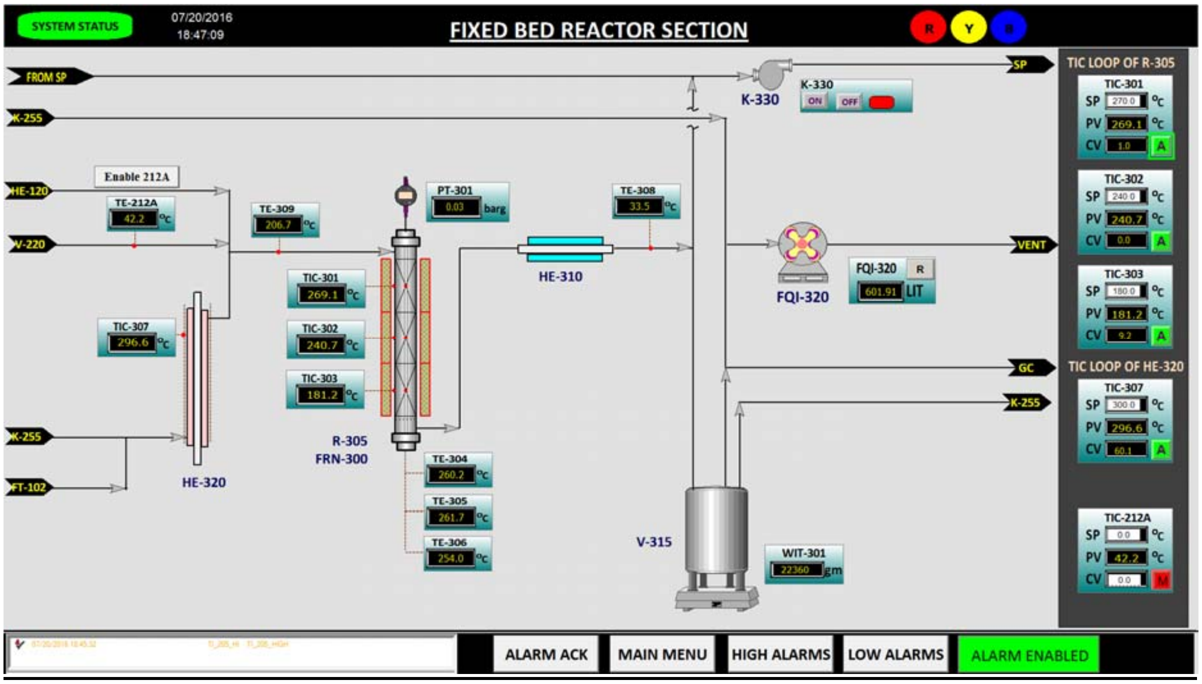

Fig. A.3. Section-III: SCADA screenshot of the second stage fixed bed conversion of continuous process for hydrogen production

Appendix- IV

Product gas molecular weight determination

GC Analysis data:

Sample	Spl1	Spl2	Spl3	Spl4	Avg.%	Norm%
H_2	20.2	20.50	18.00	17.8	19.13	20.72
CO_2	4.27	4.42	3.99	4.42	4.28	4.63
I-C_{4-}	0.54	0.5	0.75	0.32	0.53	0.57
C_3-	0	0.18	0	0	0.05	0.05
C_3=	0.17	0.00	0.16	0.39	0.18	0.20
C_2=	0.34	2.26	3.02	3.04	2.17	2.35
C_2-	0.34	0.23	0.32	0.66	0.39	0.42
N_2	19.43	23.85	23.37	21.10	21.94	23.77
CH_4	6.57	5.56	6.93	5.52	6.15	6.66
CO	38.96	34.65	37.42	39	37.51	40.64
	90.82	92.15	93.96	92.25	92.295	100

Average molecular weight of product gas

= (20.72*2.02 + 4.63*44 + 0.57*58 + 0.05*44 + 0.20*42 + 2.35*28 + 0.42*30+23.77*28 + 6.66*16 + 40.64*28)/ 100

= **22. 77 gm/mol**